OPERATING CHARACTERISTICS AND ENERGY EFFICIENCY OF HEAT PUMP DRYER FOR INDUSTRIAL ELECTROPLATING SLUDGE DRYING

CHIN YEN WEI, B.ENG. (HONS)

Thesis submitted to the University of Nottingham
for the degree of Doctor of Philosophy

JUNE, 2022

I declare that this thesis entitled “Operating Characteristics and Energy Efficiency of Heat Pump Dryer for Industrial Electroplating Sludge Drying” is the result of my own research except as cited in the references. The thesis has not been accepted for any degree and is not concurrently submitted in candidature of any other degree.

Signature	:	
Name	:	Chin Yen Wei
Date	:	31 May 2022

Publications and commercial achievement

Parts of the studies in this dissertation have been submitted for publications and actual application in the commercial industrial area.

Conference papers

1. YW Chin and SP Ong (2015). DRYING FRUITS AND VEGETABLES WITH SOLAR ASSISTED HYDROCARBON GAS HEAT PUMP DRYER. The 8th Asia-Pacific Drying Conference (ADC2015), August 10-12, 2015, Kuala Lumpur, Malaysia

2. YW Chin and SP Ong (2022). Drying Characteristics & Energy Efficiency of Heat Pump Dryer for Industrial Electroplating Sludge Drying. APCChE 2022 (19th Asia Pacific Confederation of Chemical Engineering (APCChE) Congress)

3. Technical presentation to Refine Sdn Bhd and successfully installed heat pump dryer for their sludge drying application in the year 2021.

4. Technical presentation to Refine Sdn Bhd and successfully installed heat pump dryer hot water type for their electroplating production line instead of using diesel driven type hot water boiler system in year 2022

5. Technical presentation to DSM Nutritional Material Sdn Bhd and successfully installed two unit of hybrid heat pump dryer for their drum filter drying process in the year 2019 and 2020

6. Technical presentation to Carrier Malaysia Sdn Bhd and successfully installed a heat pump system for their product testing facilities in the year 2018

7. Technical presentation to George Fisher Sdn Bhd and successfully installed a heat pump hot water unit for their product testing facilities (Quality Assurance Department) in the year 2018.

8. Product line up for heat pump energy saving unit for Aire Master Engineering (M) Sdn Bhd in year 2018. Energy heat pump unit is capable for chilled and hot water generation for industrial application. The chilled water for comfort cooling while hot water for production facilities application.

Dedicated to my beloved family

ACKNOWLEDGEMENT

First of all, I would like to express my deepest appreciation to my supervisor Associate Professor Ir. Dr. Ong Sze Pheng for her valuable guidance and support throughout this journey of research and study. Her patience and immense knowledge in drying technology has helped me a lot in the research and completion of this thesis. I especially want to thank her for accommodating my hectic schedule as a part-time student who needs to juggle between career, family and study.

Deep gratitude is expressed to Associate Professor Ir. Dr. Hii Ching Lik for his valuable advices in my research works and also his generosity and kindness in sharing his temperature measuring devices and probes that needed in my drying trials. My sincere thanks go to Professor Ir. Dr. Show Pau Loke as well for his valuable feedbacks in my annual review reports and suggestions for improvements.

I would like to express my sincere gratitude to Refine Sdn. Bhd. for providing me the sludge sample for my research. I also want to thank my workers for helping me to fabricate the heat pump dryer and also my business partner for the stimulating discussion on the design and operation characteristics of the dryer.

Last but not least, I would like to thank my family for always supporting me spiritually throughout this research project.

ABSTRACT

Conventionally, an electroplating coating factory would handle its process sludge waste from discharge point source until the dewatering stage only. Huge amount of dewatered sludge cake would incur high hidden cost to the production particularly in sludge transportation, storage and disposal. Therefore, further reduction of moisture content in the sludge after dewatering stage is essential in order to diminish the sludge handling cost. Nonetheless, the energy cost for sludge drying must be justifiable and low enough to take the advantage of it. An energy efficient sludge drying technology is indeed greatly in need. Heat pump dryer is known to be energy efficient due to its ability of heat recovery. Therefore, in the present study, a pilot-scale heat pump dryer was developed to evaluate the potential of heat pump dryer in sludge drying. Experiments were conducted to determine the drying characteristics and energy efficiency under drying temperature of 35°C-50°C and air humidity of 10%RH-52%RH. Comparisons were made against samples from conventional hot air drying (35°C-70°C). Results revealed that the drying rate would increase in proportion to wet bulb depression of drying air, where the highest effective diffusivity was recorded at 1.09765 x 10^{-8} m^2/s in heat pump drying at 50°C. Due to the dehumidification function of heat pump dryer, when under same drying temperature, drying air in heat pump dryer would possess higher wet bulb depression as compared to hot air dryer. Therefore, drying rates of heat pump dried samples were higher than hot air dried samples.

In term of energy performance, for hot air dryer, higher drying air temperature would consume more energy. The highest power consumption was recorded at 51 kWh in 35°C heat pump drying while the lowest power consumption was recorded at 14 kWh 35°C hot air drying. While lower drying air temperature consumed lesser energy, however, longer drying time was required to dry the same amount of sample. For heat pump dryer, it was found that improper configuration and control strategy could result in high power consumption as compared to hot air dryer. Findings showed that even though a heat pump dryer could possess higher heating COP theoretically, improper configurations of heat pump components (e.g. condenser type, compressor capacity, bypass duct and evaporator) and control strategy (e.g. relative humidity control and air flow rate control) could end up consuming more energy than it supposed to be (37 kWh more than hot air drying). Testing result shows that using condenser to heat the air directly would give different energy consumption profile compare to heat the air through secondary medium such as water. Direct heating would consume lesser energy at the early stage of drying compare to indirect heating. However, once the heating medium of indirect heating mode reaching its temperature limit, the energy consumption will drop and eventually having similar SMER as direct heating mode. Air volume flow rate would play a more significant role in heat pump drying compare to hot air drying. Lower airflow in heat pump drying would increase the moisture extraction rate and thus causing lower relative humidity in the drying air. Lower drying air humidity would have better drying kinetic.

In heat pump drying, some air is bypass from going through evaporator to reduce the sensible heat ratio so that more latent heat could be recovered.

Finding showed that the drying kinetic would drop significantly when there is no bypass air. This could be due to poor dehumidification of the drying air at the evaporator of the heat pump.

Improper strategy in dehumidification control was one of the major issues for heat pump dryer in term of energy efficiency. It was found that when relative humidity of drying air was too low (i.e. when dew point was near to the surface temperature of evaporator) for effective dehumidification, kept running the compressor would decrease energy efficiency as the input energy did not bring any meaningful work. In addition, it was observed that using secondary media (hot water) for heating would limit the temperature that could be achieved by a heat pump and the thermal energy that being stored in the hot water tank was not being used and wasted.

Furthermore, proper matching of heat pump size and drying load was playing an important role in the energy efficiency of the heat pump dryer as well. When the heat pump capacity was relatively too large for the drying load, then a huge amount of energy would be wasted due to frequent start/stop of the compressor and operation of auxiliary condenser. However, if the heat pump size was too small, it might not able to achieve the targeted drying air condition. Therefore, for efficient operation of a heat pump dryer, the compressor size could not deviate too much from the drying load, unless the heat pump system had means of capacity control for instance using a variable speed compressor.

Keyword: Sludge drying, energy efficiency, diffusivity, SMER

TABLE OF CONTENTS

LIST OF TABLES

LIST OF FIGURES

LIST OF ABBREVIATIONS

A = psy^c^hometric coefficient

$^\circ C$ = degree Celsius

d_v = water vapor density (kg/m^3)

$f\ (p_s,t)$ = enhancement factor at saturator pressure and temperature t

h = specific enthalpy of moist air mixture (kJ/kg)

h_a^* = specific enthalpy of dry air (kJ/kg)

h_{fg} = latent heat of vaporization of t* (kJ/kg)

h_g = specific enthalpy of saturated water vapor (kJ/kg)

$h\ (p,t,W)$ = specific enthalpy of moist air mixture at p, t, W (kJ/kg)

h_s* = specific enthalpy of a saturated mixture at p, $t*$, W_s* (kJ/kg)

h_w* = specific enthalpy of water at t* (kJ/kg)

K = Kelvin (273.16 + ˚C)

m_a = mass of dry air in mixture (kg)

m_w = mass of water vapor in mixture (kg)

N = total moles in a mixture (mole)

N_a = moles of dry air in a mixture (mole)

N_i = moles of component i in a mixture (mole)

$\mathrm{N_w}$ = moles of water vapor in a mixture (mole)

p = pressure of the moist air mixture (kPa)

p_a = partial pressure of dry air in a mixture (kPa)

p_s = vapor pressure of water in saturated moist air (kPa)

p_t = test chamber pressure in two pressure humidity generators (kPa)

p_w = partial pressure of water vapor in a mixture (kPa)

$p_{ws}{}^{(t)}$ = saturation pressure of water vapor at t ((kPa)

$p_{ws}{}^{(t*)}$ or $p_{ws}*$ = saturation pressure of water vapor at $t*$ (kPa)

$p_{ws}\,({}^{t}{}_{d})$ = saturation pressure of water vapor at ${}^{t}{}_{d}$ (kPa)

q = specific humidity

R = universal gas constant (Pa·m^3/mole·K)

R_a = specific gas constant for dry air (Pa·m^3/mole·K)

t = temperature of the moist air mixture (dry bulb) (˚C)

$t*$ = thermodynamic wet-bulb temperature (˚C)

t_d = thermodynamic dew-point temperature (˚C)

t_d' = frost-point temperature (˚C)

$t_d(p,W)$ = dew-point temperature of moist air mixture at p and W (˚C)

T = absolute temperature of the moist air mixture (˚C)

V = volume of the mixture (m^3)

W = mixing (humidity) ratio

W_s* = saturation mixing (humidity) ratio at $t*$ and p

$W_s(t,p)$ = saturation mixing (humidity) ratio at t and p

$W_s({}^{t}{}_{d})$ or $W_s(p, {}^{t}{}_{d})$ = saturation mixing (humidity) ratio at ${}^{t}{}_{d}$ and p

x_a = mole fraction of dry air in a mixture

x_i = mole fraction of component i in a mixture

x_w = mole fraction of water vapor in a mixture

x_{ws} = mole fraction of water vapor in a saturated mixture

ρ = density of an air-water vapor mixture (kg/m^3)

v = specific volume of a moist air mixture (m^3/kg)

μ = degree of saturation

ϕ = relative humidity

CHAPTER 1

INTRODUCTION

1.1 Sludge management in Malaysia

Malaysia is one of the fast-growing nations in global economy and it ranked at 27^{th} in the global competitive index in 2019 edition of World Economic Forum's Global Competitiveness Report (WEC, 2019). Though the ranking has dropped 2 places compare to previous year, Malaysia manages to achieve higher score in the index. As a result, the amount of industrial sludge in Malaysia keeps increasing due to its heavy industrialization and the archaic wastewater treatment technology. Industrial sludge is the sludge generated from industrial wastewater treatment. Its compositions vary depends on the type of industrial processes. Meanwhile, sewage sludge is generally referred to sludge originated from domestic or municipal wastewater treatment. Sewage sludge contains largely organic compositions as domestic wastewater usually carry faeces, urines, food waste, detergent, etc.

In Malaysia, the sludge management policy is centralized and governed by the National Water Services Commission (SPAN). The task of the SPAN is to:

a. Limit the production of sludge

b. Process the sludge to safe and hygienic material

c. Recycle or reuse sludge instead of disposal

With fast development in Malaysia, the volume of sludge produced has been increase proportionally with the increase of generated wastewater annually. National sewage company, Indah Water Konsortium (IWK) has produced about 5.3 million cubic meter of sewage sludge per year based on the perspective sludge production factor (SPF). While landfilling has been the most common and simple way for sludge disposal, other ways of sludge disposal such as forestry, composting and agricultural application have been studied and gaining acceptance. Table 1-1 shows the amounts of sludge produced in Malaysia per year. The projected sludge generation for year 2035 is estimated at 10 million m^3 per year with 2% dry solid content.

Table 1-1: Amount of sludge produced in Malaysia

Type of sludge	Generation rate (million m^3)	Centralized facilities (million m^3)	Non-centralised facilities (million m^3)
Sewage sludge	7.40	5.30	2.10
Industrial sludge	9.90	6.40	3.50

Before disposal, sludge need to go through dewatering process. Usually this is done at the in-plant facilities. Various types of mechanical dewatering facilities are normally used for instances belt-press, filter-press, screw-press and centrifugal. There are also dedicated sludge treatment facilities to handle sludge from factories that without in-plant dewatering facilities. Like any other places in the world, industries in Malaysia usually have in-plant sludge treatment from thickening process up to dewatering process. The sludge is first sent to a settlement tank for thickening and then pumped to a filter press for dewatering. After dewatering process, the effluent is sent to a centralized treatment plant for further treatment. Then, the dewatered and pre-treated sludge will be sent to the Kualiti Alam for further processing and finally disposed either in landfill or incinerated.

In Malaysia, the basis directive for waste and scheduled waste is governed by the Environmental Quality (Sewage and Industrial Effluents) Regulations 2010 (Spinosa, 2011). This means that the requirements derived from other directives that addressed to sludge will apply additionally to the above directive. Therefore, the management of sludge must also fulfil the requirements that spelled out by specific normative measures, such as:

a. Malaysia Sewerage Industry Guidelines (Volume II) by Sewerage Service Department
b. Department of Environment (DOE)'s site selection guidelines for sludge disposal
c. Interim guidelines for utilization of biosolids as fertilizer for non-food crops

The direction of sludge management in Malaysia is going toward 3R i.e. reduce, reuse and recycle (Indah Water Konsortium Sdn Bhd, Effects Of The Reuse of Sludge To Environment Health, 2015). The Malaysia government encourages the use of sludge (after proper treatment) as fertilizers, energy source and also for resource recovery. The same effort is also encouraged in private sector. Continuous efforts in research and development in public university and research institute will provide the support for the government to meet its objective in protecting the environment while the related authority will continue monitor and assess the impact of sludge application to the environment.

The growing environmental awareness has caused more stringent requirements on treatment, handling and storage of industrial sludge (Aja & Joo, 2016). Currently, the operations at most wastewater treatment plants are relatively inadequate and most of the time they solely rely on normal sewage treatment to handle the sludge. Consequently, the large amount of sludge, even after thickening and dewatering processes, has put tremendous pressure on sludge management cost and operating cost of the factories. Hence, additional treatment on the dewatered sludge is needed in order to further reduce the water content in the sludge before sending it for solid waste treatment or disposal. New technology in sludge treatment, management and utilization is greatly in demand.

It is estimated that approximate 6% of the total possible dry solids (DS) concentration can be obtained by thickening treatment (e.g. gravity settlement, gravity belt thickener, drum thickener), further 32% of the total possible DS concentration can be obtained by mechanical dewatering (e.g. filter press, belt press, screw press) and the remaining 62% of the total possible DS concentration (or about 90% of DS) can be obtained by thermal drying (Flaga, 2015). If water content in sludge has to be reduced to minimum (> 90% of DS), lower than that is guaranteed by mechanical dewatering, then additional sludge drying is necessary.

Sludge drying is a thermal treatment in which heat energy is delivered to the sludge in order to evaporate water. Thermal processing of sludge could reduce mass and volume of the product significantly, making its storage, transport, packaging and retail much easier. It also enables incineration or co-incineration of sludge at lower-cost and better efficiency. Sludge drying is necessary and it is an integral process for effective sludge treatment. While achieving carbon neutrality is a practical path for many countries to deal with energy crises and climate change, drying is one of the typical energy-intensive process and source of carbon emission. Hence, a proper technology and method must be employed to make the sludge drying harmless, stabilized and possess higher degree of electrification as well as decarbonization.

Traditionally, sludge drying using thermal process are based on the evaporation of water content under high temperature. The sources of heat are either by direct fire or electrical heaters. These drying process setups consume a lot of energy and thus they are expensive besides bringing the negative impacts to the environment. In addition, scarce literature on sludge drying technology shows that it is still an uncommon practice currently in the industry due to lack of awareness and knowledge. Some factories will just use direct fire and electric heater dryer to reduce the water content of the sludge, mainly due to the simplicity of the method and technology. However, what waiting for them is the expensive utility cost and high carbon footprint.

Heat pump dryers have been applied in the drying process of various materials namely fruit, vegetable, grain and wood. With past experience and positive results in using heat pump dryer to dry agricultural products, drying sludge with heat pump system might be a viable alternative for the traditional method of sludge drying. Table 1-2 shows the amount of energy that is consumed by different types of dryers to remove 1 kg of water from the sludge. The comparison is done among the common drying technologies that available in the industry. It can be clearly seen that electric heater has the highest energy cost though the thermal efficiency is higher compare to the boilers. On the other hand, heat pump dryer is an ideal choice for sludge drying as it is highly efficient, safe and clean.

Therefore, in order to reduce the energy usage, an efficient drying system such as heat pump dryer should be used for the thermal drying process. Direct fire is not taken into consideration in the present study because it is an inadequate and unsafe method. It is prone to toxic gases generation and discharge that will cause environmental issues as well as health problems.

Table 1-2: Energy cost for a dryer to remove 1 kg of water

Dryer Type	**Electric heater**	**Coal Boiler**	**Diesel Boiler**	**Gas Boiler**	**Heat Pump**
Fuel/Energy Type	Electric	Coal	Diesel	Gas (LPG)	Electric
Heat Value	3600 kJ/kWh	23027 kJ/kg	33494 kJ/L	49000 kJ/kg	3600 kJ/kWh
Thermal Efficiency	95%	30%	85%	85%	400%
Effective Thermal Value	3420 kJ/kWh	6906 kJ/kg	28469 kJ/L	41650 kJ/kg	14400 kJ/kWh
Fuel/Energy Cost	RM0.44/kWh	RM0.40/kg	RM2.05/L	RM1.90/kg	RM0.44/kWh
Fuel/Energy Consumption	1.42 kWh	0.7 kg	0.17 L	0.117kg	0.337 kWh
Total Cost (RM)	0.62	0.28	0.35	0.22	0.15
Safety	Unsafe	Unsafe	Unsafe	Unsafe	Safe
Direct Pollution	None	Very Serious	Serious	Serious	None
Equipment Life	5 -8 years	6 -9 years	6 -9 years	6 -9 years	10 -15 years

**Source: GuangZhou Kaineng Electric Equipment Co. Ltd.*

1.2 Sludge handling at electroplating coating factory

Sludge sample used in the present study was obtained from a coating company located in Banting, Selangor, Malaysia. The sludge is classified as scheduled waste by the Waste Management Centre Malaysia (Kualiti Alam) with code SW204. According to the company's normal practice, the sludge waste would first undergone dewatering process using a filter press. After that, the sludge would be packed and sent to Kualiti Alam for further treatment and disposal.

However, there are 2 major issues with their current sludge handling practice. Firstly, the cost of the sludge disposal is high with a charge of RM500 per ton. With monthly disposal range in weight of around 11 ton (after dewatering process), the cost of disposal would be about RM5500 per month. Secondly, the company is allocated with a quota of 10 tons (waste) per month by the Kualiti Alam. In other words, they would need to pay the fines if subjected to penalty when exceeding their quota.

Hence, the company is looking for ways to further reduce the weight of the sludge. Currently, they are using direct gas fire to heat the sludge cake after dewatering in order to further reduce the moisture content. According to the data given, 45 kg of sludge can be reduced to 35 kg after direct gas fire burning process, which accounts about 22% in weight reduction or equivalent to 2.44 ton per month. The gas utilisation cost for the direct fire burning is estimated at RM2340 per month. Thus, the saving gained through the weight reduction is about RM1220 per month and also avoid the overweight fines. However, they will still have the deficit of RM1120 by using direct gas fire drying method due to the utility cost. Therefore, there is essential to explore a better way of sludge drying in order to achieve the net saving.

Figure 1-1: Sludge cake and drying with direct fire burning

1.3 Problem statement

Heat pump dryer is known to be energy efficient due to its ability of heat recovery (Chua et al, 2010). Energy that is used to dehumidify air can be recovered for sensible heating, thus reducing (or totally eliminating) the usage of electric heaters. However, economic feasibility of heat pump dryer is still debatable because of its electricity consumption, high cost of construction and maintenance (Kivevele & Huan, 2014). Currently, majority of studies of heat pump drying are focus on agricultural products such as fruit, vegetable, timber etc. Study of using heat pump technology on sludge drying is still relatively uncommon though thermal drying of sludge has been gaining attention due to worldwide sludge management issue.

Heat pump dryer is relatively a complicated system. The matching of system components and their control would have affected the system efficiency greatly. Therefore, system integration is a major issue when developing any kind of heat pump dryers (Minea, 2010). As sludge from different origin posts different characteristics, the performance and operating requirement of heat pump varies accordingly. Thus, some components and system configurations are required for proper operation and optimization. The complexity of the heat pump system may be one of major factor that hinder its adoption in sludge drying considered that sludge is relatively low value compare to agricultural product. Therefore, there is a need to investigate how the configuration and integration of heat pump dryer's components would affect the performance of a heat pump dryer in terms of drying quality and energy efficiency.

1.4 Objectives

The aim of this study was to investigate the feasibility of a heat pump dryer in industrial sludge drying. Drying kinetics and characteristics of sludge samples were examined at various drying conditions, operating parameters and configurations of heat pump components. The main objectives of this research were:

i. To evaluate the drying kinetics and characteristics of the industrial sludge undergoing heat pump drying.

ii. To study and evaluate the energy efficiency of a heat pump dryer for sludge drying application.
iii. To investigate the impacts of the configurations of heat pump components (condenser type, compressor capacity, bypass duct and evaporator) and control strategy (e.g. relative humidity control and air flow rate control) on the dryer's performance and energy consumption.
iv. To determine the quality of dried sludge sample.
v. To compare the performance of the heat pump dryer with a hot air dryer.

1.5 Scope of study

A pilot-scale heat pump dryer was developed to investigate the drying of sludge sample from an electroplating coating factory with waste code of SW204. The sludge sample principally is inorganic constituents that containing metals and small amount of organic material. The scopes of this research are as followings:

i. **Design of pilot-scale heat pump dryer**

   A heat pump dryer with built in electrical heater was designed and fabricated to facilitate the study of heat pump drying. Major components of the heat pump system i.e. compressor, evaporator, condenser and circulating fan were properly studied and investigated to get proper operation. A bypass duct was fitted to control the air flow through the evaporator, and thus provided control over the evaporating temperature without affecting the condenser operation. An auxiliary evaporator was fitted to enable the evaluation of the performance of the heat pump with and without dehumidification process. This unit could transform into a hot air dryer by switching off the heat pump system.

ii. Determination of drying characteristics

Sludge samples were dried under constant temperature (35°C and 50°C) using the pilot-scale heat pump dryer. Moisture content of samples was measured and recorded throughout drying. Drying kinetics, drying rates and moisture diffusivities were determined from drying curves that were constructed based on the moisture content profile and Fick’s second law.

iii. Evaluation on the configuration of heat pump and control strategy

Sludge samples were dried under different heat pump configurations like the condenser type (dehumidifying mode and heating mode), compressor capacity (0.5 to 4 HP), bypass duct (open-, partial open- and closed modes) and evaporator (dehumidifying mode and non-dehumidifying mode), as well as various control strategies (e.g. relative humidity control and air flow rate control). Moisture content of samples and energy consumption were measured and recorded throughout drying. Comparison was made based on the moisture content profile, drying rate and specific moisture extraction rate (SMER). A 3D modelling of the heat pump dryer was constructed and computational fluid dynamic (CFD) simulations were performed to examine the temperature profile and air flow dynamics inside the drying chamber. The performance of the heat pump system under the effects of abovementioned configurations and control strategies were examined and evaluated.

iv. **Determination of the quality of sludge sample after drying**

Simulation results were studied and verified against actual measurement.

v. **Comparison with a conventional hot air dryer**

Sludge samples were dried under constant temperature (35°C, 50°C and 70°C) using the hot air dryer mode. Moisture content of sample was measured and recorded throughout drying. Drying kinetics, drying rates and moisture diffusivities were determined from drying curves that were constructed based on the moisture content profile and Fick's second law. Comparison was made against heat pump drying based on drying kinetics, drying rates, moisture diffusivities, specific moisture extraction rate (SMER) and total energy consumption.

1.6 Contribution of study

The present study had provided field measurements and experimental studies of a pilot-scale heat pump dryer to give realistic reference and data for operational optimization and technology promotion of heat pump dyer in sludge drying. The field data had validated the basic principles and working theories of a heat pump dryer and fill up the research gap by illustrating the energy efficiency, safety and reliability of the heat pump dryer in industrial sludge drying. Findings from the present study could provide the industrial sludge producers an alternative option to handle their sludge waste. Instead of stopping at the dewatering stage, now they have a possible option to further treat their sludge without much additional financial burden. The dried product that with lower moisture content and high calorific value could then be reused or recycled. In academic sector, the present study could serve as future research in advancing the technology maturity and operational improvement.

CHAPTER 2

LITERATURE REVIEW

2.1 Type and characteristics of sludge

Property and characteristic of sludge can vary greatly depending on the sources. Municipal sewerage sludge tends to have large number of organic matter while metallurgy industrial sludge may contain large number of inorganic materials. Types of sludge can be classified according to their origin and composition. Table 2-1 below shows the categories of sludge and their characteristics.

Table 2-1: Category and composition of various types of sludge

Main Sludge Category	Origin	Composition
Organic-Hydrophilic	❖ Sewerage wastewater ➢ Primary sludge ➢ Biological sludge ➢ Separate or mixed tertiary sludge ➢ Mixed sludge	❖ Prevailing organic matter: Volatile Solid/Dry Matter: 40 to 90%

Main Sludge Category	Origin	Composition
	❖ Industrial wastewater from agri-food industries ❖ Industrial wastewater from textile, organic chemical, petrochemical industries, etc. ➢ From their biological polishing treatment.	❖ Fermentable organic matter ❖ Al or Fe hydroxides that have coagulated flocculated the above products ❖ Biological floc ❖ Phosphate Fe
Hydrophobic mineral	❖ Wastewater from steel making, mining and metallurgy industries ❖ Drinking water (DW). Drillings and rivers ❖ Drinking water. Heavily laden rivers ❖ Flue gas washing wastewater ❖ Sewerage wastewater/Agri-food industries	❖ Oxides, ash, dense mineral particles, Calcium sulphate ❖ Carbonates < 80-90%, Fe, Mn oxides ❖ Silt, fine sand ❖ Dense mineral particles: gypsum ❖ Mineral matter. Mass/Volume<5%
Hydrophilic mineral	❖ DW. Medium loading rivers, lakes, reservoirs ❖ DW. Laden rivers	❖ Clay Fe, Al: 20 to 60% Activated carbon if applicable Organic matter: 10 to 25% ❖ Fe, Al:15% to 25%

Main Sludge Category	Origin	Composition
	❖ DW. Rivers and drillings ❖ Wastewater, Mineral chemical, surface treatment industrial ❖ Reuse (Sewerage/Industrial wastewater) ❖ Wastewater Dyeing and tanning industries	Clay, silt, sand ❖ Carbonates 50 to 65% Fe, Al hydroxides ❖ Metal hydroxides ❖ Fe, Al hydroxides ❖ Mineral (hydroxides) + organic (biological, grease)
Oily hydrophobic	❖ Wastewater ❖ Rolling mills (steel mills)	❖ Dense mineral particles (oxides, scales) coated in oil ❖ Oil-laden hydroxides ❖ Mineral oils
Oily hydrophilic	❖ Wastewater ❖ Refineries ❖ Mechanical workshop	❖ Emulsified or soluble oils/ Hydroxides after flocculation. ❖ Biological OM (occasionally)
Fibrous	❖ Wastewater from, ❖ Papermills ❖ Board mills ❖ Paper making pulp	❖ Cellulosic fibres: 20 to 90% ❖ Mineral fillers (kaolin, alum, carbonates): 10 to 80% ❖ Biological sludge: 10 to 20%

Source: Suez water handbook (www.suezwaterhanbook.com)

Generally, classification of sludge is based on 2 major properties: organic/mineral nature or hydrophilic/hydrophobic nature. Organic sludge usually requires organic matter stabilisation or heat oxidation stage while hydrophilic sludge will make dewatering difficult because the solids are strongly bound to water.

Organic-hydrophilic sludge. This type of sludge contains a significant proportion of hydrophilic colloids, thus it is difficult to dewater. This type of sludge is usually produced from wastewater biological treatment plant or facility. Volatile matter content is usually reaching 90% of the total dry solid (DS) content.

Mineral-hydrophilic sludge. This type of sludge contains metal hydroxides that are formed during physical-chemical precipitation processes of the metal ions in the water.

Oily sludge. This type of sludge contains oils that are found as emulsions or absorbed over hydrophilic or hydrophobic particles.

Mineral-hydrophobic sludge. This type of sludge contains large quantity of particulate matter with low level of associated water (e.g. sand, silt, slag, etc).

Mineral-hydrophilic-hydrophobic sludge. This type of sludge mainly contains hydrophobic matter that incorporates hydrophilic matter to ensure the predominance of the latter’s effect during dewatering. Hydrophilic matter is usually found in metal hydroxides that are caused by the precipitation of mineral coagulants (Fe and Al salt).

Fibrous sludge. This type of sludge is usually easy to dewater. However, if the fibres in it is being recovered, the sludge will become more hydrophilic due to the presence of hydroxides or biological sludge.

2.2 Sludge treatment

Sludge is a semi-liquid residue that is generated from municipal wastewater treatment or industrial wastewater treatment or refining processes. It is typically a viscous mixture of liquid and solid that is thick, soft and wet. The solid is suspended in liquid and in between the solid, there is large quantity of interstitial water. The sludge produced from the wastewater treatment basically consists of primary sludge and secondary sludge (www.iwapublishing.com, Sludge Drying view) Figure 2-1 below shows the typical wastewater treatment process.

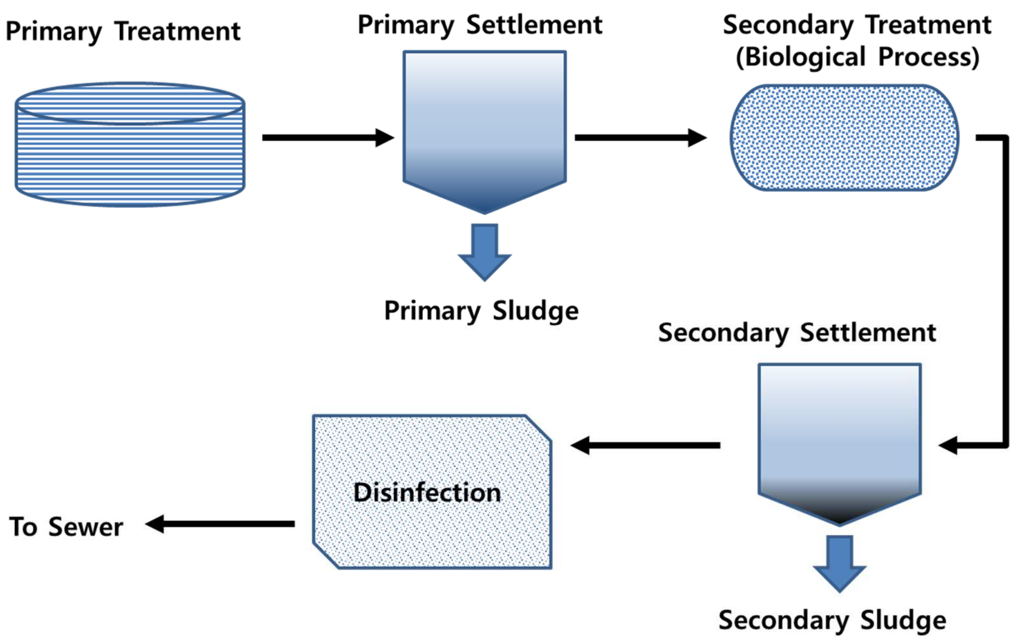

Figure 2-1: Typical wastewater treatment process

Primary treatment is the treatment stage where solids and non-polar liquids are removed from wastewater by gravity. Gravity separation of solids during primary treatment is carried out in the primary sedimentation tanks. Solids that are heavier than water will accumulate at the bottom of the settling basins. The remaining liquid usually contain less than half of the initial solids content and about two-third of the Biochemical Oxygen Demand (BOD) and the form of colloids and dissolved organic compounds (Wikipedia, Wastewater Treatment).

Secondary treatment is known as activated sludge process. The process involves adding seed sludge to the wastewater and then pump air into aeration tank to fuels the growth of bacteria that consume oxygen and also the growth of other microorganisms consume the remaining organic matter. This process produces large particles that will settle down in the huge aeration tank (Patel and Vashi, 2015).

The sludge produced from primary and secondary treatment is required to be further treated by removing the water content from the sludge. Sludge treatment is necessary due the following reasons:

a. Reduce volume (removal of water)
b. Reduce/remove odour
c. Stabilise organic material
d. Remove pathogens
e. Reclaim useful by-products (biogas, soil conditioners)
f. Safe/appropriate disposal & recycling

The remaining water content in sludge can be further reduced in order to minimize its volume and weight. Water removal process of sludge commonly consist of the followings:

Stage 1: Thickening

The sludge that generated from wastewater treatment typically contain about 0.5% to 3% dry solid (DS). During sludge thickening, the free water inside the sludge is reduced by separation of liquid and solid using gravitational force. The process is usually done inside a tank, which is called gravity thickener. Gravity thickening is one of the simplest ways to separate the solid from the liquid and requires only very low energy input. After thickening process, the dry solid (DS) of the sludge can be increase to about 6% and thus the total volume of sludge can be reduced to about half of its original volume.

Stage 2: Dewatering

Dewatering can further reduce the water content and increase the DS content of the sludge up to about 40 % DS. The sludge can then be handled like a solid material. Usually dewatering process are done mechanically using a filter press, belt press or screw press. Sludge drying bed, however, provide the simplest method of dewatering. Inside the sludge drying bed, sludge is spread on an open bed filled with sands. Drying of sludge is done though evaporation and drainage by gravity. However, the drying capability of drying bed is much lower than mechanical dewatering.

Stage 3: Sludge drying

If the water content of the sludge needs to be further removed, then drying process is required. Sludge drying is basically a thermal drying process where the water content inside the sludge is evaporated using thermal energy. The volume and the weight of sludge thus can be further reduced by sludge drying process and make it easier for storage, transportation and packaging. Thermal drying is becoming more popular as a means of decreasing sludge volume by removing the water content and achieving a DS content of 90%. This could reduce the volume of sludge by approximately 4 to 5 times and therefore make the transportation cost lower and the storage easier. It also reduces the environmental impact by producing a stabilized dry granular product that is suitable for agricultural use. Sludge drying can also increase sludge calorific value, so that it could be incinerated with lesser fuel consumption. Figure 2-2 shows weight reduction after each treatment. With the clear benefit of sludge drying, there are many researchers have conducted studies on sludge drying.

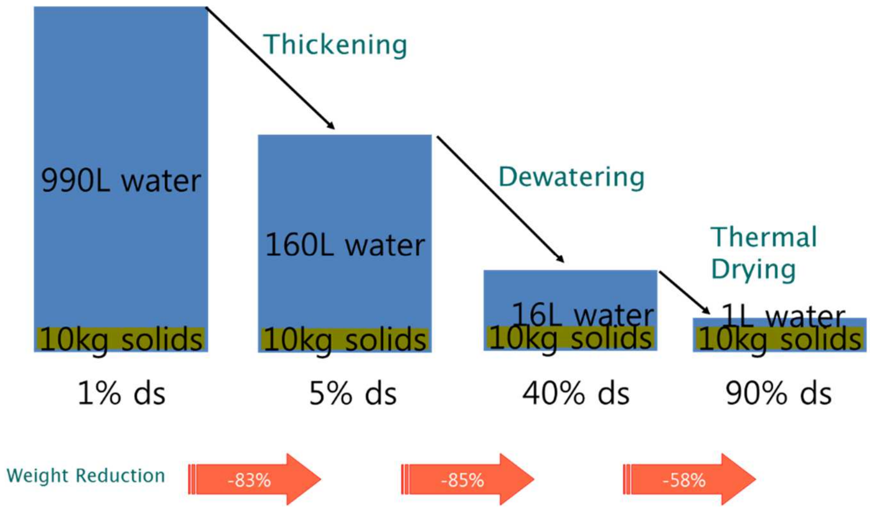

Figure 2-2 : Weight reduction of dry solid

2.3 Sludge drying

Unlike other products that are dried in the industry, sludge is very complex material and its property varies depends on its origin. Sludge with high content of volatile matter tends to emit biochemical gases during drying process. Some of the gases would cause unpleasant odour to the environment while some might be flammable and pose the risk of explosion. Another phenomenon that creates problems for some of the dryers is its sticky phase. When sludge is being dried and change its state from liquid phase to paste form, and about 40 – 60% DS, the sludge will become a substance comparable to sticky rubber. Refer to Table 2-2 for the evolution of rheological state with dry solid content. This sticky phase of sludge could affect the operation of indirect dryer or event cause damage to the equipment. The rheological change of sludge could also affect the moisture diffusivity within the sludge and thus affecting the drying rate adversely.

Table 2-2: Evolution of rheological state with dry solid content.

%DS	**<10**	**10-40**	**40-60**	**60-90**	**>90**
Sludge State	Liquid	Viscous Liquid-Pasty	Sticky phase	Granular solid	Dry solid

Source from (Léonard, 2010)

As sludge from different sources vary greatly, it is difficult to design a dryer that is suitable or optimized for all sludge. (Leonard, 2004) had conducted drying test on sludge from different origin and found that the drying flux variation could go up to a factor of 3. The experiment was performed using a micro-dryer (a small size hot air dryer) specifically designed to treat small amount of sample.

Léonard (2010) found that by simply pumping the sludge will also affect the drying behaviour of the sludge. After pumping the drying rate of sludge is reduced. This is normally counteracted by adding lime to the sludge. Lime can strengthen the texture of the sludge and thus partially counteract the effect of pumping. Liming at different stage will also have different outcome on the sludge drying kinetic. Liming before the dewatering process (i.e. pre-liming) has better effect compare to liming after dewatering process (i.e. post-liming). This is because the shear stress that impose to the sludge by the dewatering machine will reduce the texturing effect of lime.

Besides the effects of rheological changes on the sludge drying kinetic, heating itself could create another issue for sludge drying. High temperature heating could induce break down of organic matter, causing the emission of volatile organic compounds. In this case heat pump dryer may be used to reduce the volatiles emission by drying sludge at lower temperature.

Zhang et al. (2016) has reported that it is better to conduct thermal drying of sludge at a lower temperature (<100^{o}C) to reduce the release of benzene, thus reducing the danger of carcinogenic formation. Hence, a conventional heat pump system is suitable for this range of drying temperature.

2.4 Sludge drying using heat pump assisted dryers

Rao & Cao (2012) found that the performance of a solar assisted heat pump system is better than that with the process of heating by oil, gas or electricity in term of economic benefit for sludge drying. Throughout the drying process using heat pump dryer, no peculiar smell was observed.

Yi et al. (2014) had conducted a wastewater treatment project using solar assisted heat pump dryer to dry the sludge in a printing and dyeing industrial park in Xintang town of Guangzhou city. In Yu city of Shandong, a solar assisted heat pump which was similar to the one presented by Slim et al. (2008) was built.

Figure 2-3 shows the schematic of the system. The system consisted of a greenhouse, a sludge mixer, a heat pump system for heating the air and another heat pump system to heat the floor of the greenhouse. The humid air was used as heat source for the air heating heat pump to heat up the outside air that flow into the greenhouse. The greenhouse's floor was heated up by the other heat pump which using wastewater as the heat source.

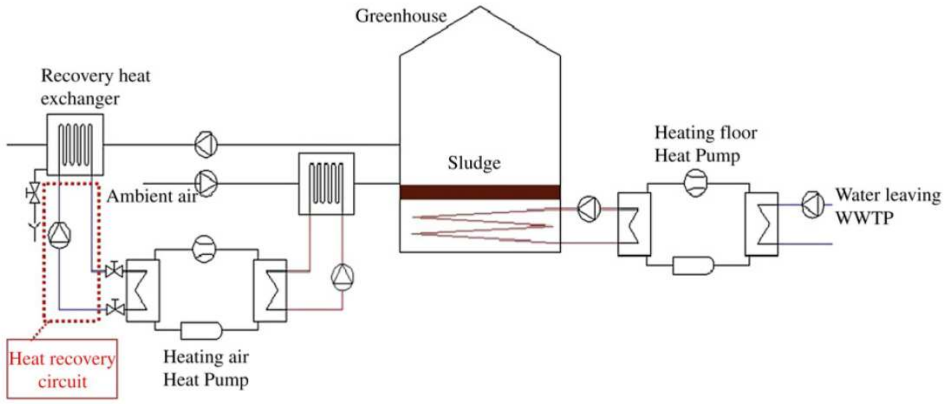

Figure 2-3 : Schematic diagram of Modelling of a solar and heat pump sludge drying system

Slim et al. (2008) had developed a slipping quasistatic model to evaluate the performance of greenhouse assisted heat pump sludge drying system. Various set point combinations had been tested to study the optimum configuration of the drying system. Slim et al. (2008) concluded that the heat pump performance and control strategy were strongly dependant on the weather in the region where the wastewater treatment plant was located.

Schnotale, (2018) had reported the use of carbon dioxide (CO_2) heat pump system to dry sludge. CO_2 is a natural refrigerant (i.e. refrigerant that exist naturally) in heat pump system as shown in Figure 2-4. It is considered as one of the alternatives to HFC as the latter is scheduled to be phased out under Kyoto Protocol. CO_2 has very low critical temperature of 31.1°C. Therefore, the heat rejection part of the system was working at the trans critical region. Hence, the heat exchanger for heating was a gas cooler instead of condenser. According to Schnotale, (2018), the trans critical cycle resulted in high compressor discharge temperature. The author took the advantage of high discharge temperature to provide additional hygienization of the sludge.

Schnotale (2018) had also done the comparison with other technologies in sludge drying. The result showed that heat pump possessed the highest efficient dryer as compared to others. The technologies that being compared are gas technology (direct drying), oil technology (indirect drying) steam technology and Watromat technology. Watromat was also a heat pump dryer but using R404a as refrigerant. R404a is a HFC refrigerant with very high global warming potential.

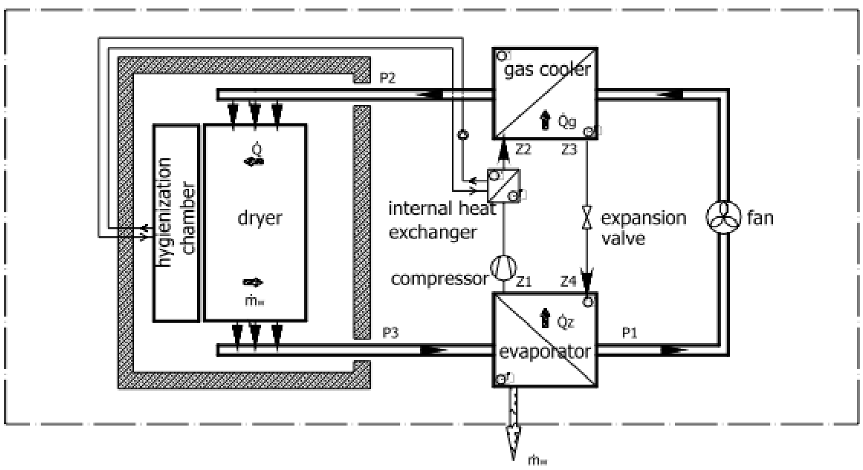

Figure 2-4: Conception of the CO_2 heat pump sludge drying system (Schnotale, 2018)

2.5 Heat pump dryer

Basically, a heat pump dryer consists of a heat pump system and a drying chamber. The heat pump system is responsible to provide heat to the drying chamber for drying purpose, as oppose to the other types of dryers that using different heat source such as electric heaters, gas fire, waste heat, etc. However, heat pump dryer has an additional function that not possessed by other types of dryers, i.e. dehumidifying the drying air. This capability of heat pump dryer enables low temperature drying and start gaining attentions from the drying industries.

Heat pump, as implied by its name, pumps heat from lower temperature region to higher temperature region which against the natural flow of heat. Similar to a water pump that pumps water from lower ground to higher ground. For electrical heat pump, the heating output is largely from the heat source instead of the input power to the heat pump. The heat that being transferred can be 3 to 4 times larger than the electrical power consumed. When compared to an electric heater which converts input electrical energy to heat, obviously, heat pump is much more energy efficient as a heating device.

Most heat pumps are working on the principle of vapour-compression refrigeration. There are 4 major components required for a complete refrigeration cycle, i.e. compressor, condenser, expansion device (throttling device) and evaporator refer to Figure 2-5. The media that used to transport heat is called refrigerant. The compressor would compress R22 refrigerant up to 21.74 bar in order to achieve 55°C condensing temperature. The high pressure superheated refrigerant is then directed to a heat exchanger for heat exchange. Inside the heat exchanger, the vapour refrigerant would be de-superheated, then condensed and sub-cooled to liquid refrigerant at temperature of 51°C (design at 4.0°C sub-cool) at constant pressure. The expansion valve would reduce liquid refrigerant pressure to about 5.48 bar (corresponding to evaporating temperature of 3.0°C) in order to reduce the temperature from 51°C to 3.0°C. The cold refrigerant would absorb the heat from the hot drying air, while the refrigerant start boiling and eventually change from the liquid form to vapour form again. The circulation keeps continue until the process water temperature achieved the desired set point.

Besides the four main components, there are other necessary probing and control instruments such as solenoid valves, filter drier, temperature and pressure sensors, and switches for safe operation of heat pump system.

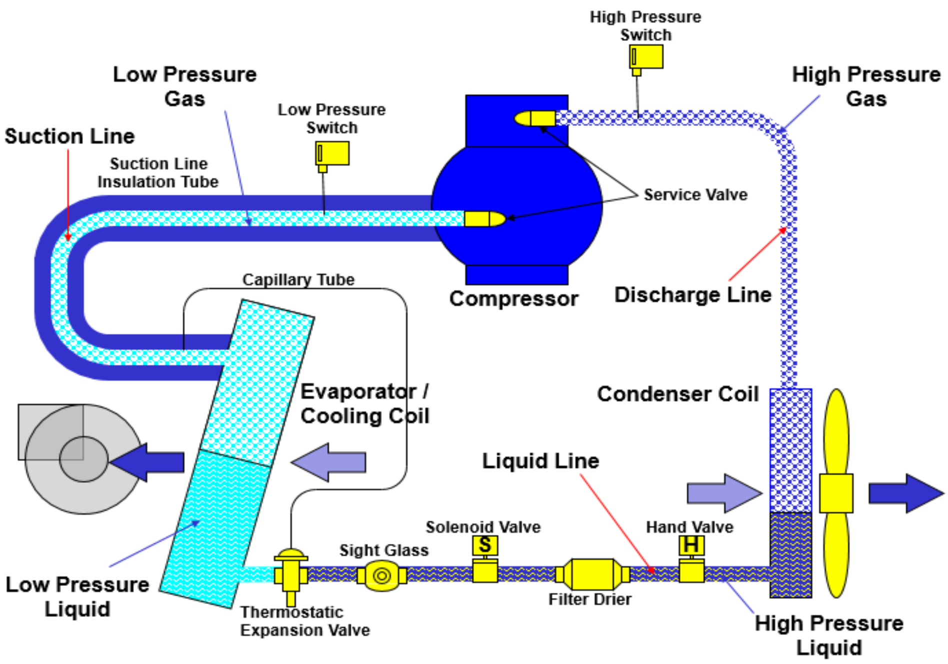

Figure 2-5 : Basic refrigeration cycle

There are many ways to integrate the heat pump system to drying chamber. Depends on application and resources available, the heat pump can be either air source, water source or ground source which extract heat from the air, water and ground, respectively. The heat pump also can be configured to provide heating directly or through secondary medium. Figure 2-6 illustrates a typical heat pump dryer using water as secondary medium. The heat pump dryer consists of a heat pump system, a heat storage tank, a circulation pump (or fan, or both pump and fan) and other necessary probing and control instruments such as solenoid valves, three-way valves, temperature and pressure sensors. This heat pump dryer can facilitate the integration of solar system or other hot water sources.

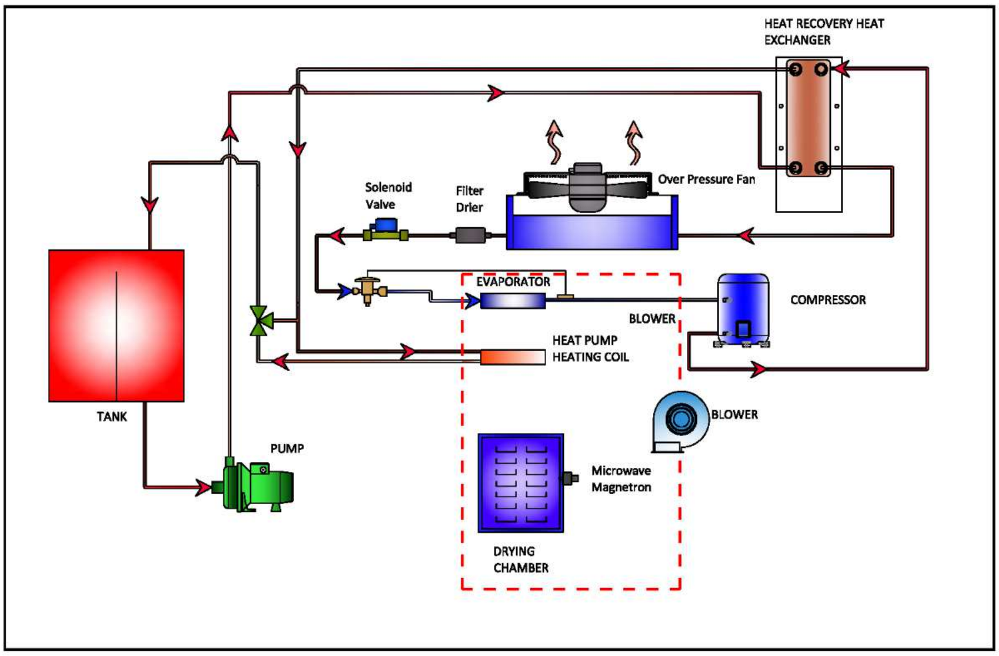

Figure 2-6 : Heat pump dryer system with heat storage

Air flow configuration plays an important role as well. Drying air flow is responsible of transporting moisture and heat within the dryer. Effectiveness of the drying air in transporting heat and moisture would affect the efficiency of the system as well. The air cycle of a HPD can be either open type, semi-open type or closed type. Type of the air cycle to be used depends on the environment conditions. For an example, if ambient air is relatively dry, the open type might be more efficient to operate. If ambient air is relatively humid, then closed type is a better choice.

2.5.1 Configuration of heat pump dryer

The basic components of heat pump dryer include a compressor, at least 2 heat exchangers and an expansion valve. However, there are other consideration for the proper operation of a heat pump dryer. For an example, in a closed loop air circulation, the air flow through condenser and evaporator should be independently control. This can be done by adding a bypass passage across the evaporator. Compressor with over bypass will facing low pressure trip while small bypass opening would reduce the dehumidification capability of the dryer.

Improper design of a heat pump system can lead to inefficient operation of the heat pump dryer. In more serious case, it might lead to frequent break down of the dryer, thus citing claims of high maintenance cost. Inappropriate matching of refrigeration component could lead to coil freezing, compressor overheating and etc. which will cause dryer downtime and interrupting the drying process.

Usage of less efficient components will make the dryer to operate less efficiently. For instance, scroll compressor has higher capacity and co-efficient of performance (COP) as compared to reciprocating compressor (Iain Grace, 2002). Thus, obviously heat pump system with scroll compressor will be more efficient than those with reciprocating compressor. Other more advanced component like Electronic Expansion Valve (EXV) can have more precise control in refrigerant flow compare to the conventional Thermostatic Expansion Valve (TXV). EXV can enhance the efficiency of the heat pump system by accurately regulate the refrigerant flow (Moon, 2003).

After all the components are correctly selected, a good control strategy is essential for efficient operation of the dryer. The control strategy might involve the correct operation of each component as well as determining the right operating set point. For example, in process of dehumidification, the surface temperature of evaporator must be sufficiently lower than the dew point temperature of the on-coil air for effective moisture extraction. If this parameter is not controlled correctly, the dryer would not operate efficiently.

2.5.2 Criteria and design consideration for a heat pump dryer

A heat pump dryer (HPD) basically consists of a heat pump system and a drying chamber. Heat pump system is responsible for the heating as well as dehumidification of drying air. It consumes large portion of the dryer's input power. Therefore, the performance of a HPD is greatly affected by the performance of its heat pump system. A different refrigerant can affect the performance of the heat pump system. Right choice of refrigerant can improve the performance of heat pump. For an example, R134A having lower operating pressure can deliver a temperature that higher than R22. Shen et al. (2018) had designed an air source HPD in which refrigerants R22 and R134a were adopted as the working medium for the high-stage and low-stage, respectively. According to their study, the supplying temperature can reach up to 70°C. On the other hand, Lee et al. (2010) had designed a two-cycle HPD, where one cycle used the refrigerant R124 to get a temperature greater than 80°C and the other cycle used the refrigerant R134A to cover the low temperature range.

Heat pump dryer with closed-loop configuration that consists of a conventional drying chamber with air circulation system and the usual components of an air-conditioning refrigeration system enables the dryer to operate at a wide range of drying conditions with temperature ranges from -20°C to 100°C (with auxiliary heating) and relative humidity ranges from 15% to 80% (Chou and Chua, 2007). Hence, heat pump dryer can be used to dry a wide range of agriculture products.

Control strategy is very important in improving the performance of a HPD. Not only the control of heat pump system components but also the control of drying air circulation. Yang et al. (2016) proposed a synchronous control strategy to improve the control accuracy of a closed-loop HPD's superheat and drying temperature. Ju et al. (2018) provided an evaluation method for the convection hot air-drying method to improve drying efficiency and reduce energy consumption by controlling relative humidity. Table 2-3 lists the design consideration based on the past experience when constructing and testing the self-developed HPD.

Table 2-3: Phenomena finding for the developed new heat pump dryer.

Item	**Design phenomena**	**Design considerations**	**Consequences of improper design**
Air velocity	The opening size of outlet discharge affected the effective air velocity In the new dryer, the outlet discharge size is: 0.25m x 0.8 m which applying 1.2m^3/s blower and resulting the air velocity = 6m/s The blower selection is based on delivered air volume and static pressure in the system. Blower motor will be integrated with a frequency inverter to regulate the air velocity	> Size of drying chamber must suite to available space > Check the maximum current electricity supply > Expected drying time and energy consumption required > Minimum and maximum drying air stream > Range of humidity inside the drying chamber	Lower air velocity causes poor drying rate while too high air velocity will cause sample fly over inside the drying chamber and high power consumption.
Evaporator	The size of an evaporator can affect the following capability: > Moisture removal from the air stream	Construction of evaporator depend on: > Row of coil	Undersize evaporator will cause lesser moisture removal due to icing and excessive liquid

Item	Design phenomena	Design considerations	Consequences of improper design
	> Coil air leaving condition such as temperature and humidity > Position or placement of the evaporator is important since vertical position will have better condensation water flow down to drain pan. While horizontal placement cause condensate water hardly to drain due to direction against air flow	> Tube height > Fin per inch > Fin length > Air volume across the coil > Type of fluid media inside the tube > Type of material	refrigerant will flush back and cause compressor failure. Evaporator with small opening will cause higher air velocity across the coil, if > 3 m/s then moisture may carry over and cause wetted drain pan. Oversize evaporator may cause poor moisture removal and starvation of liquid while having poor cooling to compressor.

Item	Design phenomena	Design considerations	Consequences of improper design
Compressor	Type of compressor would affect the energy consumption, for instance scroll is better than reciprocating in term of COP. Matching of compressor to condenser and evaporator is very important since it will affect the stability of the system	To size the compressor, it depends on: > Evaporating temperature > Condensing temperature As long as the selected point is under the compressor performance envelope, the compressor will be saved to be used under the required capacity.	Oversize compressor will cause icing and liquid flush back. Undersize will cause compressor overheated and tripping due to safety cut off.
Condenser	Condenser or heating coil will affect the system operating pressure; smaller coil will cause high pressure and oversize require bigger space and overloaded compressor due to higher refrigerant charge.	Depend on: > Row of coil > Tube height > Fin per inch > Fin length	Too big condenser coil will cause wastage of material and higher manufacturing cost and bigger space requirement.

Item	Design phenomena	Design considerations	Consequences of improper design
		> Air volume across the coil > Type of fluid media inside the tube > Type of material > Capacity of rejected heat	Undersize condenser coil will cause system running in high discharge pressure and less energy efficient.
Expansion valve	Refrigerant control device Normally refer to thermal expansion valve (TXV) which will bring down the liquid refrigerant pressure and temperature before entering into evaporator. However, to gain better flexibility control, the refrigerant control valve is upgraded to electronic expansion valve (EEV) which will have better control by referring to pressure and temperature at the suction pipe. The opening mechanism of the	Selected TXV / EEV must be based on capacity required, type of refrigerant and superheat requirement	Oversize will cause refrigerant flow hunting and unstable while undersize will cause insufficient cooling effect at the evaporator.

Item	Design phenomena	Design considerations	Consequences of improper design
	valve can be adjusted with software setting based on required evaporating temperature, type of refrigerant and superheat required.		
Control system	Design a control panel which will control the components to work accordingly to the desired control logic plus integration of safety device to minimise system operation failure.	Consider the pressure control of the system. If R22 then high pressure not more than 26 bar while low pressure not less than 2 bar. Circulation fan or pump must operate prior running of compressor. In case of less heat demand due to saturation condition, the over	If system running under pressure, then will cause insufficient cooling to compressor and cause the compressor overheated. If over pressure due to blockage or heat rejection device failure, then will be danger to operators.

Item	Design phenomena	Design considerations	Consequences of improper design
		pressure heat rejecter fan must turn on to lower the operating pressure. Electrical safety components such as current circuit breaker, current overload, residual circuit breaker must be integrated to avoid short circuit and provide protection to the components such as motor and compressor	
Control system	Humidity controller	To get humidity level indication or control of compressor status	

Item	Design phenomena	Design considerations	Consequences of improper design
Control system	Temperature controller	To control the amount of hot water flowing into three-way valve hence to achieve drying air temperature. Can be used to control the compressor on/off status since compressor can be turn off whenever achieving the setting of air stream temperature.	
Auxiliary heaters	Built in heater	In case to get higher air temperature which unable to achieve by heat pump system	Oversize cause energy wastage and undersize is unable to get higher air temperature.

Item	Design phenomena	Design considerations	Consequences of improper design
System integration	During start up, the simultaneously cooling and heating causing the temperature take longer time to raise to desired temperature. The net heating power solely depends on the compressor input power and latent capacity of cooling coil. This has reduced the heating power of the whole heat pump system during start up.	Evaporator should not be permanently located inside the drying air stream.	Lower net heating power prolong the heating period and waste time and energy
System integration	During heat pump mode, when the compressor is off, the drying air will pick up the condensate water on the cooling coil/evaporator.	Evaporator should not be permanently located inside the drying air stream, when compressor is off, the drying air stream should be diverted away from the evaporator.	Re-humidification of the drying air will waste the previous energy that are used to dehumidify the air and cause humidity fluctuation.

2.6 Sludge drying kinetic

Drying characteristic of a product can be elucidated with drying curve which is the plot of moisture content versus time. Moisture content of a product can be described as wet basis or dry basis. The wet basis moisture content M_w is defined as the mass of water in the product m_w divided by the total mass of the product m_t.

Wet basis moisture content, M_w

$$M_w = \frac{m_w}{m_t} \qquad [2.1]$$

While the dry basis moisture content, M_d is defined as the mass of water in the product divided by the total mass of the product m_d,

Dry basis moisture content, M_d

$$M_d = \frac{m_w}{m_d} \qquad [2.2]$$

Generally, the drying curve can be divided into three periods as shown in Figure 2-7 and Figure 2-8, i.e. initial period (A-B), constant rate period (B-C) and falling rate period (C-D-E). At the initial period, the product surface temperature is raised to wet bulb temperature by the drying air where the moisture at the surface of product is vaporized to the air stream. At the constant rate period, the product surface temperature is maintained at wet bulb temperature and the surface of the product is saturated with the free moisture.

The drying rate is determined by the water diffusion rate through the boundary layer at the air-solid interface. The water absorb heat from the drying air and evaporated from the product surface. Some products do not show constant rate period due to shrinkage and the product surface not completely wet.

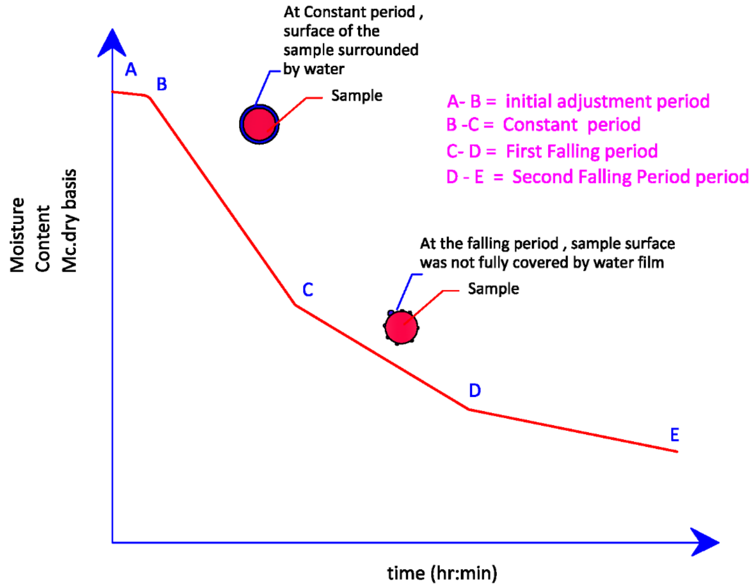

Figure 2-7: Typical drying curve. Moisture content vs drying time.

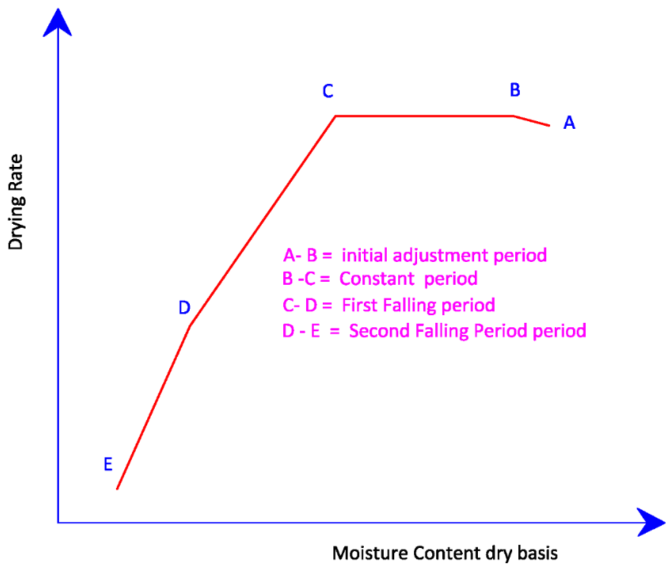

Figure 2-8 : Typical drying curve. Drying Rate vs drying time

At the falling rate period, the moisture content at the surface start to decrease, thus the evaporation rate starts to fall. The surface temperature begins to move from wet bulb temperature to dry bulb temperature. At this period, the drying rate is determined by the moisture diffusion rate inside the product. The moisture content is asymptotically approaching the equilibrium moisture content and the temperature and humidity of the drying air.

The basic mass and energy balance for the sludge drying process can be illustrated as in Figure 2-9.

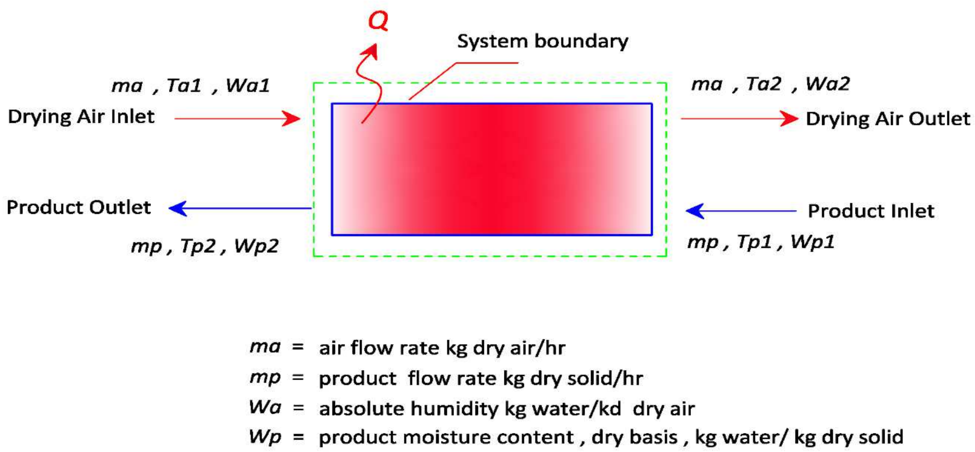

Figure 2-9 : Basic mass and energy balance for the sludge drying process

Mass Balance

$$ma \,.\, Wa1 \;+\; mp \,.\, Wp1 \;=\; ma \,.\, Wa2 \;+\; mp \,.\, Wp2 \qquad [2.3]$$

Energy Balance

$$ma \,.\, Ha1 \;+\; mp \,.\, Hp1 \;=\; ma \,.\, Ha2 \;+\; mp \,.\, Hp2 + Q \qquad [2.4]$$

where,

ma = air flow rate, kg dry air/hr

mp = product flow rate, kg dry solid /hr

Wa = absolute humidity, kg water/ kg dry air

Wp = product moisture content, dry basis (kg water/kg dry solids)

Ha = Thermal energy of air KJ/kg

$Ha = Cs\ (Ta - T_0) + Wa\ .\ HL$

Cs = Specific heat capacity of moist air = 1.005 + 1.88Wa

Hp = Thermal energy for product KJ/kg dry solids

$Hp = Cpp\ (Tp - T_0) + Wp\ .\ Cpw\ (Tp - T_0)$

Cpp = specific heat of the product

Cpw = specific heat of the water

Q = Energy loss from the drying system

2.7 Moisture diffusivity

Moisture diffusivity is the rate of movement of water molecules from a region of high vapour concentration to a region of low vapour concentration. The moisture diffusivity of agricultural product such as fruits are complicated. It not only depends on the physical structure of the product but also on the moisture content and the temperature. Most of the moisture diffusivity calculations are based on Fick's Laws of Diffusion. However, there is no standard way of applying these laws on evaluation of moisture diffusivity.

The moisture diffusion process often being described using Fick's second law of diffusion,

$$\frac{\partial M}{\partial t} = D_{eff}\nabla^2 M \qquad [2.5]$$

where,

M = local moisture content (d.b.)

= time (s)

D_{eff} = moisture diffusivity (m^2/s)

For engineering analysis, one-directional diffusion is good approximation for practical application. Thus, in the present study, the situation is assumed as one-dimensional. If the sludge is assumed to have geometry of thin slab, the general solution for Equation [2.5] can be derived using appropriate boundary conditions (Crank, 1975),

$$MR = \frac{8}{\pi^2}\sum_{n=1}^{\infty}\frac{1}{(2n-1)^2}exp\left(-(2n-1)^2\frac{\pi^2 D_{eff}t}{L^2}\right) \qquad [2.6]$$

where *MR* is moisture ratio and *L* is the thickness of the sludge. In most cases, the effective diffusivity can be estimated by using only the first term of the general solution (Zogzas et al, 1996). Thus, Equation [2.6] can be written as,

$$MR = \frac{8}{\pi^2}exp\left(-\frac{\pi^2 D_{eff}t}{L^2}\right) \qquad [2.7]$$

Then Equation [2.7] can also be written in logarithmic form as,

$$\ln MR = \ln\frac{8}{\pi^2} - D_{eff}\left(\frac{\pi}{2L}\right)^2 t \qquad [2.8]$$

The moisture ratio *MR* of the sludge can be determined by the Fick's diffusion equation as following,

$$MR = \frac{M_t - M_{eq}}{M_0 - M_{eq}} \qquad [2.9]$$

Where,

M_t = moisture content (dry basis) of the sludge at time *t*

M_{eq} = equilibrium moisture content

M_0 = initial moisture content

In this case, M_{eq} is relatively smaller compare to M_t and M_0. Thus, the equation can be simplified to,

$$MR = \frac{M_t}{M_0} \qquad [2.10]$$

CHAPTER 3

METHODOLOGY

3.1 Sludge sample preparation

Sludge cake sample (after dewatering) was obtained from a coating company located in Banting, Selangor, Malaysia according to the standard method of ASTM D346-90. The sludge sample was categorized as waste coating chemical (SW204) by the Waste Management Centre Malaysia (Kualiti Alam). The sludge cake sample was properly sealed in an air tight container to avoid water evaporation. The weight of the sample was pre-defined and recorded before the drying experiment. The initial moisture content of the sludge cake sample was about 71%. The major components of the sludge sample are copper (65,530 ppm), nickel (61,144 ppm), chromium (50,578 ppm), iron (5551 ppm), platinum (163 ppm), lead (135 ppm) and zinc (53 ppm).

3.2 Prototype heat pump dryer

A prototype heat pump dryer was designed and fabricated by Aire Master Engineering (M) Sdn Bhd located at No.30, Jalan Sungai Jeluh 32/189, Taman Perindustrian Bukit Naga, 40460 Shah Alam , Selangor, Malaysia to facilitate the study of sludge drying using heat pump system in . This heat pump dryer (HPD) was fitted with multiple heating elements and flexible control systems to study sludge drying under various drying modes. There were with 3 heating elements: (i) auxiliary electric heaters; (ii) direct expansion heating coil (condenser); and (iii) hot water coil (utilised water as secondary medium). When performing conventional hot air drying, the heat pump system would be switched off and heating element (i) was used. On the other hand, when heat pump drying was performed, then either heating element (ii) or (iii) was used.

Meanwhile, the dehumidifier of the HPD could be either enabled or disabled as required in the experiment setting in order to study the effects of dehumidification in sludge drying. In addition, the circulation fan was connected to a variable frequency drive (VFD), so that the fan speed could be adjusted to study the effects of air flow on the sludge drying. Figure 3-1 shows the conceptual design configuration of the prototype heat pump dryer.

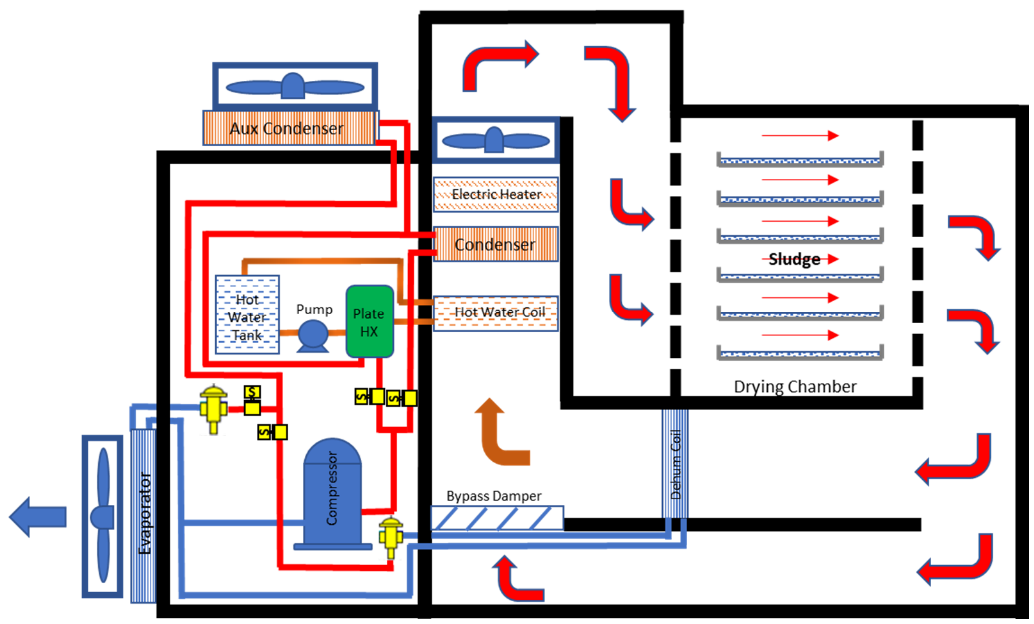

Figure 3-1 System configuration of the prototype heat pump dryer (closed mode)

Besides the default closed loop (Closed Mode) configuration as shown in Figure 3-1, the HPD can also be configured into open loop configuration (Open Mode) and partially open configuration (Partially Open Mode) as illustrated in Figure 3-2 and Figure 3-3, respectively. In the Open Mode, the drying air was exhausted out of the system after the drying process and was not recirculated back to the system. Then the blower would draw in fresh air and the drying air was heated up to the desired temperature. When the hot drying air passed through the sludge sample which located inside the drying chamber, it would pick up moisture from the sample and then this moisture laden drying air would be exhausted to the ambient in the end. In the Partially Open Mode, part of the drying air was recirculated back to the system and mixed with fresh air before it was heated up to perform drying. The blower would recirculate part of the drying air inside the drying chamber. A small amount of air change was required to keep the drying air humidity below desired level. Minimum heating was needed to maintain the recirculating air temperature.

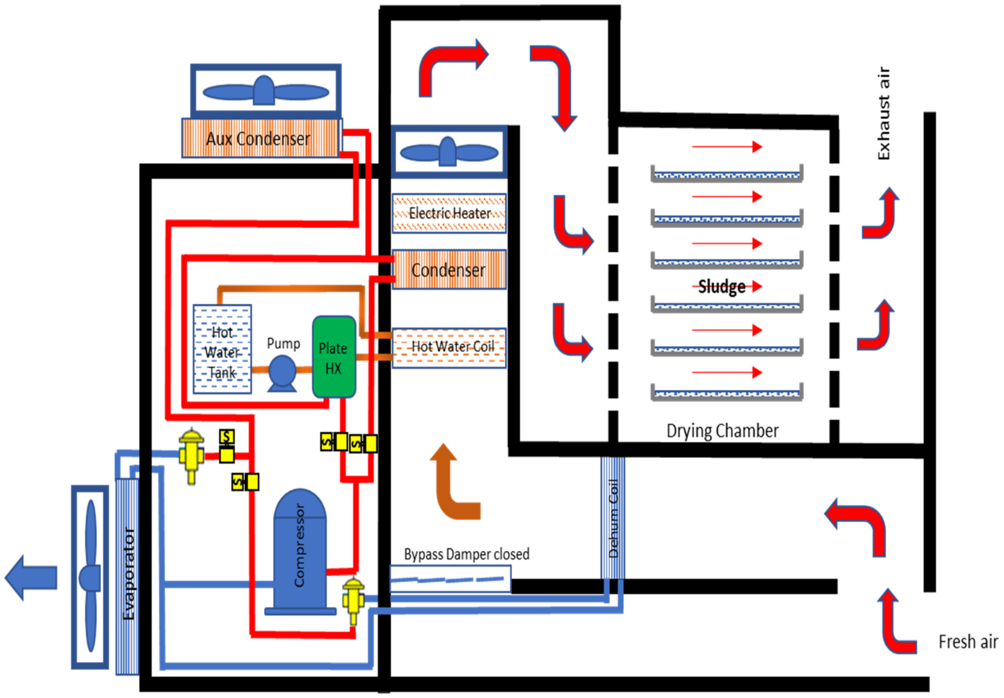

Figure 3-2 Schematic of open mode drying configuration

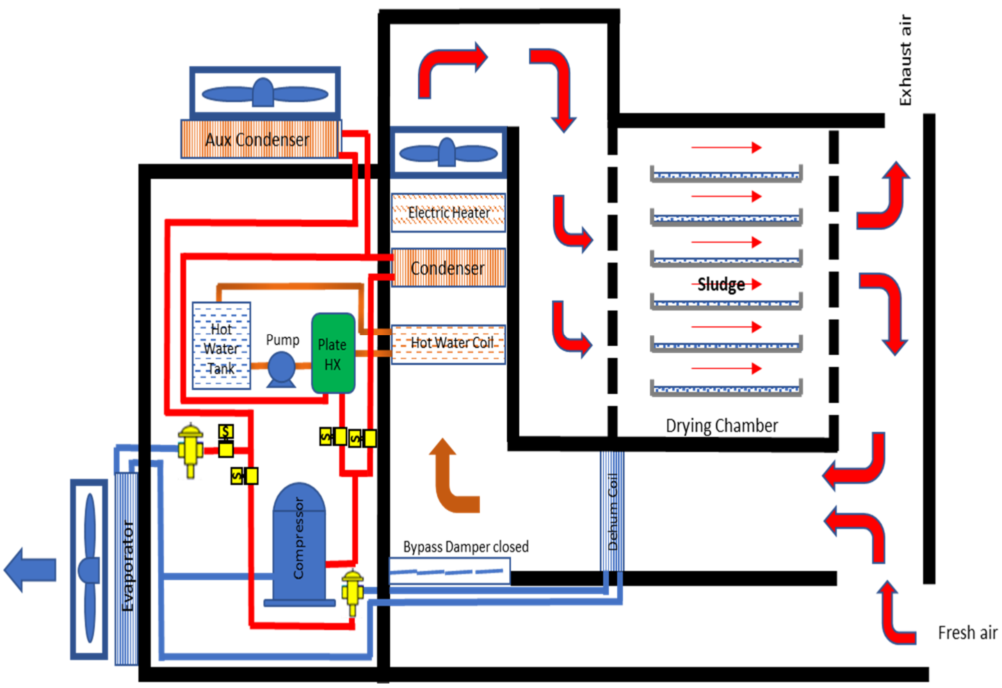

Figure 3-3 Schematic of partially open mode drying configuration

Figure 3-4 shows the overall dimension and general component layout of the pilot-scale heat pump dryer. The overall dimension of the heat pump dryer was 1941 mm (width) x 1544 mm (depth) x 2265 mm (height).

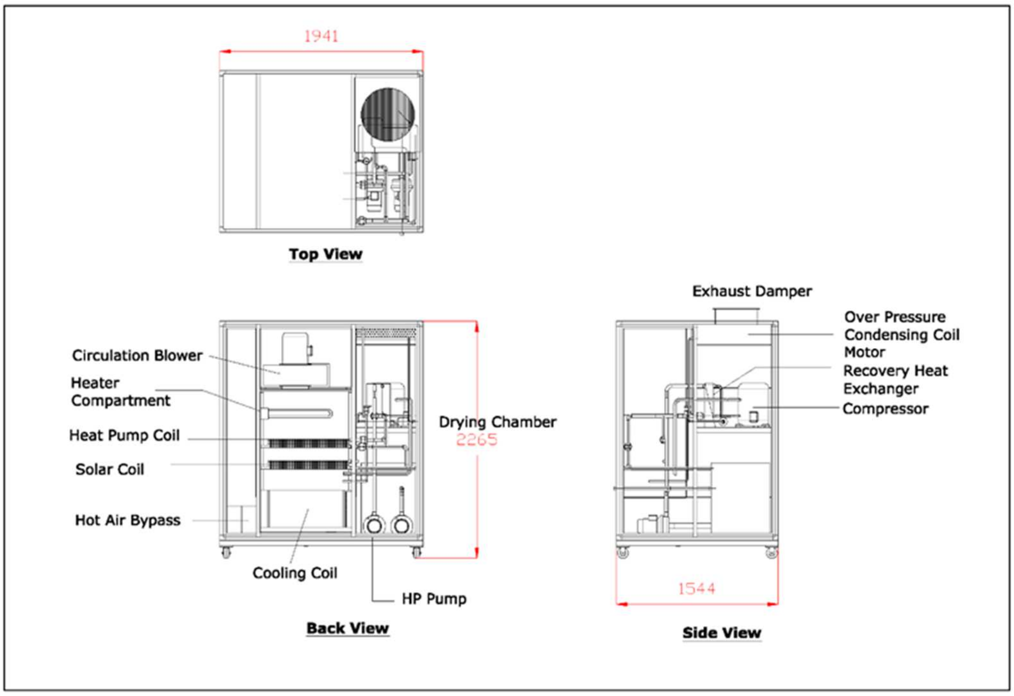

Figure 3-4: General layout and overall dimension of the prototype heat pump dryer

Figure 3-5 shows that the front view of the heat pump dryer where the drying chamber was located at the centre and the air duct was connected to the drying chamber from the top. On the left-hand side was the heat pump system compartment, housing of the compressor, hot water tank, pump and piping system. The control panel and electrical switch gears were at the right-hand side of the heat pump dryer.

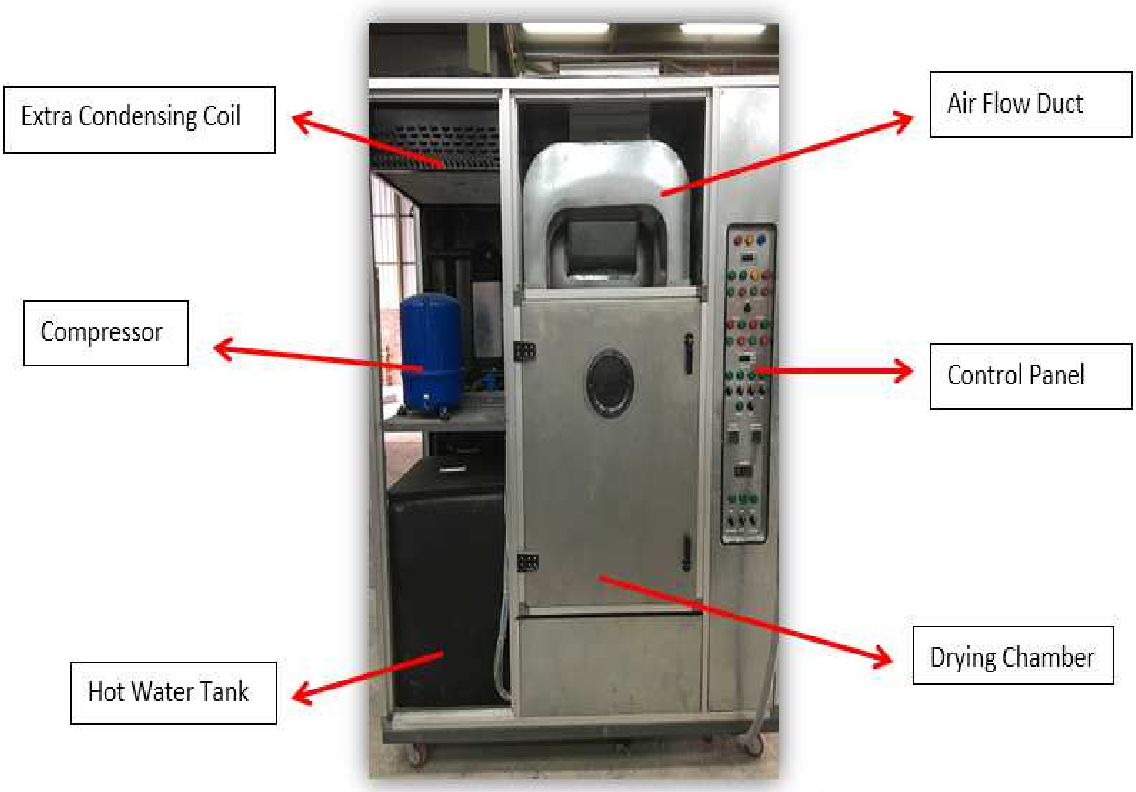

Figure 3-5: Front view of heat pump dryer

Figure 3-6 shows the layout of the control panel and electrical switch board. At the top section of the control panel was the heat pump system control section which controlling the compressor and circulation fan. A temperature controller was used to control the operation of the compressor based on the drying air temperature. Below the heat pump control section was the electric heater control section. The electric heaters can be switched to operate in auto mode or manual mode. A separate temperature controller was fitted to control the drying air temperature during auto mode. Below the heater control section was hot water system control. A PID controller was fitted to control the opening of the 3-way valve to regulate the water flow rate of the hot water in order to achieve the drying air temperature. At the bottom of the control panel was humidity control section. A humidity controller was inter-linked with the heat pump controller to control the operation of the compressor. When switched to humidity control mode, the humidity controller would override the temperature controller to switch on the compressor for dehumidification process.

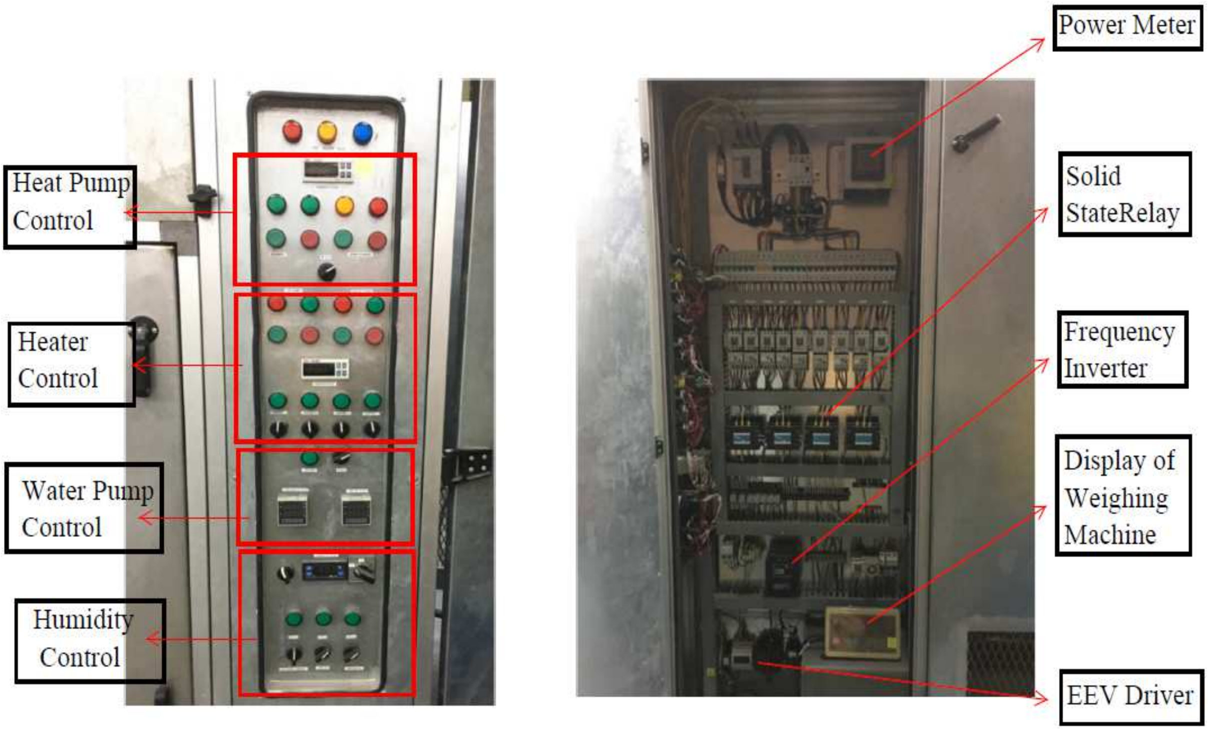

Figure 3-6: Control panel and electrical switch board

Figure 3-7 shows the internal of the drying chamber. The drying chamber was 802 mm (width) x 802 mm (depth) x 998mm (height). At the centre of the drying chamber, a metal rack was fitted to hold the drying trays. The metal rack was sitting on a weighting scale for real time weight measurement. Drying air was fed into the drying chamber from the left side of the chamber and passed through to the drying trays in parallel before discharged from the chamber through the return air grill at the right side of the chamber.

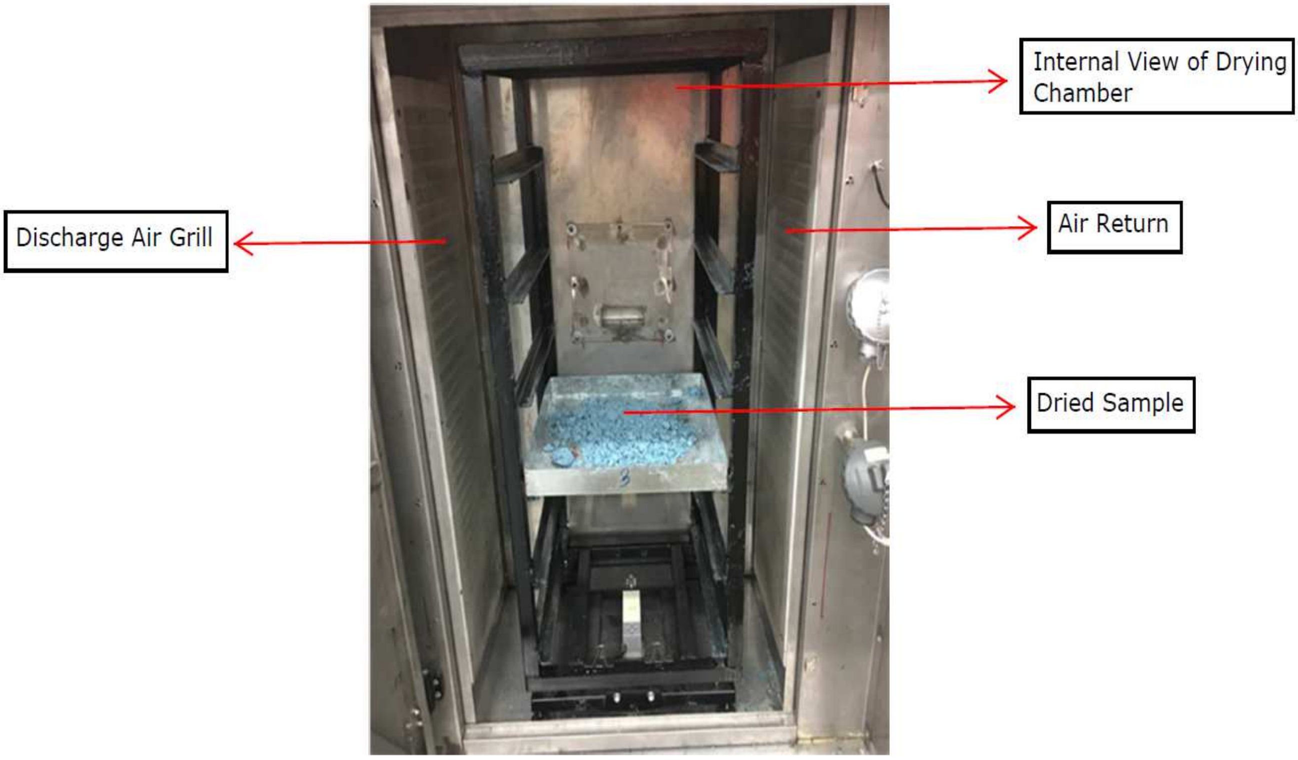

Figure 3-7: Internal view of the drying chamber

At the back of the drying chamber was the fan and heating compartments. Figure 3-8 shows the layout of the fan and heating components. Fan or blower was located at the top of the compartment, drawing air through the heating components. The drying air would pass through the hot water coil first, then the direct expansion coil (condenser) and finally the auxiliary electrical heaters. Depends on the operating mode, the drying air can be heated up by either one or combination of the heating elements.

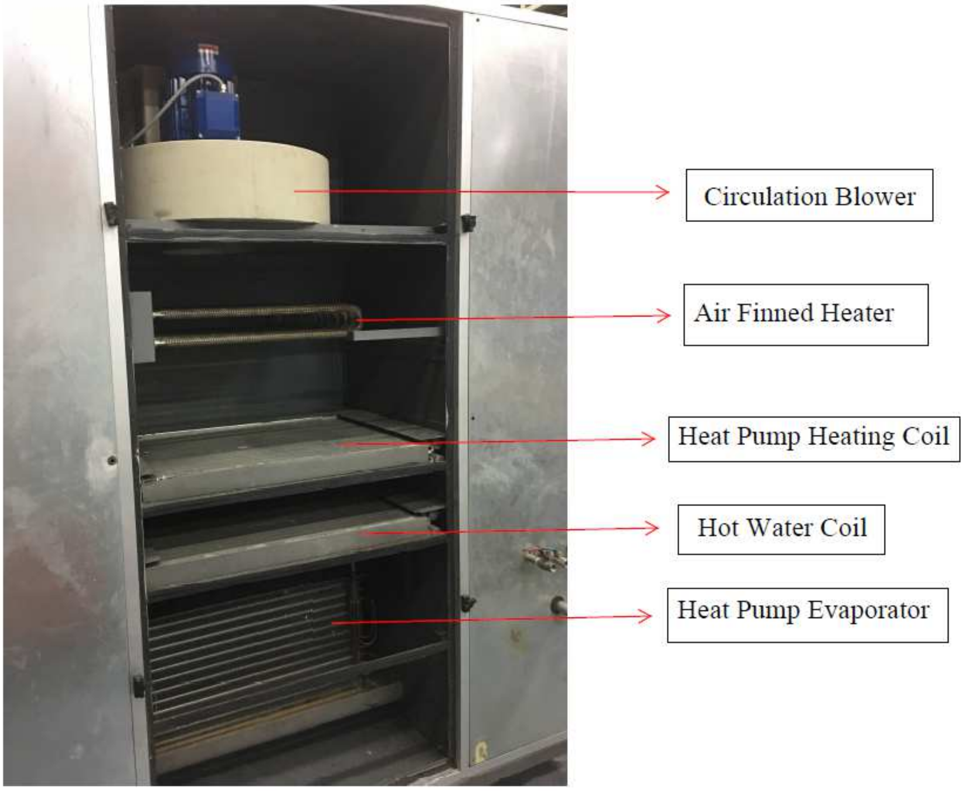

Figure 3-8: Fan and heating compartment

3.3 Control system of heat pump dryer

Control system of the prototype heat pump dryer was designed by considering the stability and safety of the dryer's operation. Upon activation of the heat pump system, the circulation fan would be activated first before other components kick in. This was to ensure proper air circulation inside the dryer so that the temperature and humidity sensors could give a more accurate reading from the airstream before the controllers could take any corrective actions. Activation of other components in the heat pump system would base on the measured process variables and set point of the controlled variables.

3.3.1 Temperature control

Each heating element corresponded to its dedicated temperature controller. For electric heating, the temperature was controlled by a temperature controller P+I control algorithm and regulated using 4-stages heaters where heating capacity for each stage was 4.5kW.

For hot water coil heating (see Figure 3-9), temperature of drying air was controlled by a PID controller and regulated using the hot water in coil (recovered heat from heat pump using the Plate HX). The required heating capacity could be adjusted by manipulating the hot water flow rate to the coil through a three-way valve. The moist laden drying air exhausted from the drying chamber was directed to an evaporator (dehumidifier-coil) and then was cooled below the dew point in order to condense the moisture from the air stream. Later, the cold air exited from the evaporator was heated up by a hot water heating coil. If the measured air temperature was below set point, then the three-way valve opening would be increased to allow higher flow rate to the heating coil. In contrary, if the measured air temperature was above set point, the three-way valve opening would be reduced to limit the hot water flow into the coil and at the same time bypass the hot water to a storage tank for thermal storage. On top of that, when dehumidification was not required while the water temperature in the hot water storage tank had achieved its set point, the heat pump system would be terminated. Thus, the hot water would not be generated further. During this time, if heating was still required, then hot water from the hot water storage tank would be directed to the heating coil.

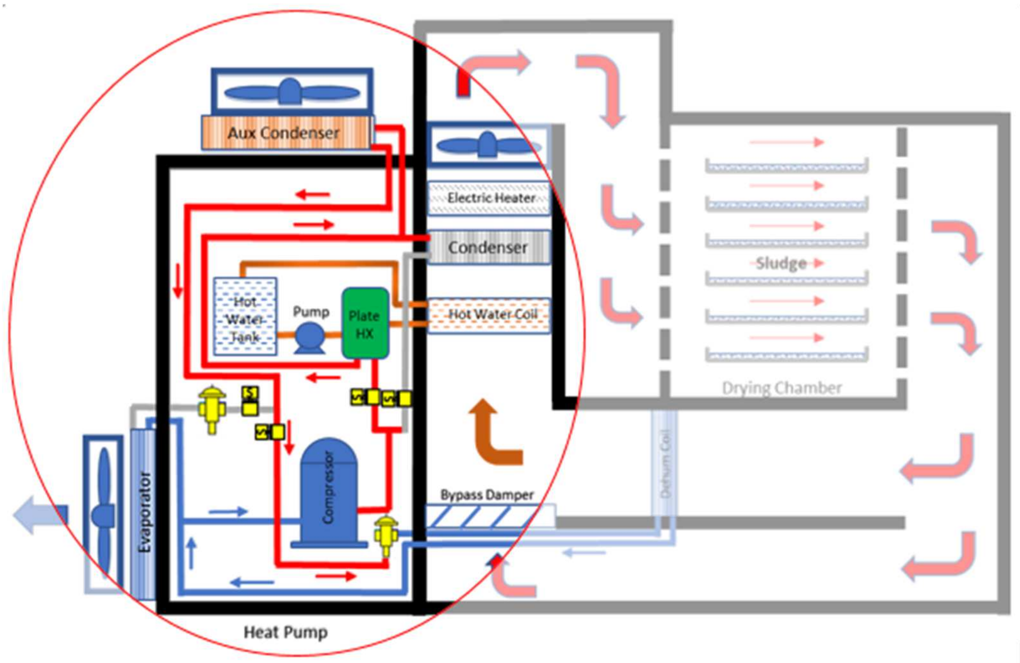

Figure 3-9 Hot water coil heating system in the HPD

For direct expansion heating (see Figure 3-10), condenser was used to directly heating the drying air instead of through the secondary medium (hot water coil). Direct air heating can achieve higher drying air temperature as compared to hot water heating. A temperature controller with P+I algorithm was used and the temperature could be regulated by switching on/off the compressor. When the drying air temperature was below set point, the compressor would be switched on for heating and vice versa. However, the temperature control would not be as precise as hot water heating due to the discrete on/off heating mode.

For in direct expansion heating without dehumidifier (see Figure 3-11), the drying air was only passed through condenser for heating. Liquid refrigerant was diverted to an external evaporator and the dehumidification coil was not operating and therefore the air was not undergoing cooling and dehumidification process. The air temperature was controlled by switch on/off the compressor. This setup was to mimic the conventional hot air drying (without dehumidifier) except that the heating source was from the heat pump and not electric heating. Due to the limitation of the heat pump system, drying experiments were done with drying temperature at or below 50°C.

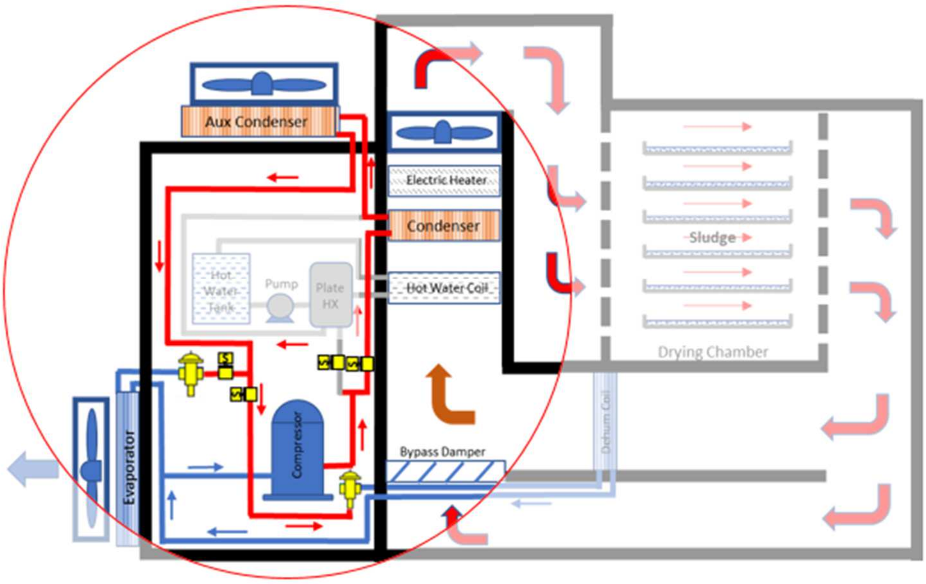

Figure 3-10 Direct expansion heating system in the HPD

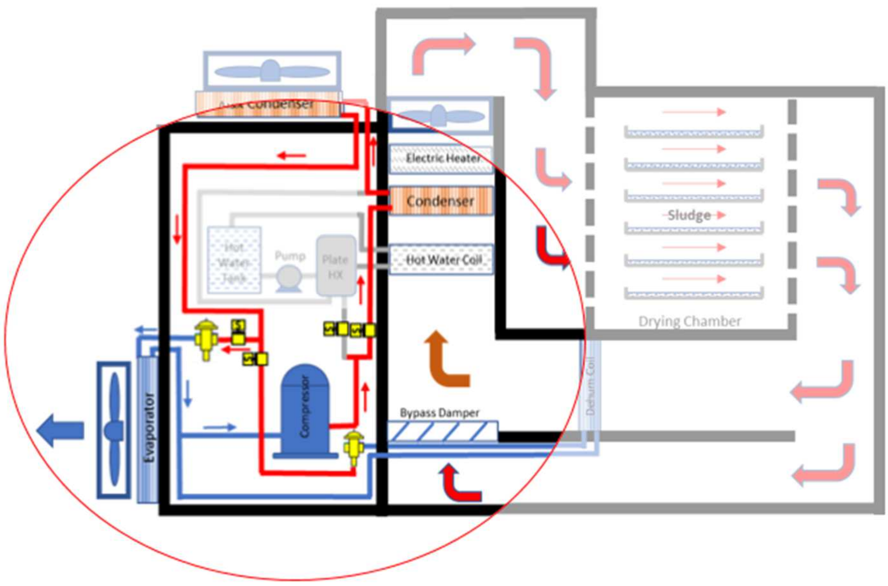

Figure 3-11 Schematic of heat pump drying in direct heating without dehumidifier

3.3.2 Humidity control

Humidity control was only available during heat pump operation. If the measured relative humidity in drying air was higher than humidity set point, the heat pump would be switched on to activate the dehumidification process. Evaporator in the heat pump system would act as a dehumidifier where moisture in the air would be condensed out at the cold surface of the evaporator. To achieve this, the surface temperature of the evaporator needed to be maintained below the dew point of drying air. Meanwhile the evaporating temperature of the evaporator could be manipulated through adjustment of air flow and suction superheat of the refrigeration system.

3.3.3 Air flow control

Drying trials were conducted with 3 different fan speeds: 30Hz, 50Hz and 60Hz to investigate the effect of air velocity on drying rate. Figure 3-12 shows the drying trays arrangement and dimension in the heat pump dryer. Basically, in the drying chamber, the air flow was passing through a stack of trays parallelly. The passages between trays were approximately 365mm x 95mm. Air flow was measured using a hot wire air flow meter and then the air velocity passing through the sample was calculated by dividing the air flow with the tray passage opening area.

Types of HPD configurations, namely the Closed Mode, Open Mode and Partially Open Mode, were evaluated by manipulating the bypass damper opening, where 0% bypass for fully-closed, 100% bypass for fully-open and 50% bypass for partially-open. Drying trails were conducted to investigate the effects of bypass air on dehumidification and drying rates. Both total air flow and bypass air flow were measured using the hot wire air flow meter.

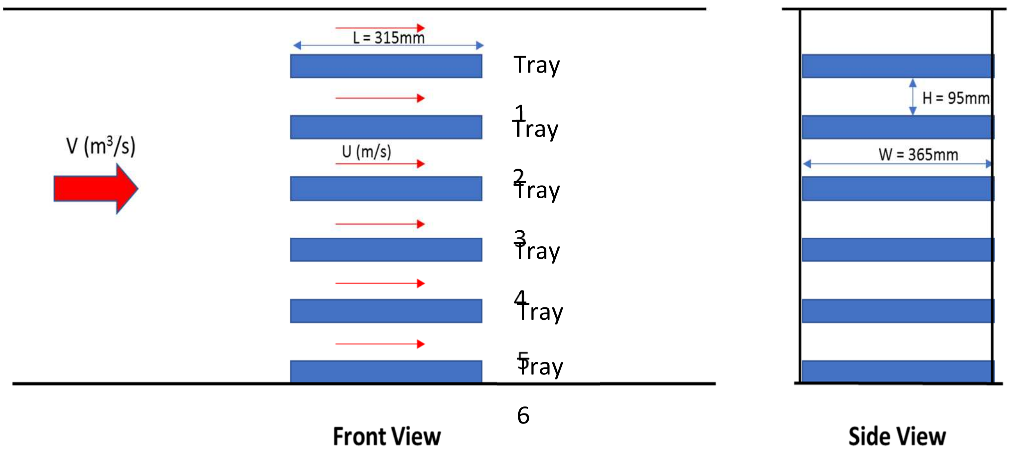

Figure 3-12 Drying trays arrangement and dimension in the heat pump dryer

Air flow dynamics in the drying chamber were further evaluated by developing a 3D modelling using Computational Fluid Dynamics (CFD) simulation. Figure 3-13 shows the computer-aided design (CAD) model and the mesh profile that were used in the simulation.

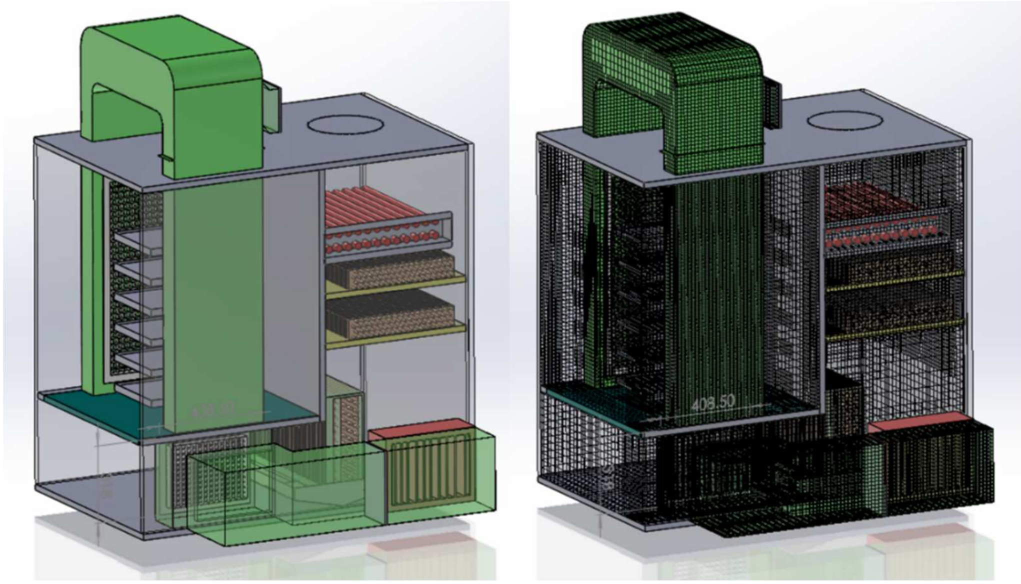

Figure 3-13 Heat pump dryer model and mesh profile

3.3.4 Process safety control

While the sensible and latent heats that absorbed by the evaporator could be fully recovered at the condenser for sensible heating, the heating capacity was always higher than required due to continuous heat input to the system through compressor work. Therefore, a heat rejecter was essential to reject this portion of extra heat out of the system. Otherwise, the heat energy would accumulate and build up in the system, subsequently cause system instability. Initially, this extra portion of heat would be stored in the hot water storage tank. When the storage tank limit was achieved, further heat input will cause the discharge pressure to increase. When the discharge pressure reaches the pre-set value, then a heat rejecter would be turned on to reject the extra heat out of the system. In contrary, if too much heat had been rejected from the system, the discharge pressure would drop. When the discharge pressure had dropped to a pre-set value, then the heat rejecter would be turned off.

Besides, various safety devices were installed at the heat pump dryer unit to ensure safe operation. Power supply to all electrical components were connected to Miniature Circuit Breakers (MCBs). On top of that, an Earth Leakage Circuit Breaker (ELCB) was fitted to protect the operators from current leakage and electric shock. All induction components such as compressor and motor were protected by means of over current protection devices. For refrigeration system, high-low pressure switches were fitted to protect the compressor and the system from abnormal operating pressure.

In addition, a power meter had been fitted to record the total power consumption of the dryer under different operating modes.

3.5 Heat pump sizing and capacity

Effects of heat pump sizing and capacity were investigated by using 2.0 HP and 0.5 HP compressors. Drying trials (HP50_0.5HP and HP50_2.0HP) were performed at 50°C using direct air heating mode only where the drying air medium was not passing through the dehumidifier. Table 3-1 shows the comparison between the 2 heat pump systems.

Table 3-1: Basic info of the heat pump systems

	HP50_0.5HP	HP50_2.0HP
Compressor size	0.5 HP	2.0 HP
Heating capacity	2.25 kW	6.30 kW
Cooling capacity	1.61 kW	4.34 kW
Evaporator air flow	233 m^3/h	880 m^3/h
Condenser air flow	800 m^3/h	1900 m^3/h

3.6 Drying experiments

Table 3-2 shows the overview of experiment trials that were conducted to evaluate the performance of the pilot-scale heat pump dryer and compare with the performance of conventional hot air dryer.

In order to perform conventional hot air drying, the heat pump system was switched off during the operation of the dryer unit. Temperature of the drying air was fully manipulated by the electric heaters. Hot air drying experiment were conducted at temperature 35°C, 50°C and 70°C. Meanwhile, effects of closed mode, open mode and partially open mode were evaluated using the dryer configurations as shown in Figure 3-1, Figure and Figure 3-3, respectively. During the drying process, all the critical parameters e.g. drying air temperature and humidity, sample weight, electric energy consumption and running hour were recorded for further data analysis.

Table 3-2: Overview of drying experiments

Item	Type of Experiment	Target	Comparison
1	Hot air drying 35°C @ 50Hz spee	Water Extraction from sample	Compare energy and drying kinetic if change of air temperature
		Energy Consumption	
2	Hot air drying 50°C @ 50Hz speed	Water Extraction from sample	
		Energy Consumption	
3	Hot air drying 70°C @ 50Hz spee	Water Extraction from sample	
		Energy Consumption	
4	Hot air drying 50°C @ 30Hz spee	Water Extraction from sample	Differences in energy consumption and drying rate with different air speed
		Energy Consumption	
5	Hot air drying 50°C @ 60Hz spee	Water Extraction from sample	
		Energy Consumption	
6	Heat Pump drying 35°C @ 50Hz s	Water Extraction from sample	Compare energy and drying kinetic if change of air temperature
		Energy Consumption	
7	Heat Pump drying 50°C @ 50Hz s	Water Extraction from sample	
		Energy Consumption	
8	Heat Pump drying 50°C @ 35Hz s	Water Extraction from sample	Check effects of air velocity on drying rate and energy consumption
		Energy Consumption	
9	Heat Pump drying 50°C @ 50Hz s	Water Extraction from sample	
		Energy Consumption	
10	Heat Pump drying 50°C @ 60Hz s	Water Extraction from sample	
		Energy Consumption	
11	Heat Pump drying 50°C @ 50Hz speed (Air Temperature Setting)	Water Extraction from sample	Compare energy and drying kinetic if change of control logic
		Energy Consumption	
12	Heat Pump drying 50°C @ 50Hz speed (Water Temperature Setting)	Water Extraction from sample	
		Energy Consumption	
13	Heat Pump drying 50°C @ 50Hz speed (Humidity Setting) with different bypass air volume	Water Extraction from sample	Compare energy consumption and drying rate under different air bypass flow rate
	i. 0 cfm	Energy consumption	
	ii. 500cfm		
	iii. 1000 cfm		
14	Heat Pump drying 50°C @ 50Hz speed (Heating Only Mode)	Water Extraction from sample	Compare energy consumption and drying rate under different operating mode
		Energy Consumption	
15	Heat Pump drying 50°C @ 50Hz speed (Dehumidification Mode)	Water Extraction from sample	
		Energy Consumption	

3.7 Drying procedures

The sludge sample was divided into batches of 10 kg. Each batch was dried under different drying mode and drying air condition for 7 hours (420 min). Inside the drying chamber, the sample was equally distributed to 6 stainless steel trays with each tray dimension 350mm x 350mm x 25 mm (width x length x height). Sample weight was recorded every 15 min. At the end of the drying experiment, total energy consumption was recorded and the total water removal was calculated. The drying efficiency was represented by specific moisture extraction rate (SMER) which was defined as follow,

$$\mathrm{SMER} = \frac{\text{Amount of water removed}}{\text{Total energy consumption}}\left(\frac{\mathrm{kg}}{\mathrm{kWh}}\right) \qquad [3.1]$$

3.8 Heavy metals and total organic carbon

Sludge samples were sent to Permulab BVAQ (Bureau Veritas and AsureQuality) laboratory (Selangor, Malaysia) for quantitative analysis of heavy metals and total organic carbon. Content of heavy metals, namely copper (Cu), nickel (Ni), chromium (Cr), iron (Fe), platinum (Pt), lead (Pb) and zinc (Zn), were determined according to method USEPA 6010B which mainly using inductively coupled plasma-atomic emission spectrometry. Meanwhile, amount of total organic carbon was determined according to method BS 1377-3:1990.

CHAPTER 4

RESULTS AND DISCUSSION

4.1 Hot air drying

Hot air drying experiments were conducted at temperature 35°C, 50°C and 70°C for purpose of comparison with heat pump drying. Effects of closed mode, open mode and partially open mode were evaluated as well.

4.1.1 Drying kinetic

Figure 4-1, Figure 4-2 and Figure 4-3 show the drying kinetics of sludge samples under the 3 types of hot air drying modes: closed mode, partial open mode and open mode, respectively, at different drying temperatures (35°C, 50°C and 70°C). However, hot air drying at temperature of 70°C was not performed for the open mode as the installed heater was undersize and not able to achieve the set temperature under the open mode condition. It was observed that all sludge samples conformed the typical drying kinetics, where the higher the drying temperature the higher drying kinetics (Putra and Ajiwiguna, 2017), regardless of type of drying mode. For closed mode, it appears that it took about 830 min to dry the sludge sample down to a moisture content of 2.00 kg/kg (dry basis) when drying was performed at 35°C. On the other hand, when drying were performed at 50°C and 70°C then it took much shorter time i.e., 440 min and 230 min, respectively, to achieve the same moisture content. By increasing temperature from 35°C to 50°C, the total drying time could be shortened by 47%. If further increasing the temperature to 70°C, the total drying time is 72% shorter as compared to that can be achieved at 35°C.

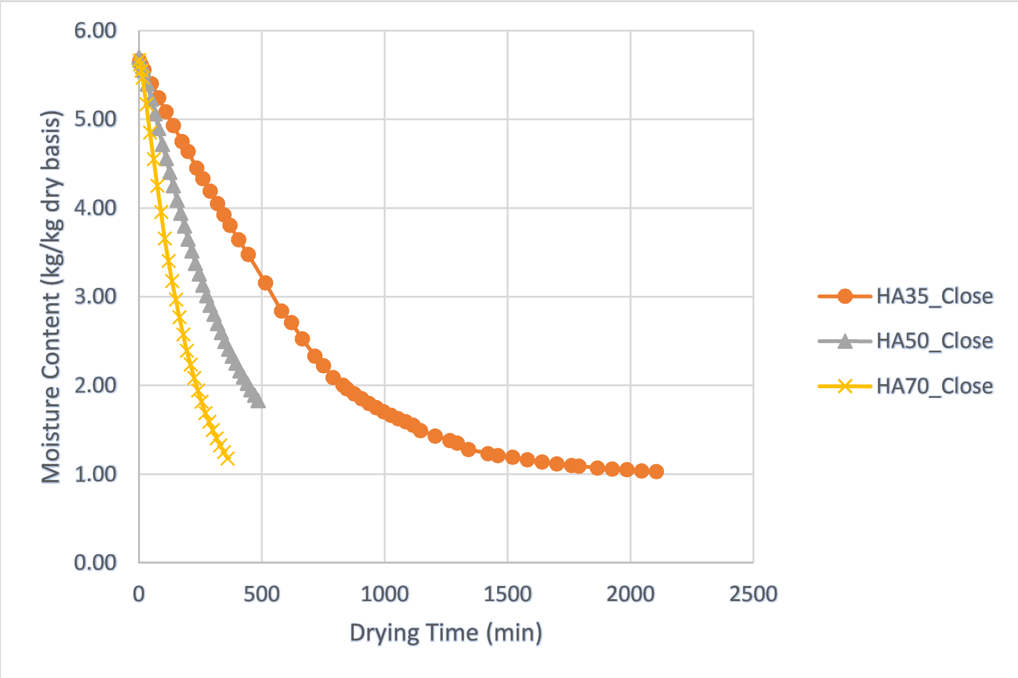

Figure 4-1 Drying kinetics of samples under hot air drying close mode at various temperatures

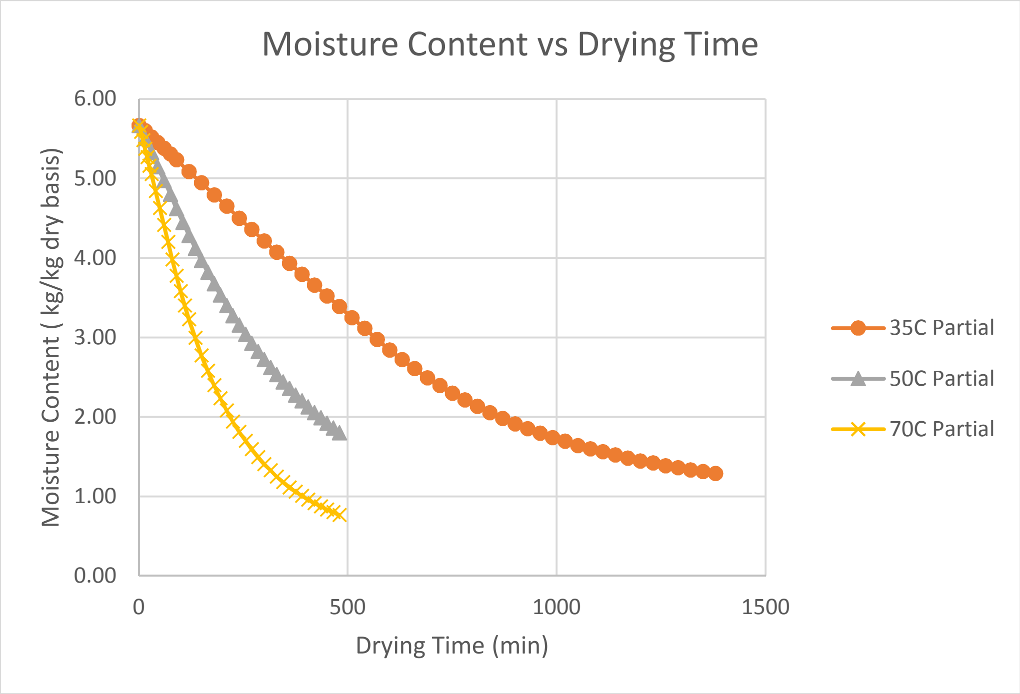

Figure 4-2 Drying kinetics of samples under hot air drying partial open mode at various temperatures

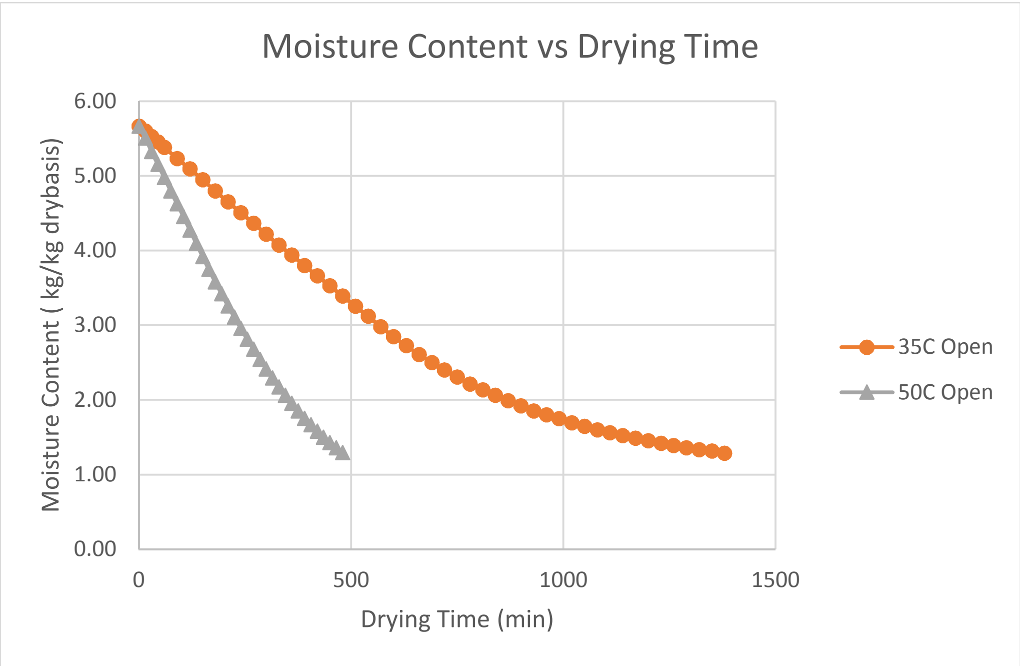

Figure 4-3 Drying kinetics of samples under hot air drying open mode at various temperatures

However, when drying was conducted at the 35°C, different drying modes did not have significant impact on the drying kinetic. Figure 4-4 shows that at 35°C drying temperature, all 3 curves of closed, partial open and open modes are superimposed to each other. This implies that the drying rates are the same for all the 3 drying modes at 35°C.

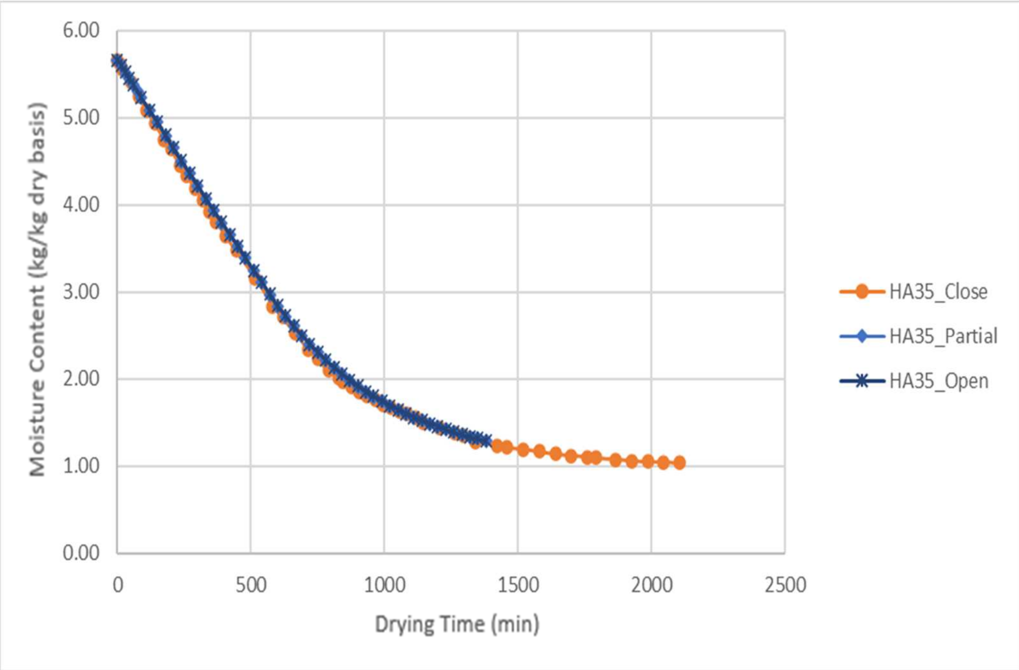

Figure 4-4 Drying kinetics of samples under hot air drying 35°C at various air ratios

However, at 50°C, the drying kinetic in closed mode is slightly slower than those in partial open and open modes. Figure 4-5 shows that at early stage, the moisture reduction under closed mode is slower as compared to partial open and open modes, whilst the drying curves of partial open and open modes are identical. This could be due to the high relative humidity in the drying chamber when undergoing closed mode drying, where the drying air has picked up moisture that being released from the drying sample and kept recirculating in the drying chamber. Due to the accumulated moisture and high relative humidity, the drying performance under closed mode is thus reduced. Meanwhile, in open and partial open modes, the moisture laden drying air is being exhausted or partially exhausted from the drying chamber during the drying. Therefore, the drying performance is not much affected as the relative humidity is always maintained at a lower level as compared to that in closed mode.

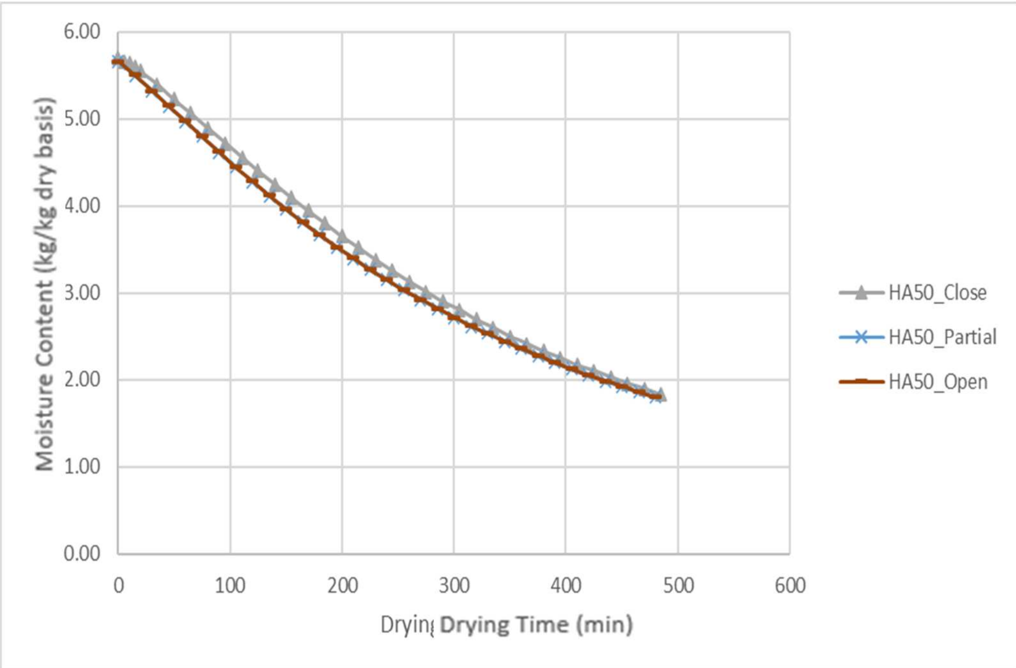

Figure 4-5 Drying kinetics of samples under hot air drying50°C at various air ratios

Figure 4-6 shows the drying rate curves of the sludge samples. It can be observed that all the samples showed 3 archetypical drying periods which consist of initial transient period, constant rate period and falling rate period. Apparently, constant rate period of hot air drying at 35°C (HA35_Close, HA35_Partial and HA35_Open) is much longer as compared to 50°C (HA50_Close, HA50_Partial and HA50_Open) and 70°C (HA70_Close and HA70_Partial). This indicates that a longer time is needed to remove the surface moisture when drying is conducted at 35°C. On the other hand, it can be postulated that the drying kinetics of drying samples at 50°C and 70°C are mainly governed by internal moisture migration where a distinctive single falling rate period can be observed at moisture content of 4.5 and 4.0 kg/kg dry basis, respectively. It was determined that the falling rate period is relatively long and take up about 64-83% of the total drying time.

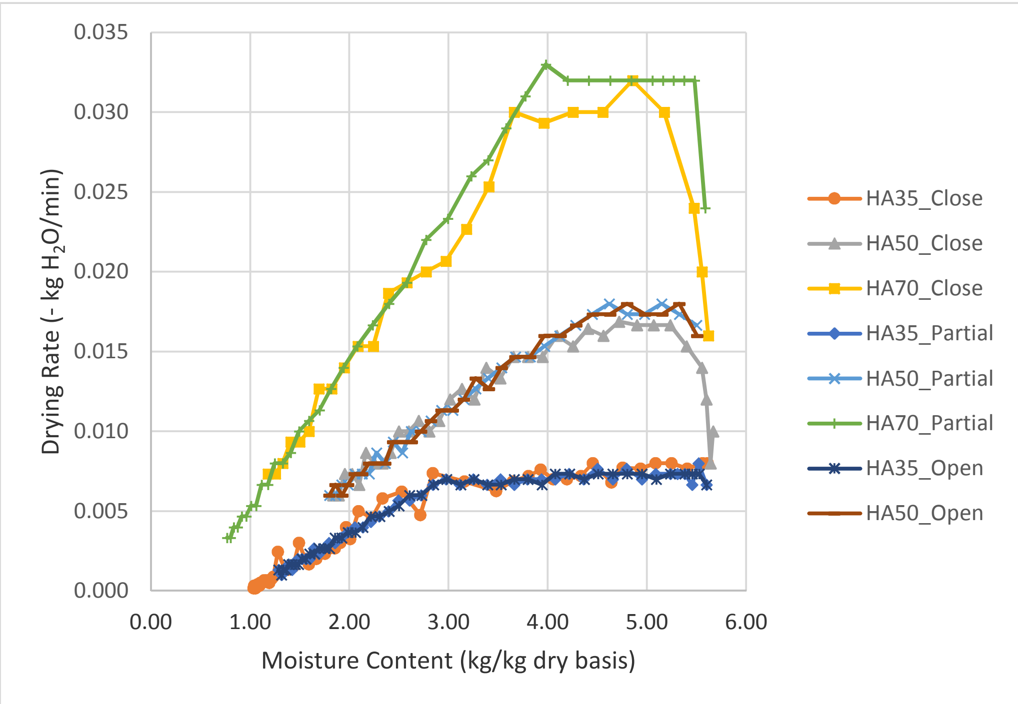

Figure 4-6 Drying rate of samples under hot air drying at various temperatures and air ratios

Generally, the drying rate is increasing with drying temperature. According to thermodynamics principle, the heat transfer between the drying air and moisture at sample's surface is very much dependent on the exposing surface area as well as the dry bulb temperature and wet bulb temperature of drying air (Fudholi *et al.*, 2011). Thus, when the air velocity and sample surface area are kept to the same, then the drying rate is directly proportional to the drying air wet bulb depression (Leniger et al, 2012). Whereby the wet bulb depression can be increased by either increasing the dry bulb temperature or reducing the humidity. However, in the present study, there was no further dehumidification stage in all 3 types of hot air drying mode as hot air dryer does not have dehumidification function, and hence the high drying rate was solely attributed by the high dry bulb temperature. As opposed to a heat pump dryer which doing heating and dehumidification simultaneously.

4.1.2 Energy performance

Figure 4-7, Figure 4-8 and Figure 4-9 show the accumulated energy consumption that required to dry the sludge sample to various moisture content at temperature of 35°C, 50°C and 70°C under closed mode, partial open mode and open mode, respectively. In order to dry the sample to moisture content of 2.00 kg/kg (dry basis), HA50_Open has recorded the highest energy consumption at 97 kWh, while HA35_Close has recorded the lowest energy consumption at 13 kWh, which is only about 13.5% of that in HA50_Open. It appears that in each drying mode, higher drying temperature would cause higher energy consumption. This is because extra energy is needed to elevate the temperature of the drying air to achieve the set temperature and to maintain the set temperature throughout the drying process. Also, when air temperature is higher, more heat lost to the ambient through conduction due to higher differential temperature.

However, it was observed that there were instances where lower drying temperature could cause higher energy consumption, particularly when trying to achieve a final moisture content that lower than 2.00 kg/kg (dry basis). It can be seen from Figure 4-7 and Figure 4-9 that HA35_Close and HA35_Open recorded higher energy consumption as compared to HA70_Close and HA50_Open, respectively. This could be due to the longer drying time took during the last stage of drying period (e.g. slower thermal conduction and internal moisture migration) when drying at a lower temperature.

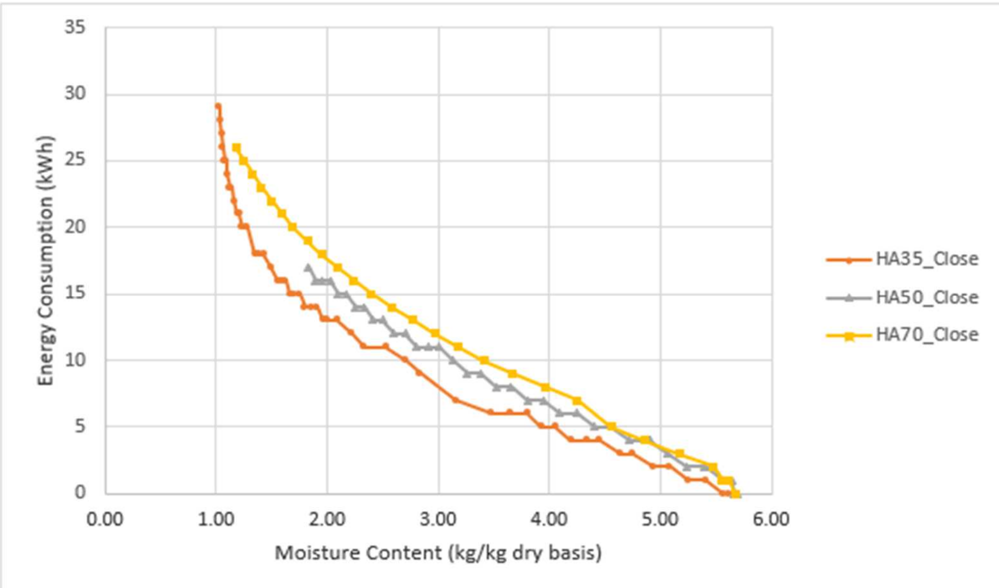

Figure 4-7 Energy consumption during hot air drying close mode at various temperatures

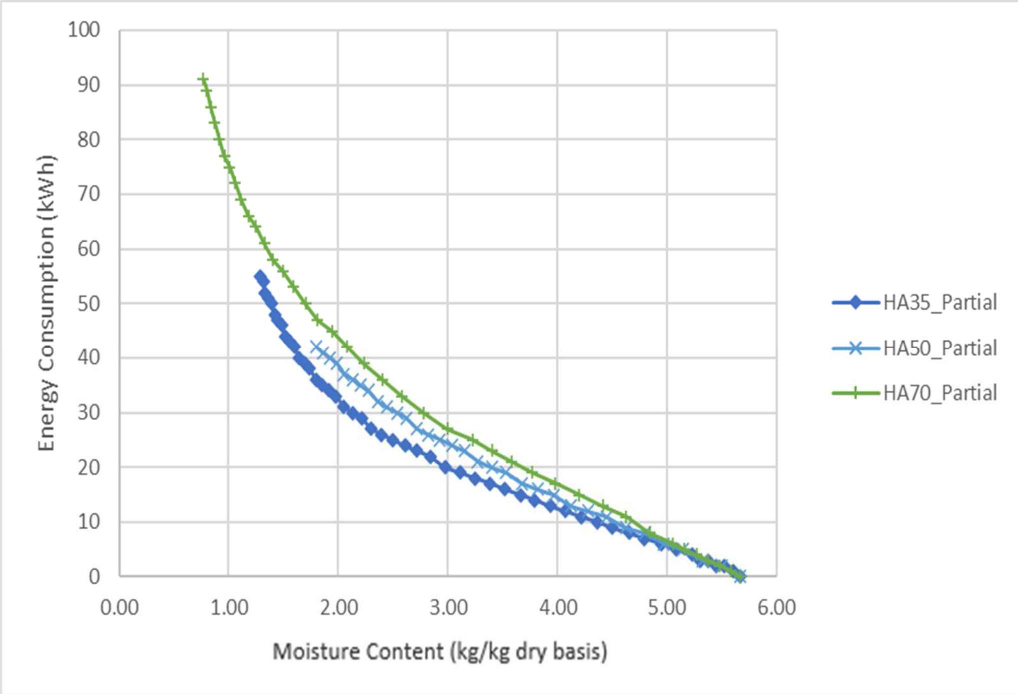

Figure 4-8 Energy consumption during partial hot air drying open mode at various temperatures

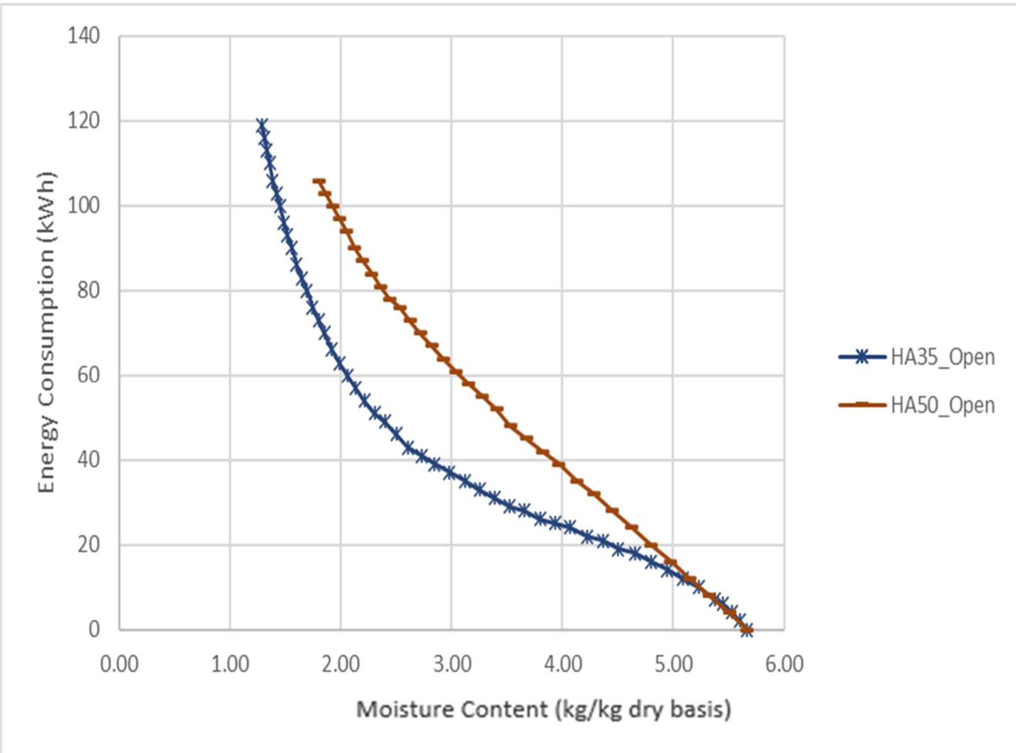

Figure 4-9 Energy consumption during hot air drying open mode at various temperatures

Figure 4-10 and Figure 4-11 show the comparison of energy consumption among the drying modes at 35°C and 50°C, respectively. It can be observed that open mode always consumes higher energy as compared to partial mode and closed mode. This is because in the open mode, a large amount of energy is used to heat up the incoming fresh air but only a small portion of the heat input is absorbed by the sludge sample to vaporise the moisture in it. Then the remaining unused portion of the heat input is being exhausted from the dryer and thus causing energy wastage. In contrary, for partial mode and closed mode, the unused heat input is recirculated back to the drying chamber for the continuous drying process. Thus, the heat input that required for these 2 modes is much lesser when compared to those in open mode. Comparatively, closed mode recirculates more drying air than partial mode, hence recovers more energy than partial mode. For instance, HA35_Partial has recorded lower energy consumption compared to its open mode because during the drying period, there are times where the recycled drying air is already at 35°C or slightly higher. When this happen, additional heat input is not required. Similar phenomenon also can be observed in the closed mode. It is just that a little extra energy is needed to raise the air temperature to higher temperature, likewise for the dried sample's surface temperature. Similar observation has been reported by Hanif et al. (2017) when drying wheat with desiccant grain dryer. The author found that desiccant grain dryer is more energy efficient as the heat that required to pre-heat the wheat is very minimal.

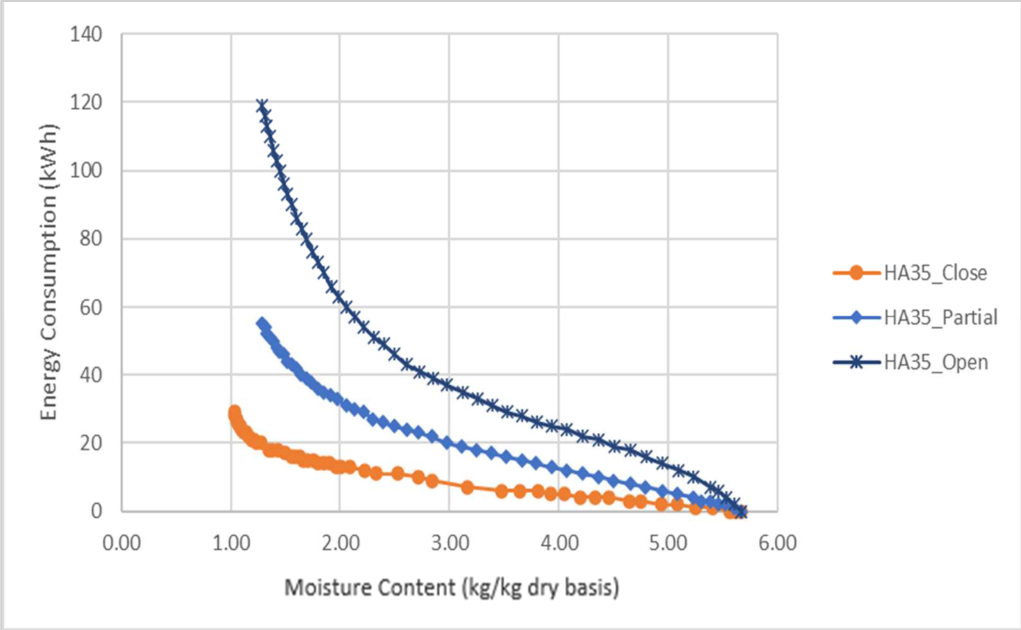

Figure 4-10 Energy consumption during hot air drying 35°C at various air ratios

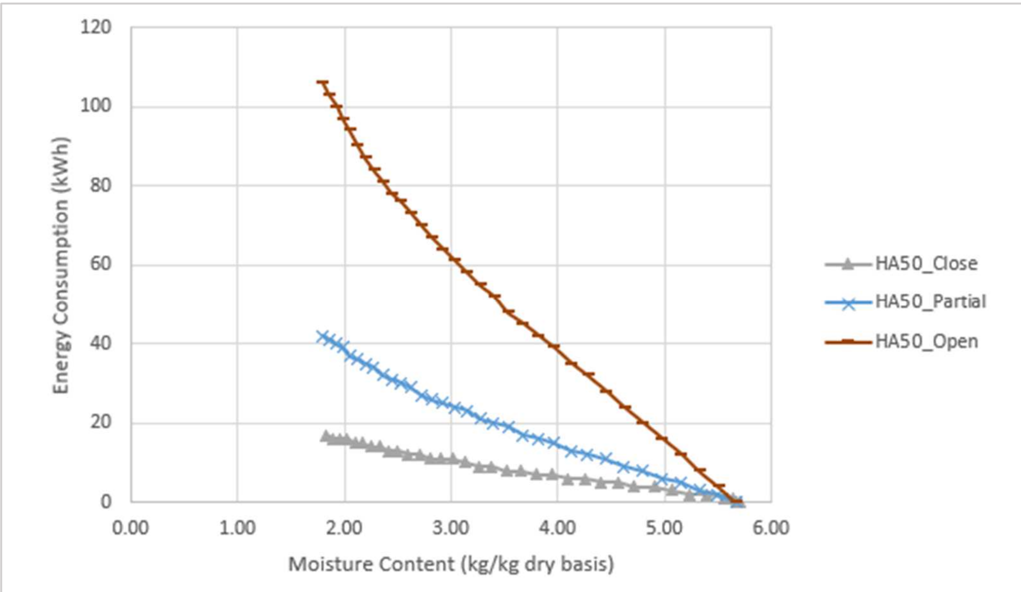

Figure 4-11 Energy consumption during hot air drying 50°C at various air ratios

Figure 4-12 shows the SMER of various hot air drying modes. In term of SMER, HA35_Close recorded the highest value at about 0.5 kg/kWh while

HA50_Open recorded the lowest value at about 0.06 kg/kWh. Generally, closed mode recorded the highest SMER while open mode recorded the lowest SMER. By considering the same drying mode, the SMER is decreasing with increasing temperature. Initially, the SMER is low as energy input is used to raise the drying air temperature and the drying rate is low before the drying air is raised to the desired temperature. Maximum SMER is achieved when the moisture content of sample weight was reduced to about 3.5 kg/kg dry basis. After that the SMER started to drop as drying is more difficult when surface water has been dried up. Lesser energy was consumed by the hot air dryer when a lower temperature was used, thus higher SMER was observed. Though lower drying temperature consume lesser energy, longer drying time is required as compared to higher drying air temperature. Yousaf et al. (2019) had observed the similar result when they investigated the drying efficiency of open loop and closed loop dryers. They found that SMER and MER for closed loop system was higher than the open loop system due to significant amount of fresh air into the system during each cycle.

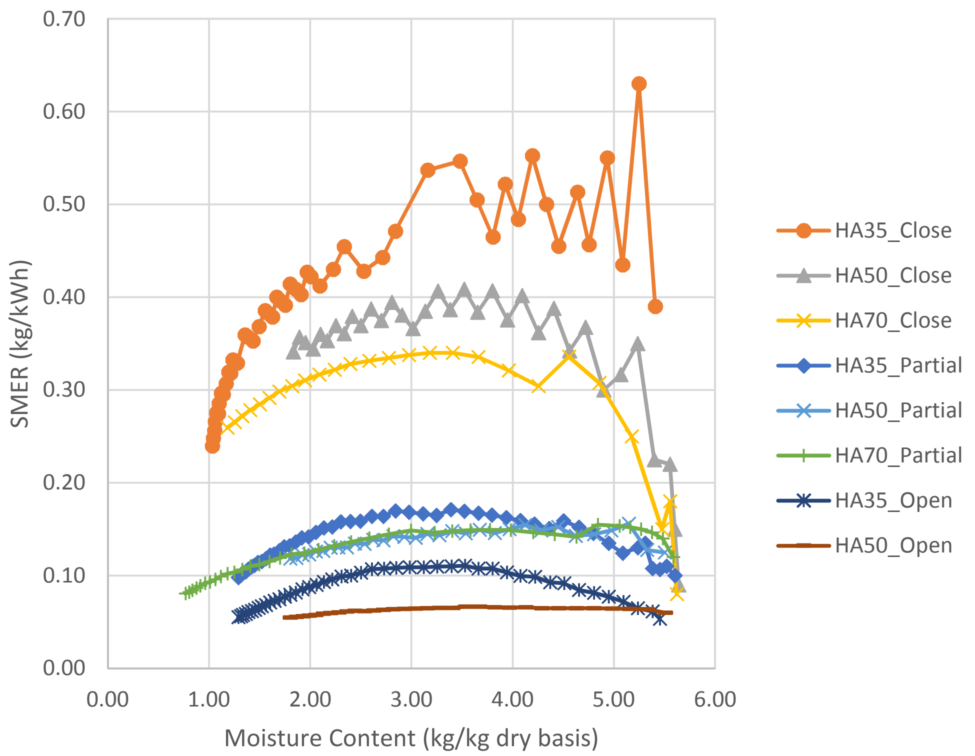

Figure 4-12 SMER of hot air drying at different temperatures and air ratios

*4.1.3 Effect*ive moisture diffusivity

Figure 4-13, Figure 4-14, Figure 4-15 and Figure 4-16 show the effect of drying temperature on the linear relationship between logarithmic moisture ratio and drying time. All the linear regression equations, correlation coefficients (R^2), slopes magnitudes, interception values and effective moisture diffusivity (*Deff*) are determined and listed in Table 4-1. The data reveals that the slopes of the logarithmic moisture content graphs are similar when drying are conducted under the same drying temperature regardless of the type of drying modes (Figure 4-16). For instance, at 35°C, the slopes for closed-, partial- and open-modes hot air drying are determined as 0.0012 min^{-1}. At 50°C, the slopes of the logarithmic moisture content graphs are with same value at around 0.0024 min^{-}

[1]. While at 70°C, the slopes of the linear graph are ranging around 0.0044 min^{-1} to 0.0045 min^{-1}. Based on the calculation, effective moisture diffusivities for all sludge drying experiments are ranging from 5.0661 x 10^{-9} m^2/s to 1.8998 x 10^{-8} m^2/s. This result shows that increasing drying temperature would increase the effective moisture diffusivity. Higher drying temperature has higher thermal energy and thus increasing the water molecules activity resulting in higher moisture diffusivity (Shi et al, 2008).

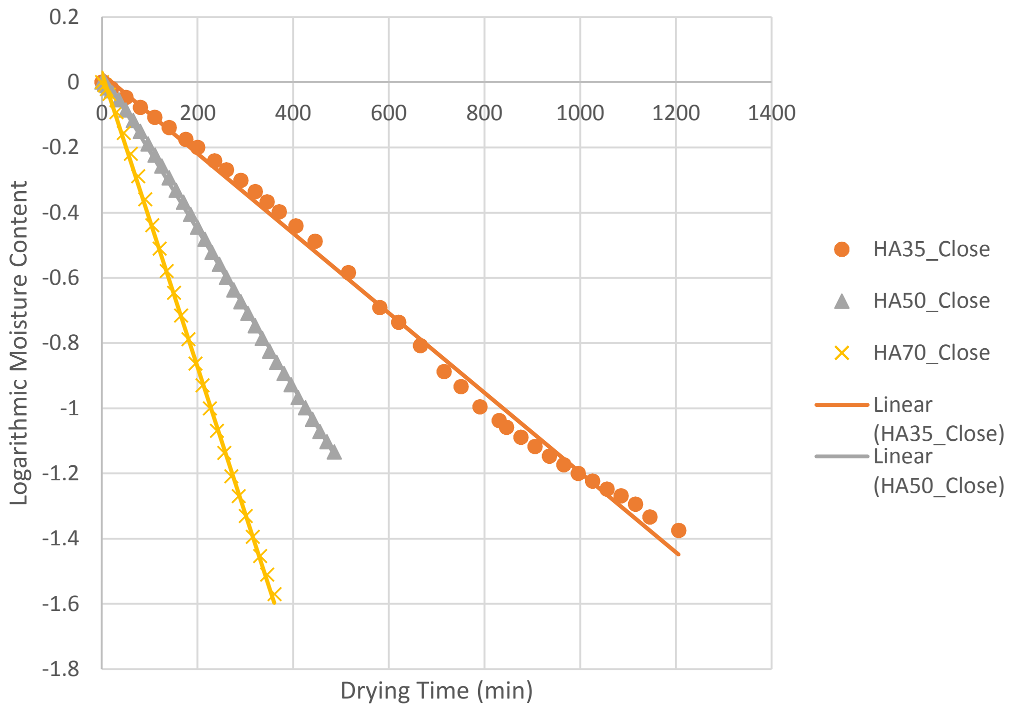

Figure 4-13 Logarithmic moisture content of samples under hot air drying close mode

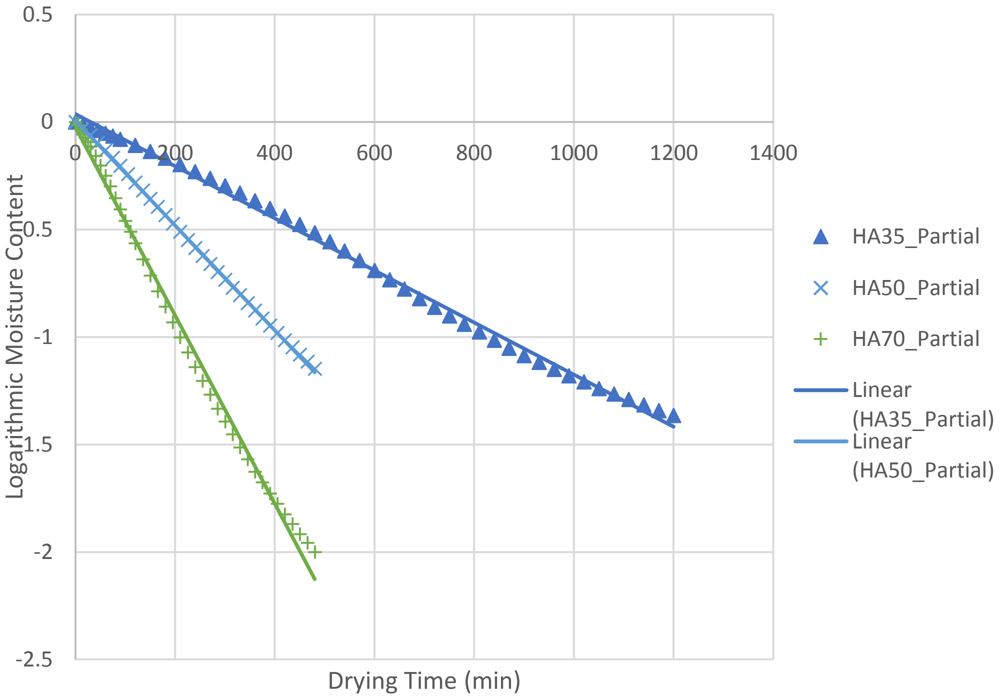

Figure 4-14 Logarithmic moisture content of samples under hot air drying partial mode

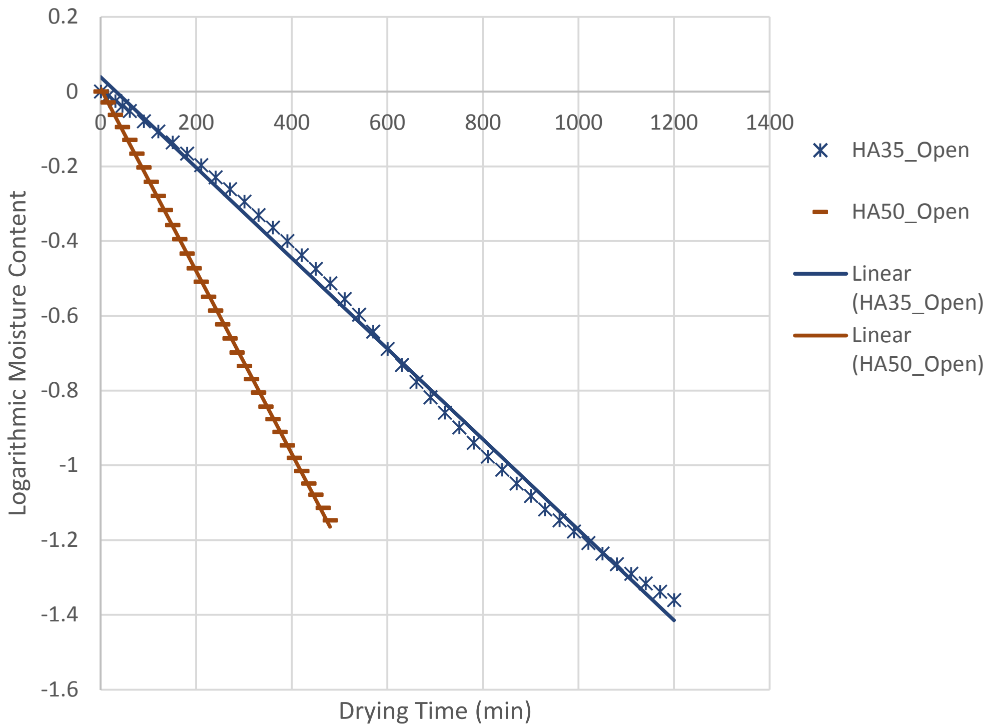

Figure 4-15 Logarithmic moisture content of samples under hot air drying open mode

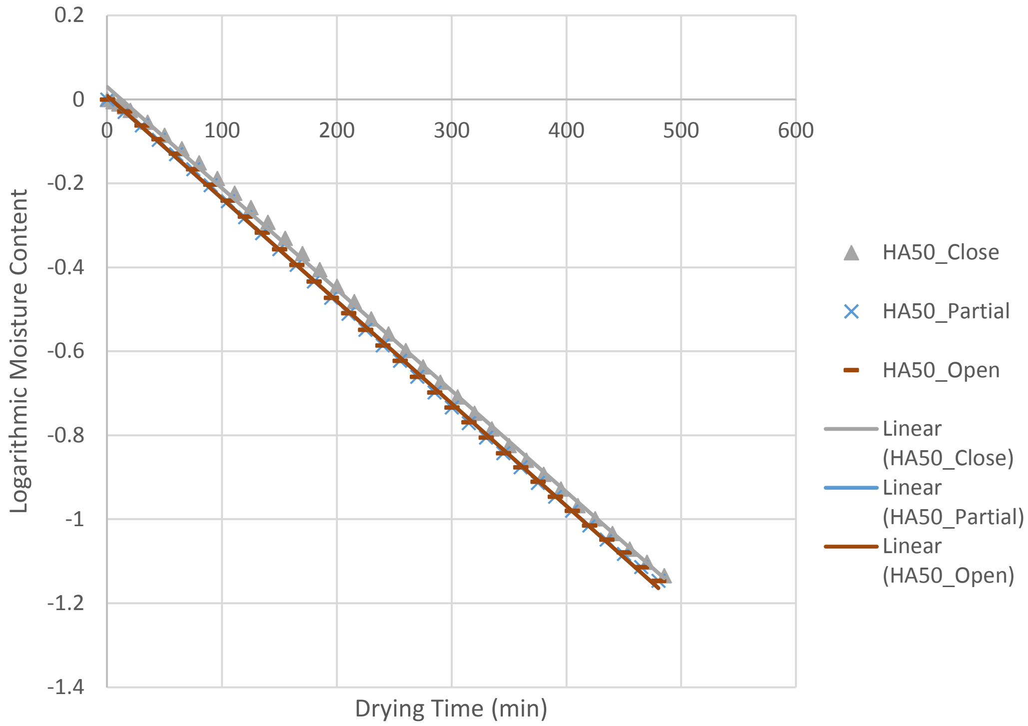

Figure 4-16: Logarithmic moisture content of samples during hot air drying at various air ratios

Table 4-1 Effective moisture diffusivity at various hot air drying mode

Condition	Linear Formula	R^2	Intercept value	Slope	Diffusivity (*Deff*) m^2/s
HA35_Close	y = -0.0012x + 0.0259	0.9955	0.0259	-0.0012	5.06606×10^{-9}
HA50_Close	y = -0.0024x + 0.0298	0.9992	0.0298	-0.0024	1.01321×10^{-8}
HA70_Close	y = -0.0045x + 0.0298	0.9992	0.0298	-0.0045	1.89977×10^{-8}
HA35_Partial	y = -0.0012x + 0.0375	0.9967	0.0375	-0.0012	5.06606×10^{-9}
HA50_Partial	y = -0.0024x + 0.0074	0.9996	0.0074	-0.0024	1.01321×10^{-8}
HA70_Partial	y = -0.0044x - 0.0277	0.9947	-0.0277	-0.0044	1.85756×10^{-8}
HA35_Open	y = -0.0012x + 0.0389	0.9966	0.0389	-0.0012	5.06606×10^{-9}
HA50_Open	y = -0.0024x + 0.0081	0.9995	0.0081	-0.0024	1.01321×10^{-8}

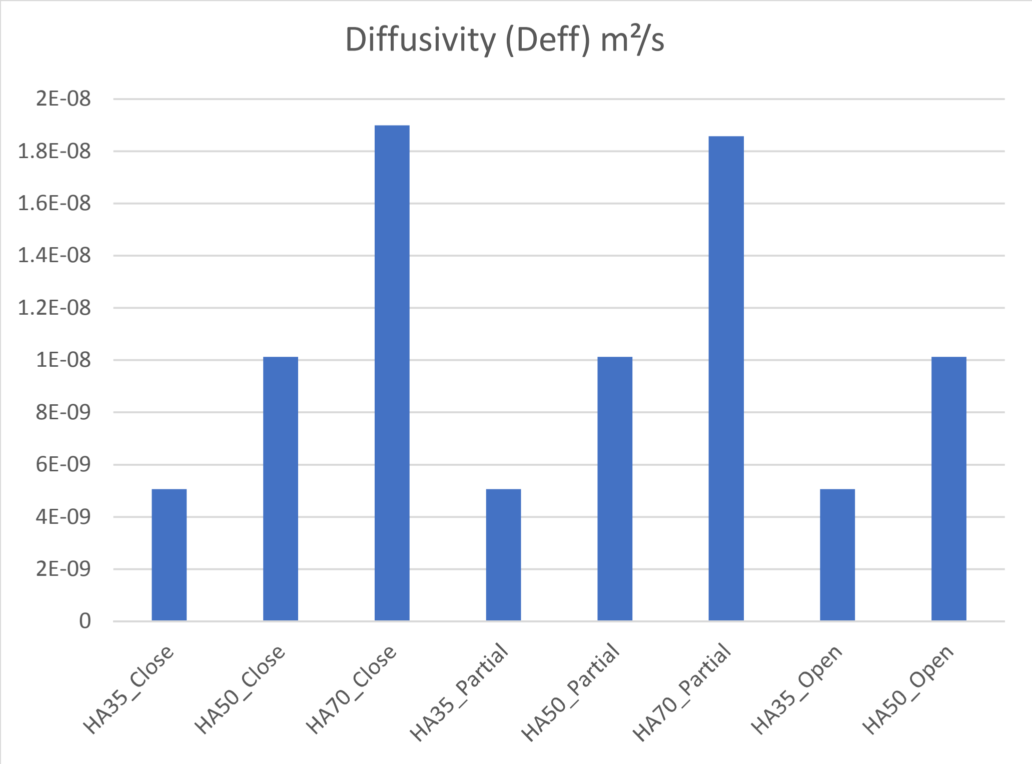

Figure 4-17 : Diffusivity of hot air drying at various air temperature and type of opening

4.2 Heat pump drying

Followings are the experimental results from heat pump drying trials.

4.2.1 Drying kinetic

Figure 4-18 shows the drying kinetics under the heat pump drying in closed mode at temperature of 35°C (HP35) and 50°C (HP50), together with drying kinetics of sludge samples under hot air drying in closed mode at temperature of 35°C (HA35) and 50°C (HA50). It was observed that dehumidified air that produced by the heat pump dryer would further promote the mass transfer efficiency. This can be verified by comparing the drying curves of hot air drying (HA35C and HA50C) and heat pump drying (HP35C and HP50C) at the same drying temperature. Moisture reduction rates of heat pump drying were always higher than the hot air drying at the same corresponding drying temperature. In line with findings reported by Yu et al. (2012) where at similar drying temperature, heat pump dryer would have higher drying rate as compared to hot air dryer. This mainly because the heat pump system could dehumidify the circulated drying air and reduce the wet bulb temperature, thus further increase the wet bulb depression.

Figure 4-19 shows the relative humidity of the drying air in both heat pump drying and hot air drying. Due to the dehumidification capability of heat pump dryer, the humidity of the drying air in heat pump dryer is always lower than the humidity of drying air in hot air dryer. In HP35, the relative humidity can even go as low as what it can be achieved in HA50. Therefore, at the same drying air temperature, heat pump dryer can have larger wet bulb depression as compared to hot air dryer. Table 4-2 shows the calculated wet bulb (WB) depression and drying rate of the corresponding drying air condition. Apparently, the results show that the drying rate increase with WB depression and the increment is almost proportional. Therefore, it can be concluded that the drying rate is largely governed by WB depression instead of temperature alone.

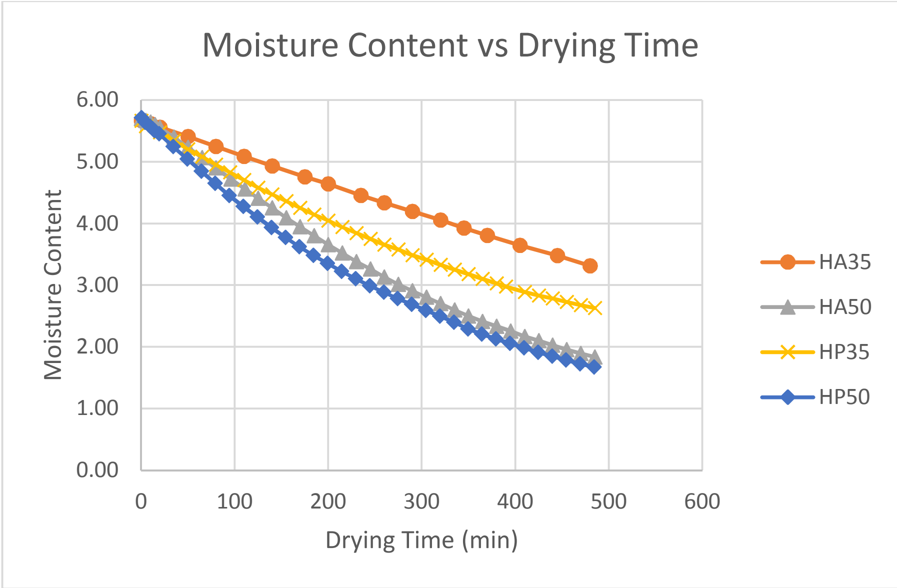

Figure 4-18 Drying kinetics of samples during heat pump drying and hot air drying

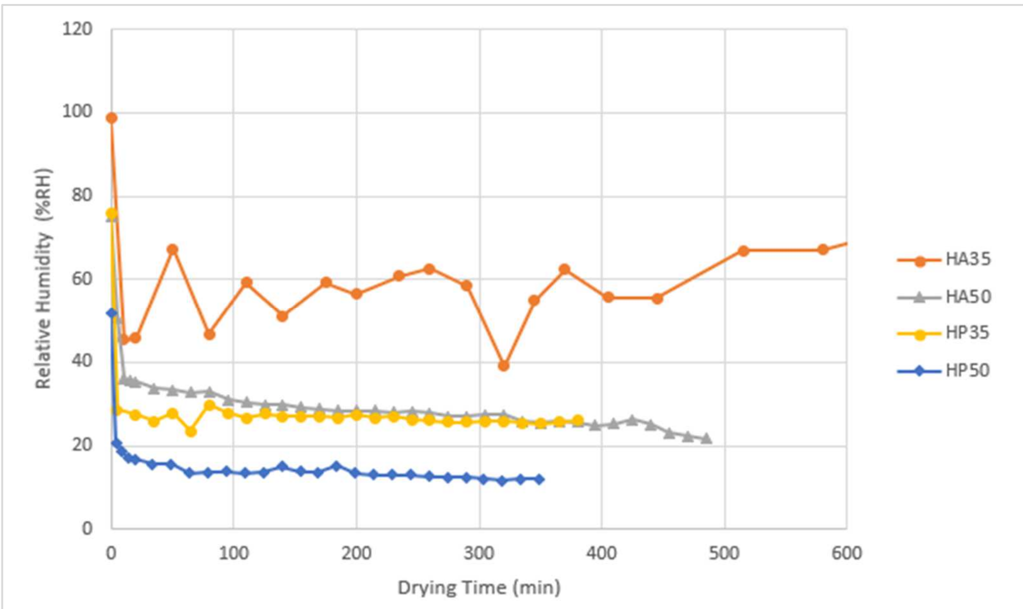

Figure 4-19 Relative humidity of drying air during heat pump drying and hot air drying

Table 4-2 Drying air properties in heat pump drying and hot air drying

	DB Temp (°C)	WB Temp (°C)	WB Depression (°C)	Drying Rate (-kg/min)
HA50	50±1.5	32.4±1.5	17.6±1.5	0.0167±0.0005
HP50	50±1.5	25.8±1.5	24.2±1.5	0.0200±0.0005
HA35	35±1.5	26.6±1.5	8.4±1.5	0.0078±0.0005
HP35	35±1.5	20.8±1.5	14.2±1.5	0.0133±0.0005

However, there will be a limitation in the heat pump system where the wet bulb temperature could not be further reduced when the dew point of drying air approaching evaporator surface temperature. At this point, relative humidity of drying air in the heat pump system would achieve its equilibrium state where the dehumidification rate (moisture extraction rate by the evaporator) is equal to the humidification rate (moisture evaporation rate or drying rate from sample). Principally, in order to maintain the low relative humidity and wet bulb temperature, compressor in the heat pump system would run continuously. Unlike a hot air dryer, where the infiltration in drying process would increase the heating load but reduce the latent load, the infiltration in drying process of a heat pump dryer would increase both the heating and latent load because the recycled drying air contains less moisture content as compared to the fresh ambient air. Hence, when there is significant amount of moisture vaporization from sample and infiltration of fresh air, a heat pump dryer would consume more energy than a hot air dryer. This is because the compressor in the heat pump system needs to be in operation continuously to bring down the relative humidity.

4.2.2 Effective moisture diffusivity

Figure 4-20 shows the effect of drying temperature on the linear relationship between logarithmic moisture ratio and drying time of the sludge sample in heat pump and hot air drying. The linear regression equations, correlation coefficient (R^2), slopes magnitude, interception values and effective moisture diffusivity (*Deff*) were determined and listed in Table 4-3.

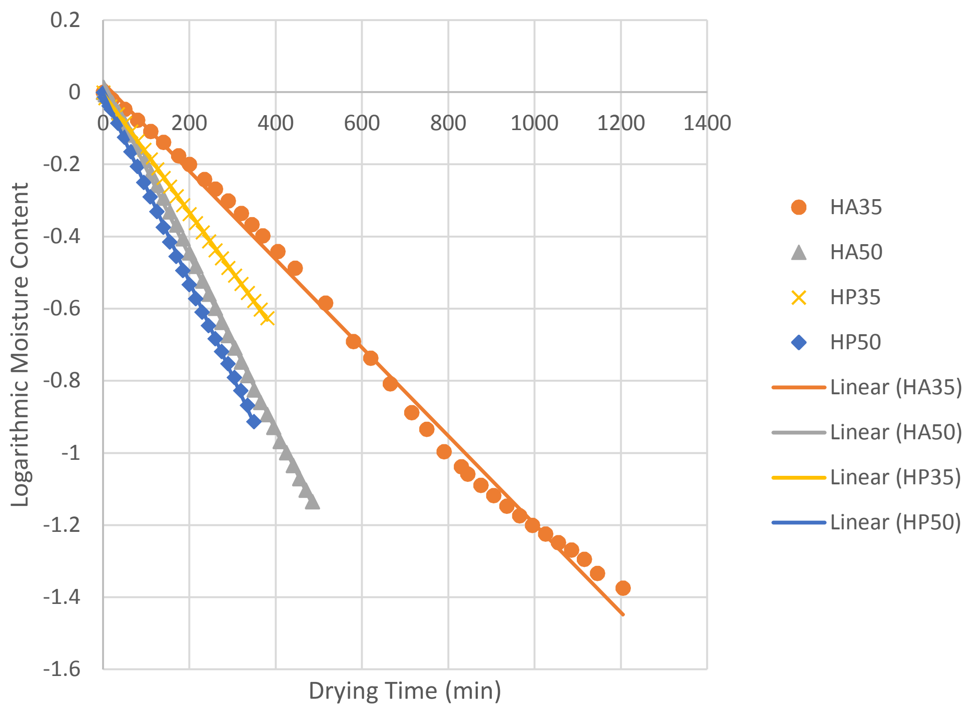

Figure 4-20 Logarithmic moisture content of samples in heat pump drying and hot air drying

Table 4-3 Effective moisture diffusivity at heat pump and hot air drying

Sample	Linear Formula	R^2	Intercept value	Slope	Diffusivity (*Deff*) m²/s
HA35	y=-0.0012x+0.0259	0.9955	0.0259	-0.0012	5.06606×10^{-9}
HA50	y=-0.0024x+0.0298	0.9992	0.0298	-0.0024	1.01321×10^{-8}
HP35	y=-0.0017x-0.0039	0.9997	-0.0039	-0.0017	7.17692×10^{-9}
HP50	y=-0.0026x-0.0024	0.9995	-0.0024	-0.0026	1.09765×10^{-8}

4.2.3 Effect of relative humidity control on energy performance

Figure 4-21 shows the energy consumption of heat pump dryer and hot air dryer. It could be observed that the curves for HP50 and HP35 were

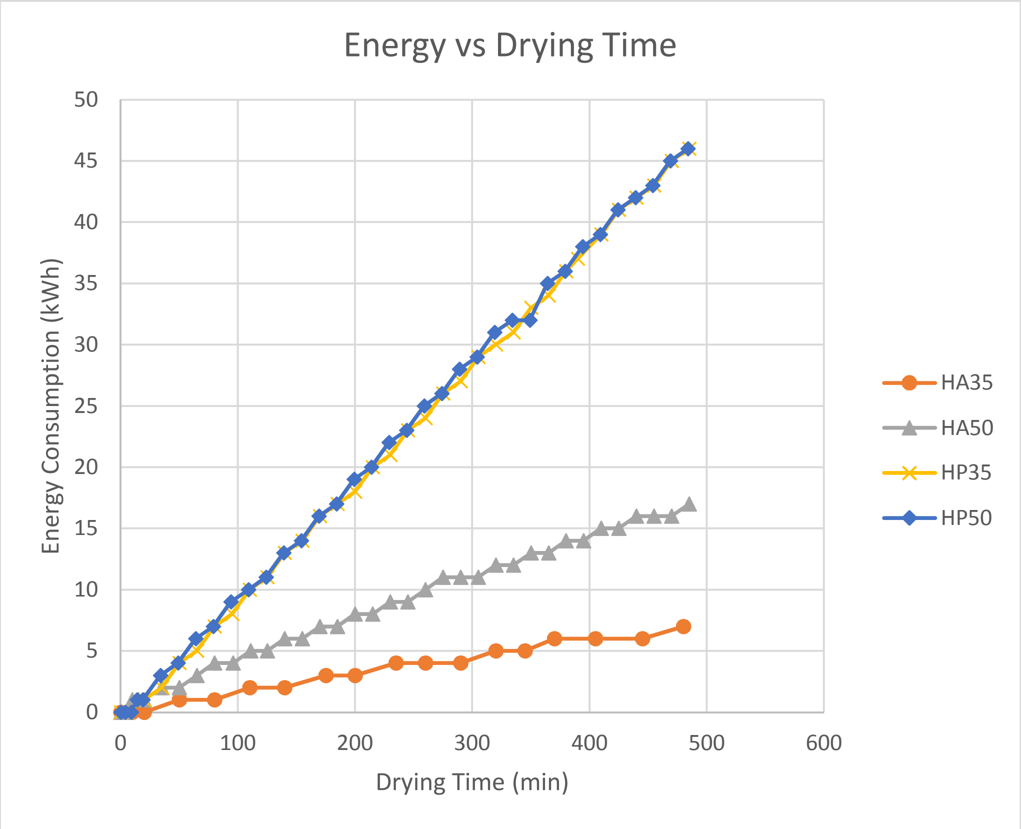

Figure 4-21 Energy consumption during heat pump drying and hot air drying

superimposed to each other despite the difference in drying temperature. In addition, the gradients of the curves under heat pump drying were much higher than the curves for hot air drying HA50 and HA35. Comparing between the hot air drying trials HA50 and HA35, the gradient of the curve for HA50 was higher than that for HA35. This had postulated that the heat pump dryer would consume similar amount of energy regardless of the drying temperature while the energy consumption for the hot air dryer was increasing with drying temperature. This occurred because the power consumption of the heat pump dryer was mainly used to run the compressor continuously in order to maintain the set relative humidity, while for hot air dryer the power consumption was used to run heaters that were switching on and off periodically to maintain the set temperature.

On top of that, higher drying temperature would require more heat input to achieve the set temperature and thus consuming more energy.

Figure 4-22 shows that in order to dry the sludge sample to moisture content of 3.0 kg/kg dry basis, HP50 had recorded energy consumption of about 22kWh while HP35 consumed even higher energy at about 36kWh. On the other hand, the hot air drying consumed much lesser energy at about 11 kWh and 8 kWh for HA50 and HA35, respectively. In this case the power consumption of heat pump dryer was almost triple higher than that in hot air drying. The high power consumption in the heat pump dryer was primarily due to the continuous running compressor in order to maintain the set humidity. However, due to the limitation on the wet bulb temperature that it could achieve in the heat pump system and also the moisture evaporation rate of sludge sample, the additional energy input did not bring much benefit to the drying rate. Thus, when there was a controller regulating the relative humidity, the heat pump dryer would consume much more energy than the hot air dryer.

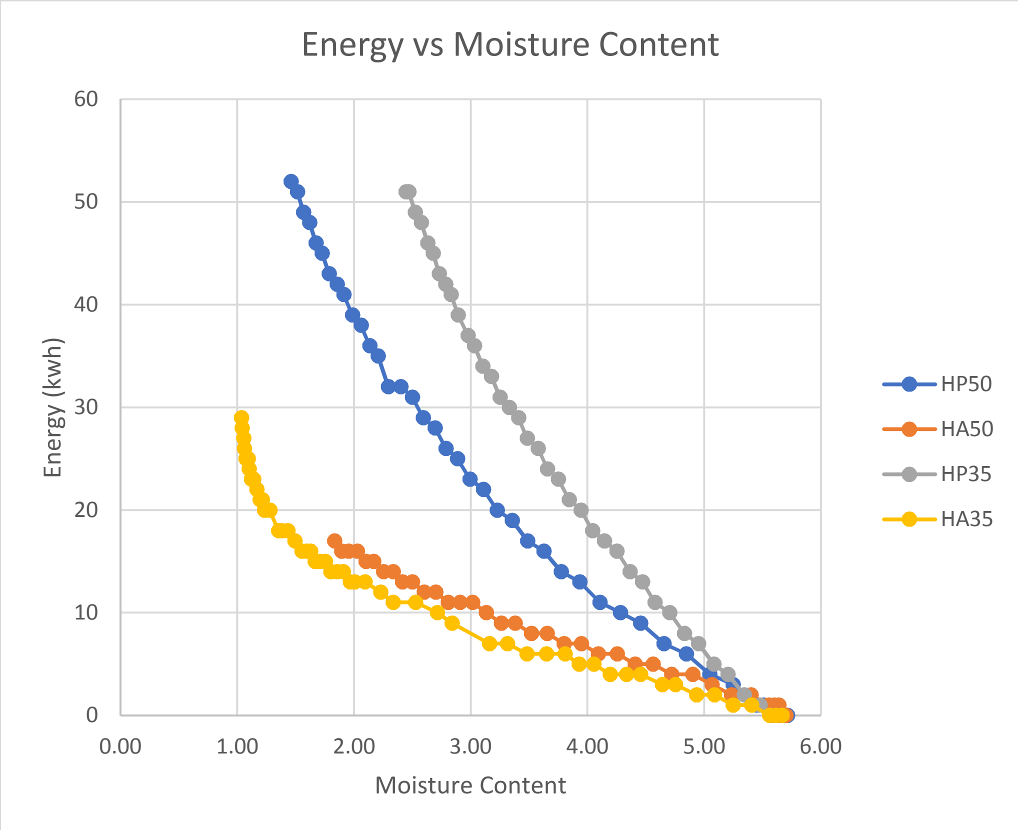

Figure 4-22: Energy consumption vs moisture content

Figure 4-23 shows the comparison of SMER for hot air dryer and heat pump dryer. The results revealed that SMER of heat pump dryer was much lower than hot air dryer. The high power consumption of heat pump dryer was due to the continuous running compressor to perform the dehumidification. The profiles of SMER curves were different between heat pump dryer (concave) and hot air dryer (convex). For the hot air dryer, the SMER tended to increase at the beginning of the drying session and then achieved maximum value when the sample weight was about 5.5 kg. After that the SMER would start to drop.

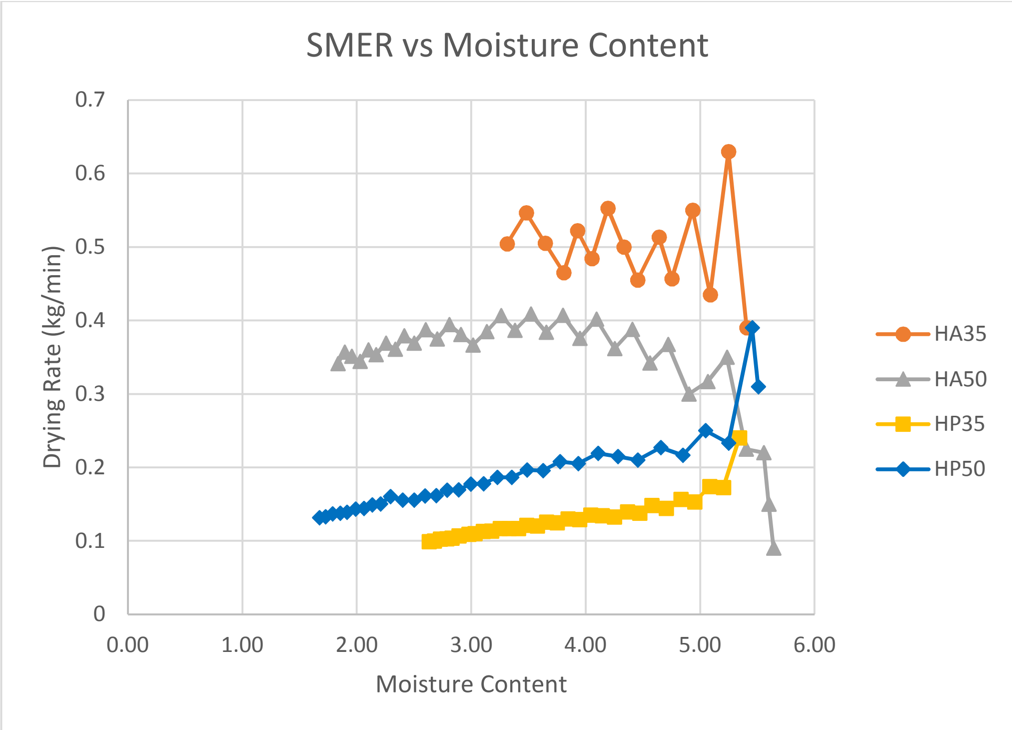

Figure 4-23: SMER during heat pump drying and hot air drying

On the other hand, SMER for the heat pump dryer was in reducing trend from the beginning. This phenomenon could be due to that the heat pump dryer was not heating the air directly but through secondary heat transfer medium, which in this case the water. Therefore, at the beginning of drying session, the heat pump system was heating the water before the water could heat up the drying air effectively. At the same time, the drying air medium that was passing through the evaporator had been cooled by the heat pump system. Thus, the temperature of the drying air medium increased much slower than the drying air medium in hot air dryer. The longer heating up time and higher power consumption had restricted the increment of SMER like what could be obtained in hot air dryer.

4.2.4 Effect of condenser type

Figure 4-24 shows the moisture content reduction over drying time when drying trials were conducted using condensers with direct air heating mode (DH) HP50_Air Temp and water heating mode (WH) HP50_Water Temp. The curve for both heating modes were superimposed to each other. The result revealed that both the drying kinetics were similar regardless of the condenser type. This indicated that both condenser types were able to produce the drying air medium with the similar properties and drying force. Nonetheless, Figure 4-25 shows that the temperature control in WH mode was more stable than DH mode.

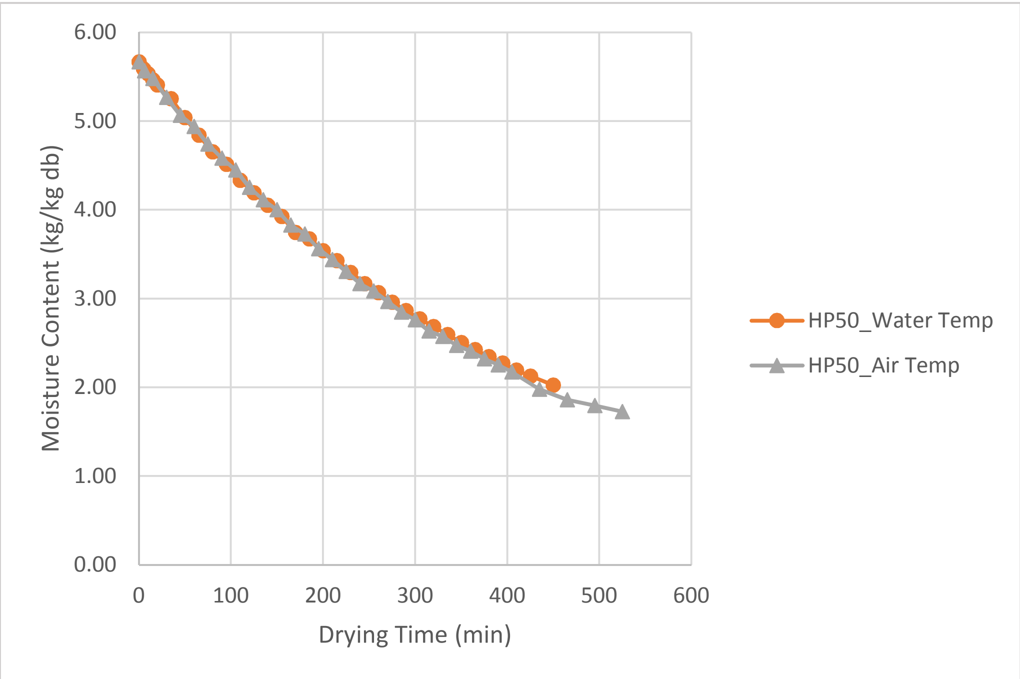

Figure 4-24 Drying kinetics of samples during heat pump drying under direct heating (Air) and water heating (Water) modes

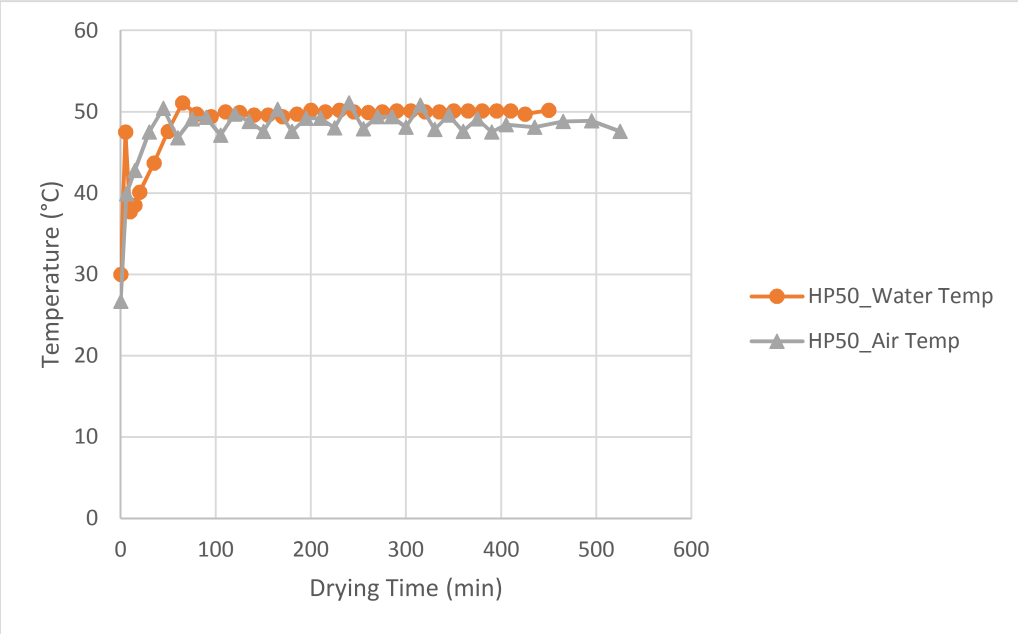

Figure 4-25 Temperature profile of drying air under direct heating (Air) and water heating (Water) modes

In addition, Figure 4-26 shows that energy consumptions of DH mode and WH mode were about the same in overall, though WH mode tended to consume slightly more electricity at the beginning of drying when it was heating and storing thermal in the water tank. Once the hot water tank reached the temperature limit, then the electricity consumption would drop and eventually consumed equal amount of electric energy as the DH mode.

Figure 4-27 shows SMER at various moisture content when undergoing heat pump drying under DH mode and WH mode. In agreement with the electric energy consumption trend, it was observed that DH mode possessed much higher SMER in the early stage of drying. Nevertheless, SMER for both operating modes were similar in the end of drying.

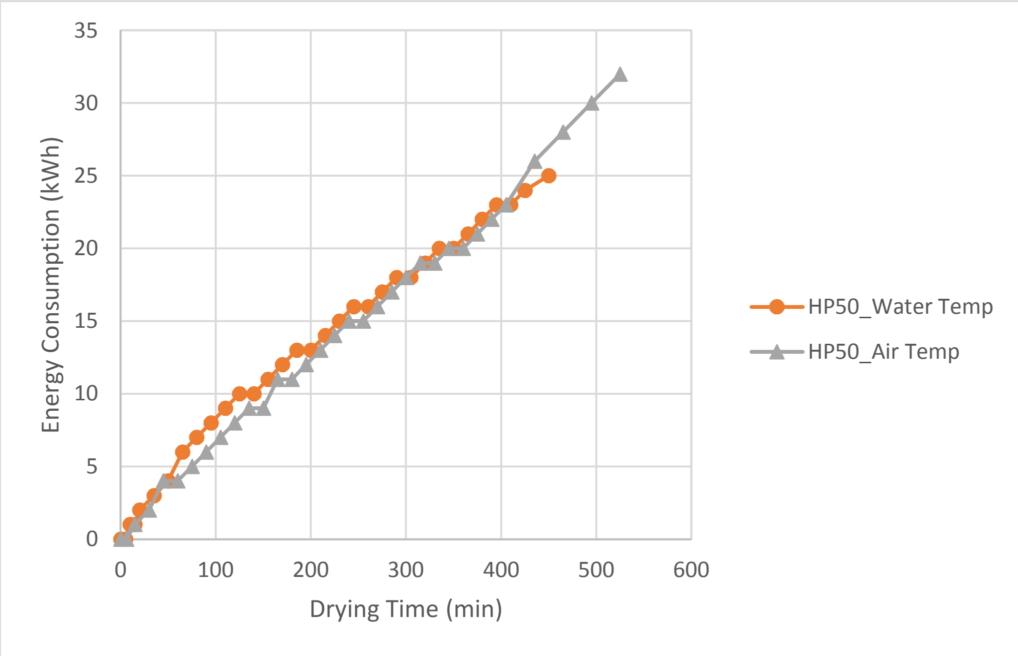

Figure 4-26 Energy consumption heat pump dryer under direct heating (Air) and water heating (Water) modes

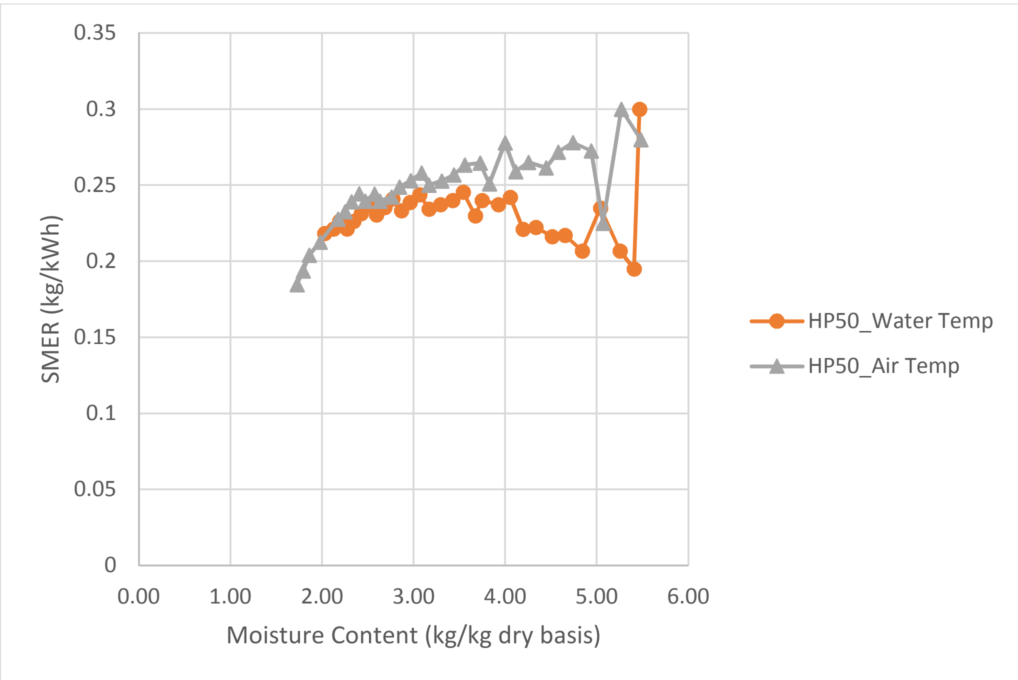

Figure 4-27 SMER of heat pump dryer under direct heating (Air) and water heating (Water) modes

4.2.5 Effect of air flow

Drying trials to evaluate the effect of air flow were conducted by varying the fan speed using a frequency inverter. The frequency was adjusted to 30Hz, 50Hz and 60Hz to obtain different air flow settings in the drying chamber. Table 4-4 shows the corresponding air flow properties to each frequency setting.

Table 4-4 Air flow rate in the drying chamber at various frequencies

Frequency	**Fan Speed (rpm)**	**Total air flow, *V* (m^3/s)**	**Air velocity, *u* (m/s)**
30Hz	870±10	0.33±0.02	1.59±0.6
50Hz	1450±10	0.53±0.02	2.55±0.6
60Hz	1740±10	0.61±0.05	2.93±1.5

Figure 4-28 and Figure 4-29 show the simulated air flow profile and dynamics in the drying chamber. It can be seen that with the current heat pump configuration and blower position, the air velocity was the highest at the lower part of the drying chamber i.e. Tray 3, 4, 5 and 6 while Tray 1 and 2 would experience the lowest air velocity (refer to Figure 3-12 for tray arrangement). Therefore, it was expected that Tray 1 and 2 would possess the lowest drying rate while Tray 3, 4, 5 and 6 would have the highest drying rate. Uneven air distribution inside the drying chamber would reduce the overall drying efficiency (Misha *et al.*, 2015), especially at the later stage of drying where the relatively dried sample kept on subjected to high air flow while the relatively wet sample was not getting enough drying air medium to promote the moisture removal. Hence, careful planning on the air flow path, strategic position of air inlet feed point, use of honeycomb sheet, rotation of sample trays and etc. could help to reduce the effect of the uneven air flow and consequently the sporadic drying kinetics.

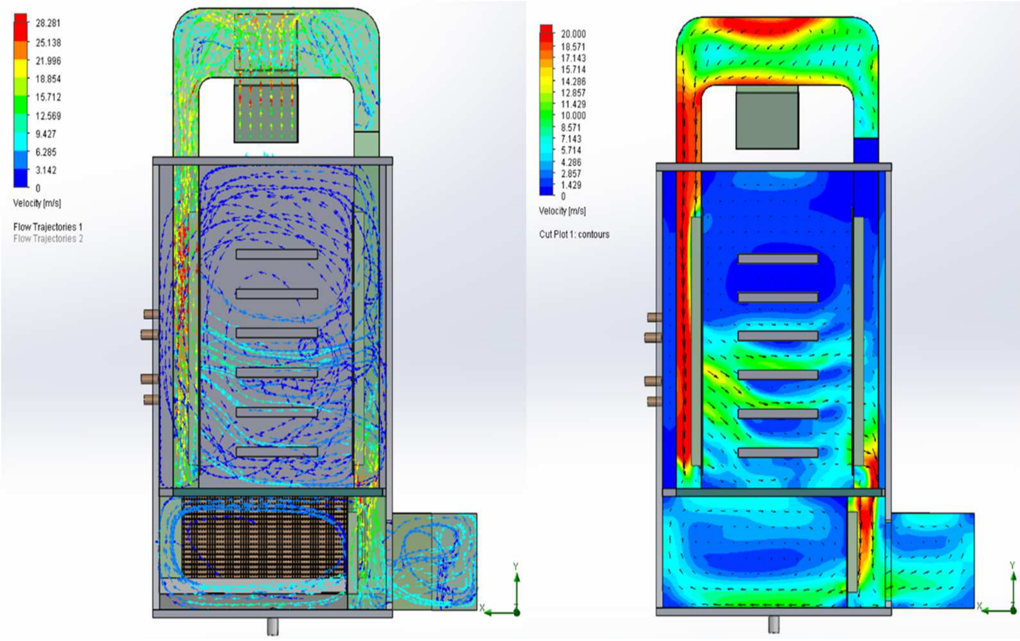

Figure 4-28 Simulation of air flow pathway inside the drying chamber (front view)

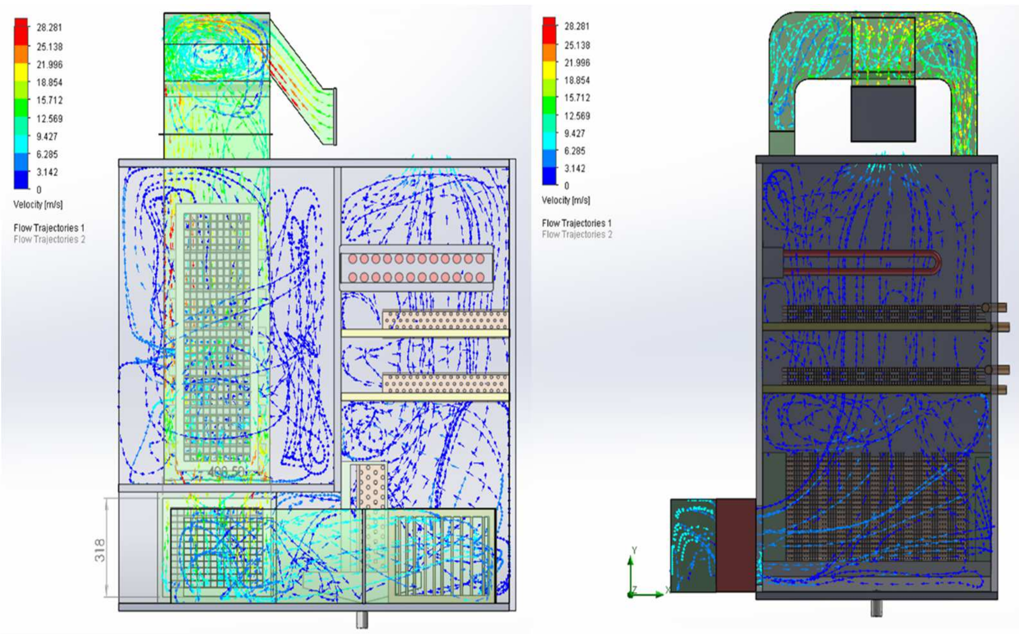

Figure 4-29 Simulation of air flow pathway inside the drying chamber (left-side view & right-back view)

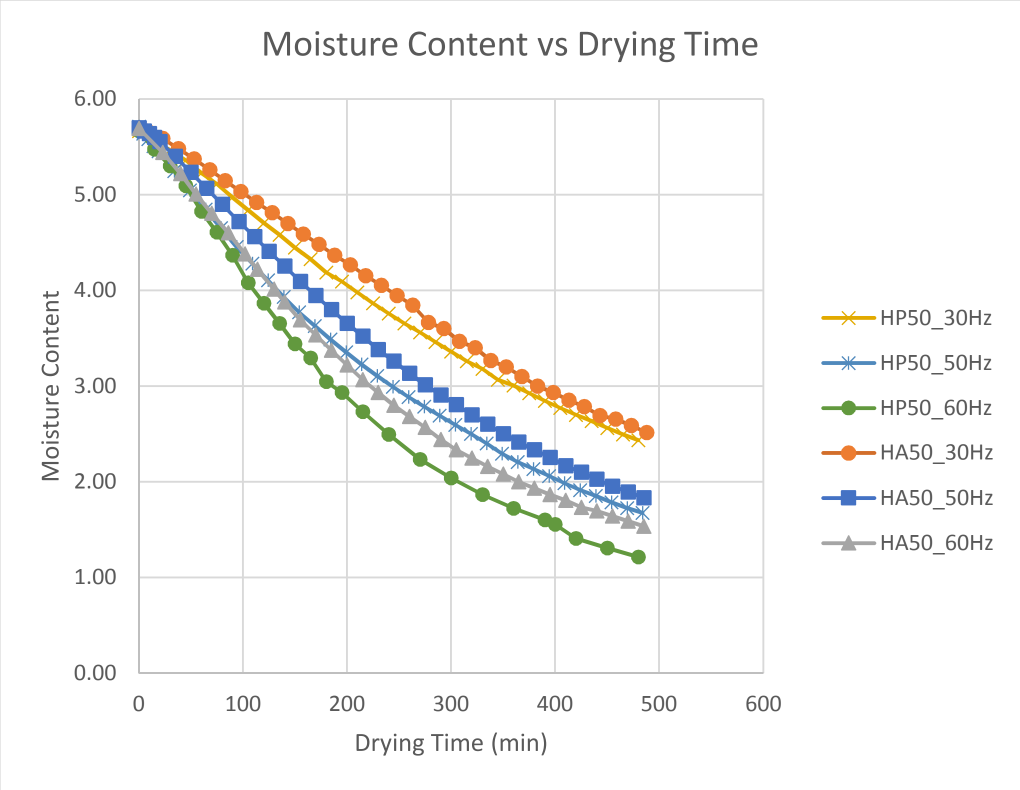

Figure 4-30 Moisture content of sample at various fan speeds

Figure 4-30 shows the sample drying kinetics under heat pump drying and hot air drying with fan speeds of 30Hz (1.59±0.6 m/s), 50Hz (2.55±0.6 m/s) and 60Hz (2.93±1.5 m/s). Results showed that when under the same drying temperature, higher air velocity would promote higher drying kinetics. Same phenomena were observed in both heat pump drying and hot air drying. However, when samples were subjected to the same drying temperature and air flow, then heat pump drying would give higher drying kinetics due to the greater drying force caused by lower relative humidity in the drying air medium.

Figure 4-31 shows the relative humidity of the drying air medium in heat pump drying and hot air drying. Apparently, the relative humidity of drying air medium in heat pump dryer was always lower than that in hot air dryer, regardless of fan speed. On top of that, it was observed in the heat pump dryer that lower air flow tended to further lower down the relative humidity. This could be due to the longer contact time between the evaporator and drying air medium, consequently resulted in increased moisture extraction rate (condensation) from the drying air medium and thus causing lower relative humidity in the drying air medium. However, when comparing the drying kinetics in Figure 4-30, it can be seen that the effect of air velocity was more prominent than relative humidity where drying kinetics of HP50_60Hz (2.93 ± 1.5 m/s; 12.4% RH) was higher as compared to HP50_30Hz (1.59 ± 0.6 m/s; 9.4% RH) though the relative humidity in the later was lower.

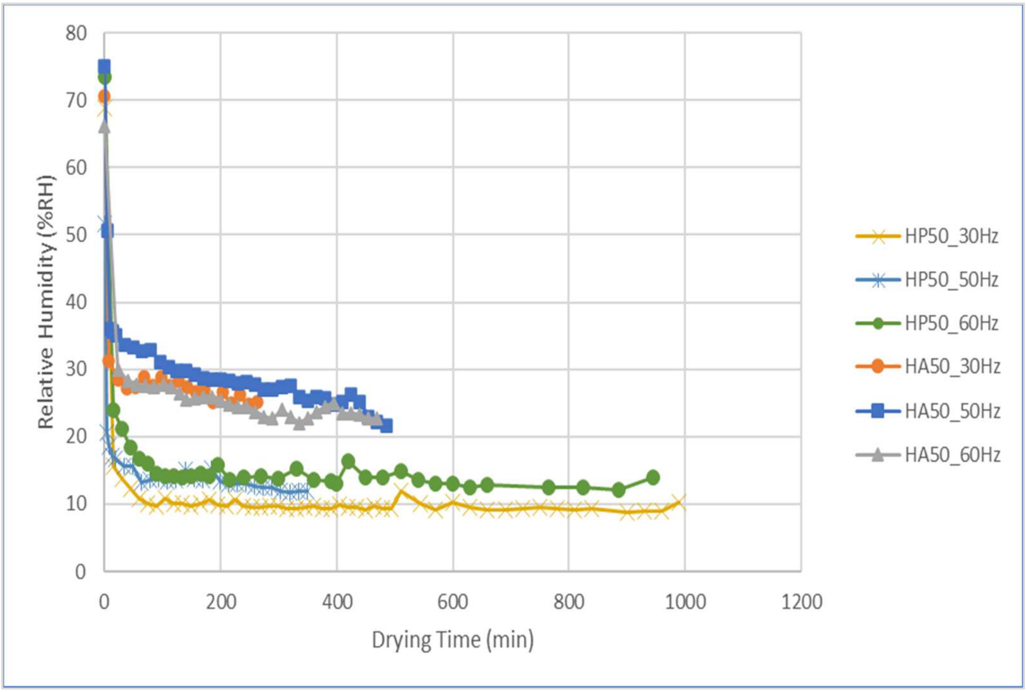

Figure 4-31 Relative humidity of drying air medium during heat pump drying and hot air drying

Figure 4-32 and Figure 4-33 show the logarithmic moisture ratios of samples at various fan speeds in heat pump drying and hot air drying, respectively. The slopes of the linear graphs and the calculated effective moisture diffusivity are listed in Table 4-5 and illustrated in Figure 4-34.

Generally, at fan speed of 30Hz (1.59 ± 0.6 m/s) the slopes of the linear graph were 0.0015 min^{-1} and 0.0017 min^{-1} for HA50_30Hz and HP50_30Hz, respectively. While at fan speed of 50Hz (2.55±0.6 m/s), the slopes were 0.0024min^{-1}.and 0.0026min^{-1} for HA50_50Hz and HP50_50Hz, respectively. Then at fan speed of 60Hz (2.93 ± 1.5 m/s), the slopes were 0.0029min^{-1}.and 0.0032min^{-1} for HA50_60Hz and HP50_60Hz, respectively. Based on the slopes from the linear regression, the effective moisture diffusivity values were determined ranging from 6.33257 x 10^{-9} m^2/s (HA50_30Hz) to 1.35095 x 10^{-8} m^2/s (HP50_60Hz). In agreement with the findings in drying kinetics, the results here show that when drying at the same temperature, higher air flow would promote higher effective moisture diffusivity. This postulated that higher air flow would carry away the moisture from the sample surface faster and thus increase the moisture gradient between sludge sample and drying air medium, which subsequently enhance the effective moisture diffusivity.

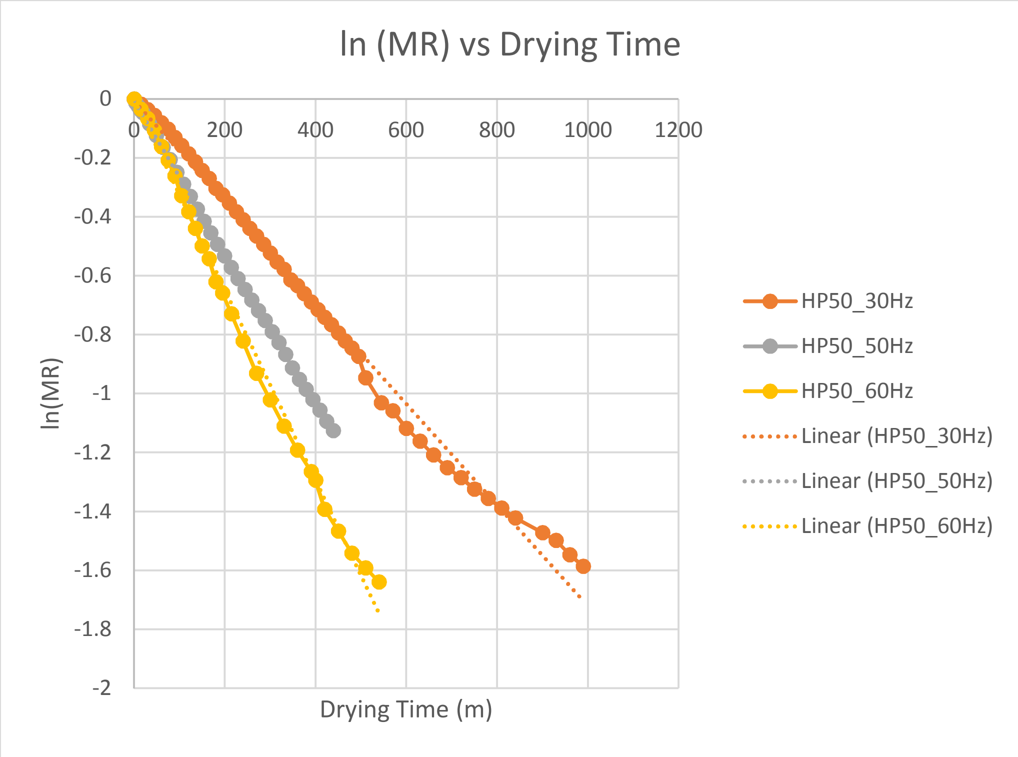

Figure 4-32 Logarithmic moisture ratio at various fan speeds in heat pump drying

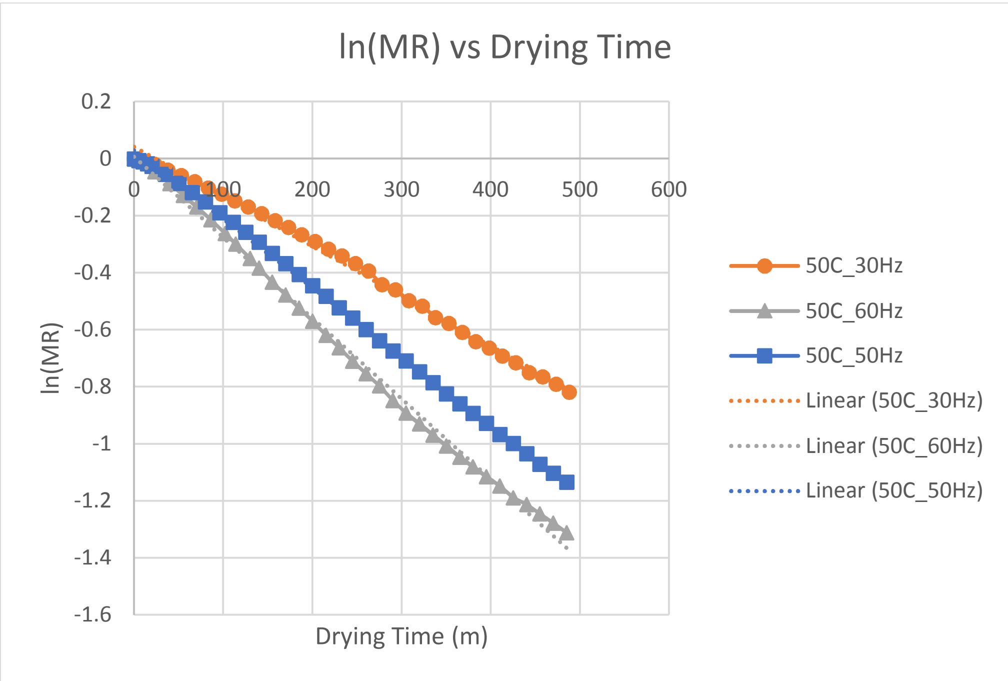

Figure 4-33 Logarithmic moisture ratio at various fan speeds in hot air drying

Table 4-5 Effective moisture diffusivity at various fan speeds in heat pump and hot air drying

Dying Trials	Linear Formula	R^2	Intercept value	Slope	Diffusivity (*Deff*) m^2/s
HP50_30Hz	y = -0.0017x - 0.0062	0.9915	-0.0062	-0.0017	7.17692×10^{-9}
HP50_50Hz	y = -0.0026x - 0.0024	0.9995	-0.0024	-0.0026	1.09765×10^{-8}
HP50_60Hz	y = -0.0032x - 0.0008	0.9951	-0.0008	-0.0032	1.35095×10^{-8}
HA50_30Hz	y = -0.0015x + 0.0175	0.9966	0.0175	-0.0015	6.33257×10^{-9}
HA50_50Hz	y = -0.0024x + 0.0298	0.9992	0.0298	-0.0024	1.01321×10^{-8}
HA50_60Hz	y = -0.0029x + 0.0105	0.9971	0.0105	-0.0029	1.2243×10^{-8}

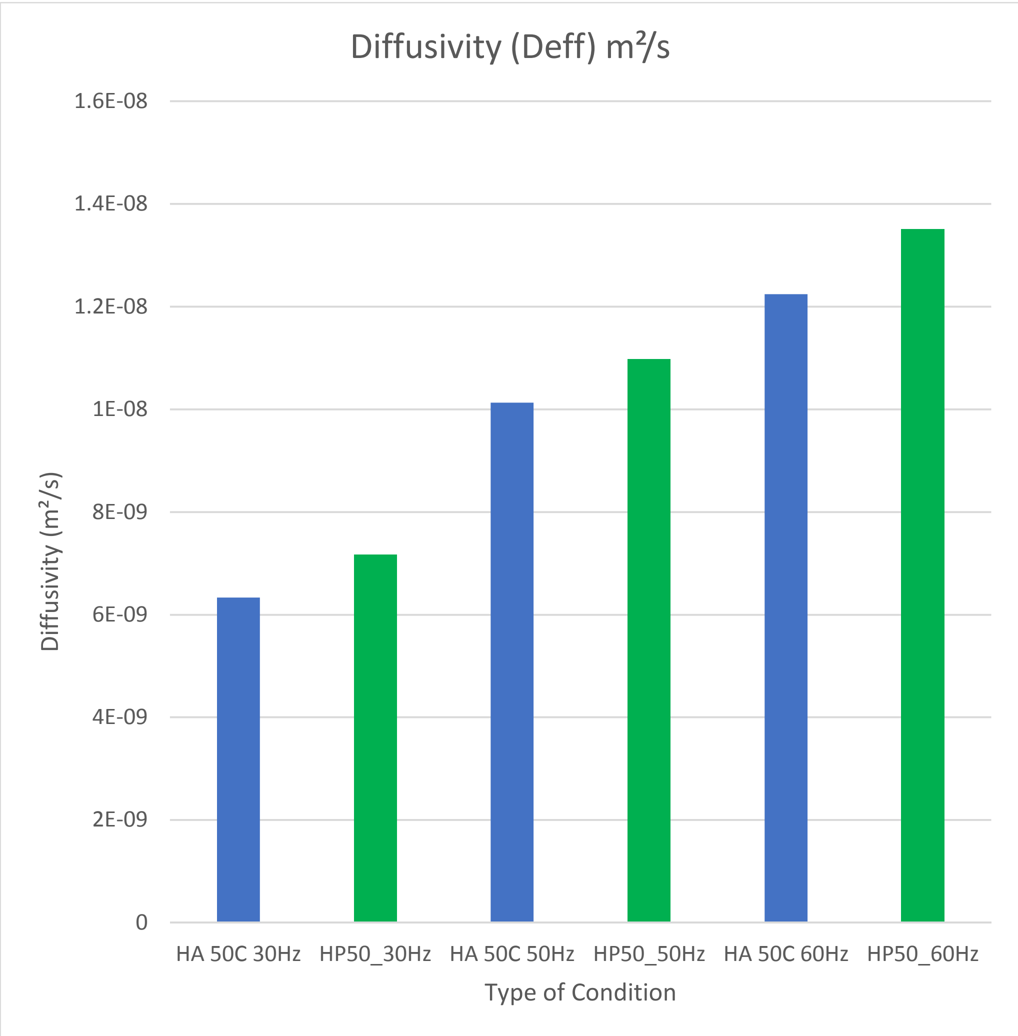

Figure 4-34: Diffusivity at various fan speed for hot air and heat pump drying

Figure 4-35 shows the total energy consumption of the heat pump drying and hot air drying at various fan speeds. Apparently, HP50_60Hz recorded the highest electricity consumption meanwhile HA50_30Hz logged the lowest. In overall, it was observed that the continuous operation of compressor in heat pump dryer was the main reason for the higher energy consumption when compared to hot air drying. Nevertheless, in both drying modes, the energy consumption was increasing with fan speed.

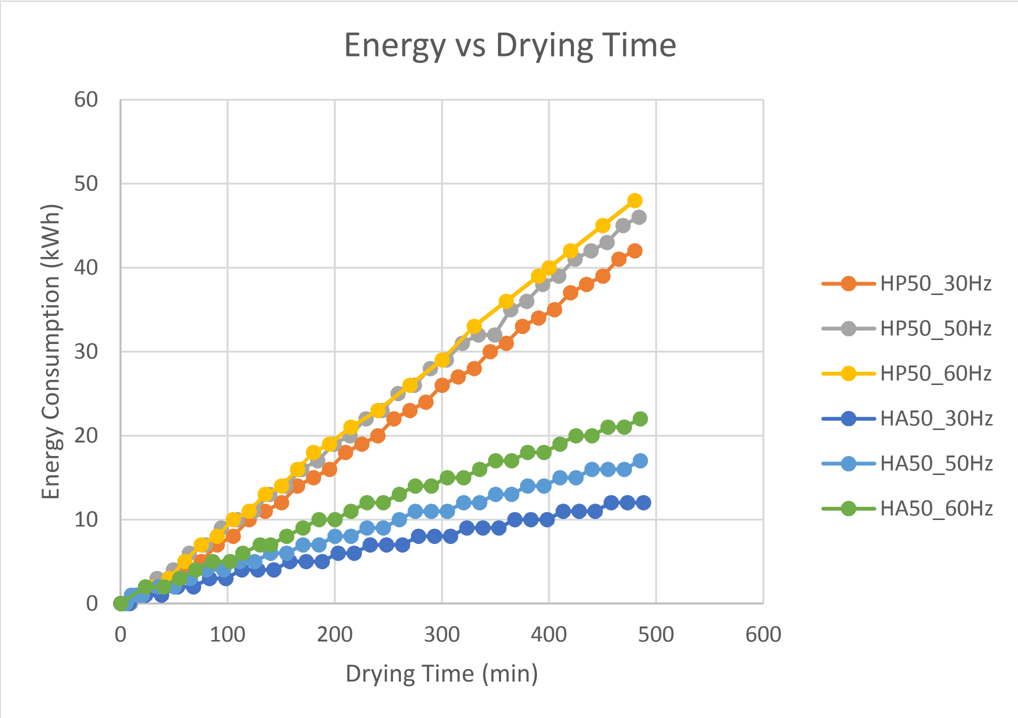

Figure 4-35 Energy consumptions of dryer during heat pump drying and hot air drying at various fan speeds

Figure 4-36 shows the SMER of heat pump drying and hot air drying at various fan speeds. Generally, SMER of hot air drying was higher than heat pump drying. It could be postulated that in heat pump drying, the energy consumption was largely attributed by the compressor. Somehow, the fan electricity consumption was relatively small as compared to the compressor electricity consumption. On top of that, it was observed that the SMER of

HP50_60Hz was the highest among the heat pump dried samples although it logged the highest electricity consumption. The result revealed that the electric power input for the fan in heat pump dryer was worthy as the higher air velocity could help to enhance the drying kinetics and hence improve the moisture extraction rate. In contrary, though the drying kinetic increased with the fan speed, the SMER in hot air drying was decreased with the electric power input for the fan. For instance, drying kinetic for sample HA50_60Hz was the highest among the hot air dried samples but in term of SMER it was the lowest. Therefore, it can be proposed that high air flow is not necessary when come to hot air drying. Air velocity around 2.5 m/s would be the optimum air flow rate to achieve the optimum drying rate and energy efficiency.

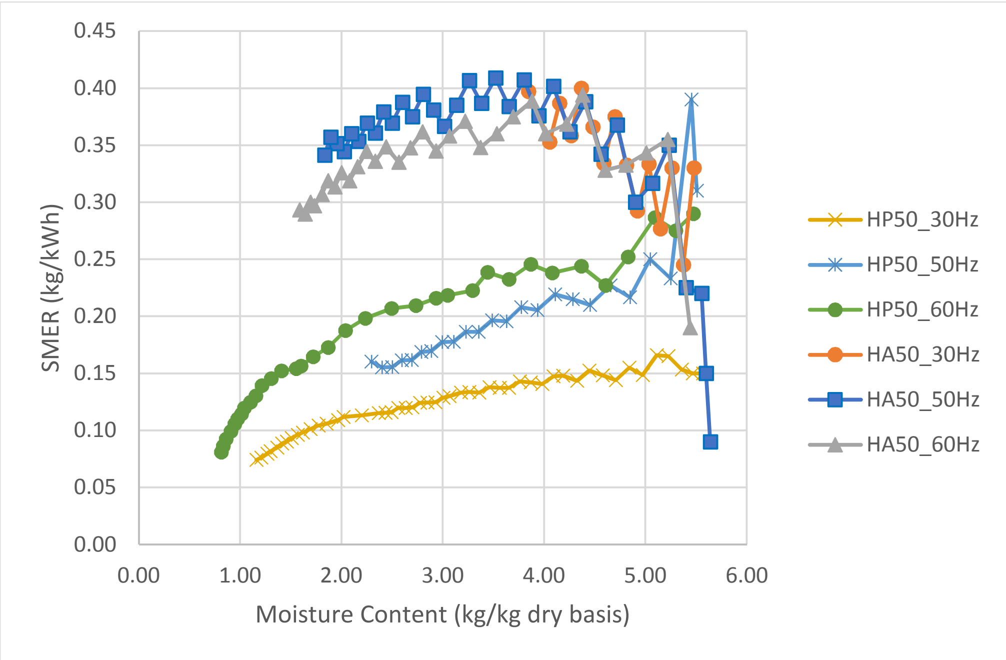

Figure 4-36 SMER of heat pump drying and hot air drying at various fan speeds

4.2.6 Effect of bypass air ratio

Drying trials were conducted to study the effect of bypass air ratio by manipulating the bypass damper opening, e.g. fully-closed (no or 0% bypass), fully-open (maximum or 100% bypass) and partially-open (half or 50% bypass). Table 4-6 shows the air flow rate in the drying chamber at the different bypass air ratio.

Table 4-6 Air flow rate in the drying chamber at different bypass air ratio

	Fully-Open		Partially-Open		Fully-closed	
	Total	Bypass	Total	Bypass	Total	Bypass
Air flow rate (m^3/s)	0.53	0.25	0.52	0.20	0.51	0.00

For heat pump drying, the main purpose of having bypass air was to reduce dehumidification load at the evaporator and thus reduce the sensible heat ratio (SHR). It was presumed that with lower SHR, more latent heat capacity could be recovered from the evaporator and subsequently enhance the dehumidification capability (Parker et al , 1997). Findings showed that when the bypass damper was partially open, the bypass air flow (0.20 m^3/s) would be just slightly lower than that when the damper was fully open (0.25 m^3/s). Therefore, it was expected that there would be a very similar drying performance among the fully open and partially open modes. Figure 4-37 shows the moisture reduction kinetics of sludge samples under heat pump drying at 50 °C with different bypass air ratio.

As expected, the drying kinetics for partially open and fully open were almost the same where the curves were nearly superimposed to each other. On the other hand as shown in Figure 4-37, it was observed that when the damper was fully closed and no bypass air (where all drying air medium being circulated back to drying chamber after passing through the evaporator), the drying kinetic would drop significantly. This could be due to the poor dehumidification of drying air medium at the evaporator when there was overwhelm of warm and moisture laden drying air medium passing through it. Moreover, the elevated temperature at the evaporator would result in an increase of sensible cooling while experiencing decrease in latent cooling. Therefore, less moisture extraction (condensation) from the drying air medium. In the worst case scenario, where the evaporator surface temperature was higher than the drying air dew point, there would be no dehumidification occur at all at the evaporator (Ananthanarayanan, 2013).

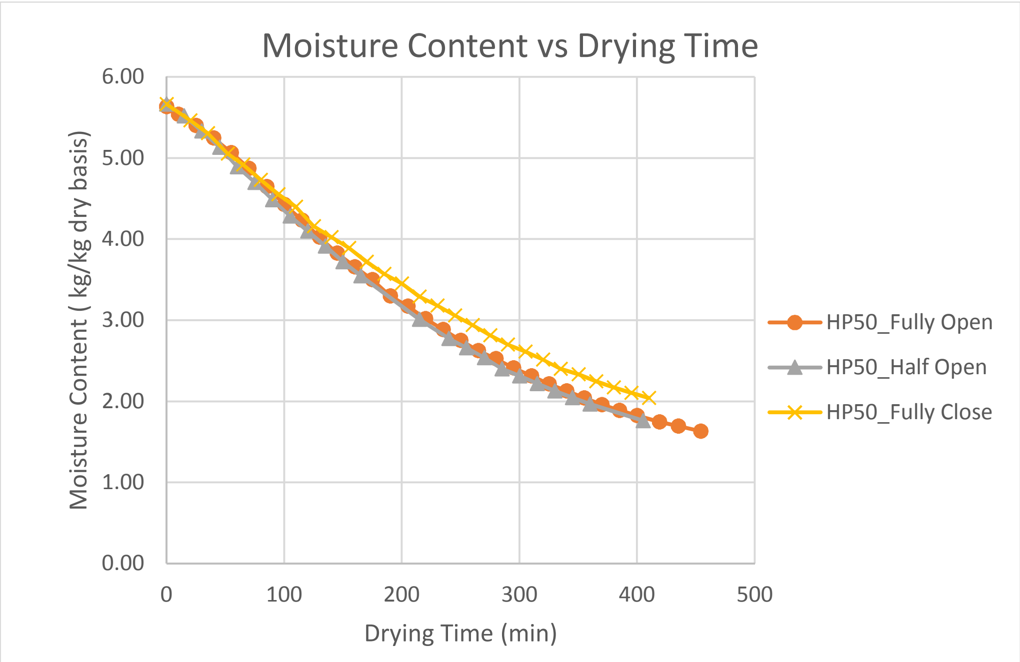

Figure 4-37: Moisture content for different bypass opening at heat pump 50°C

Figure 4-38 shows the relative humidity of drying air medium under heat pump drying at 50 °C with different bypass air ratios. When the damper was fully closed, the relative humidity was recorded at around 16% RH. Meanwhile, the relative humidity when damper partially open and fully open were logged at 13% RH and 12% RH, respectively. In agreement with the previous findings, it appeared that the high relative humidity in the fully close mode was due to the poor dehumidification at the evaporator. It can be recommended that the bypass air ratio should be adjusted and controlled based on the surface temperature of the evaporator, where ideally it should not go higher than the water dew point. Nevertheless, optimum bypass air ratio would be different depends on the application and heat pump configuration. Liu et al., (2018) had reported that the optimum SMER was obtained at 40% bypass air for food drying while Soponronnarit et al. (2000) reported that the best setting for seed drying was with 0% bypass air.

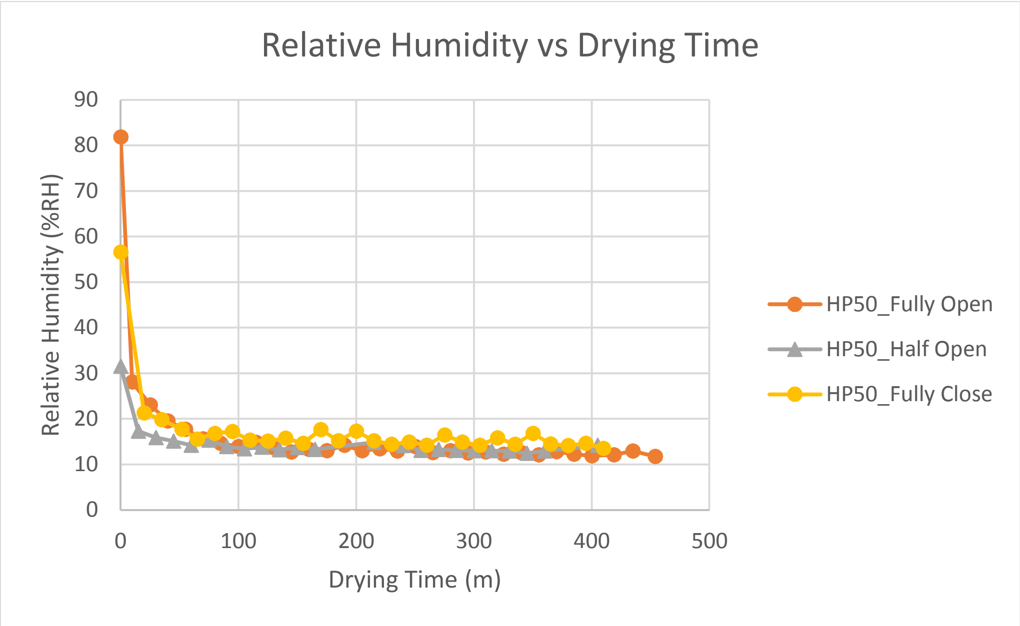

Figure 4-38: Relative humidity in the heat pump dryer at different bypass air ratios

4.2.7 Effect of dehumidification

Effect of dehumidification was evaluated together with energy consumption of the heat pump dryer. Figure 4-39 and Figure 4-40 show the drying air temperature and relative humidity, respectively when the heat pump dryer was configured with dehumidifying mode (HP50_Dehum) and heating mode (HP50_Heating).

In both modes, the temperatures increased equally fast. It took about 15 min to elevate from initial temperature at about 27°C to 50°C. However, it can be seen that temperature profile for the HP50_Heating mode was more fluctuated when compared to HP50_Dehum. Among the reasons could be due to the on-off cycle of compressor in the heat pump system which trying to control the temperature at the set temperature when the evaporator was not used to perform the dehumidification. On the other hand, in HP50_Dehum mode the compressor was continuously running for the dehumidification operation while the temperature was controlled by cycling the auxiliary condenser. Therefore, the temperature fluctuation was much smaller.

As for relative humidity profile, apparently the relative humidity of the drying air medium in the HP50_Dehum mode could rapidly reduce to about 17% RH in 30 min. Meanwhile, relative humidity of the drying air medium in the HP50_Heating mode was slightly higher which ranging from 28% RH to minimum 20% RH, where the lowest RH could be achieved at about 150 min after commencing the dryer unit.

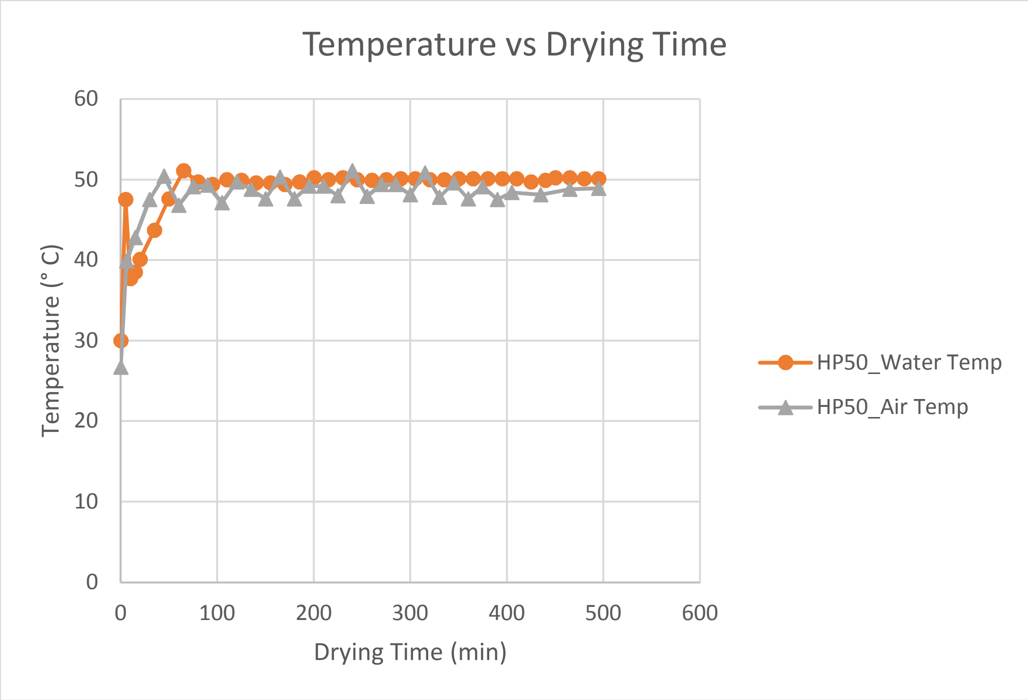

Figure 4-39 Drying air temperature during heat pump drying with dehumidifying mode and heating mode

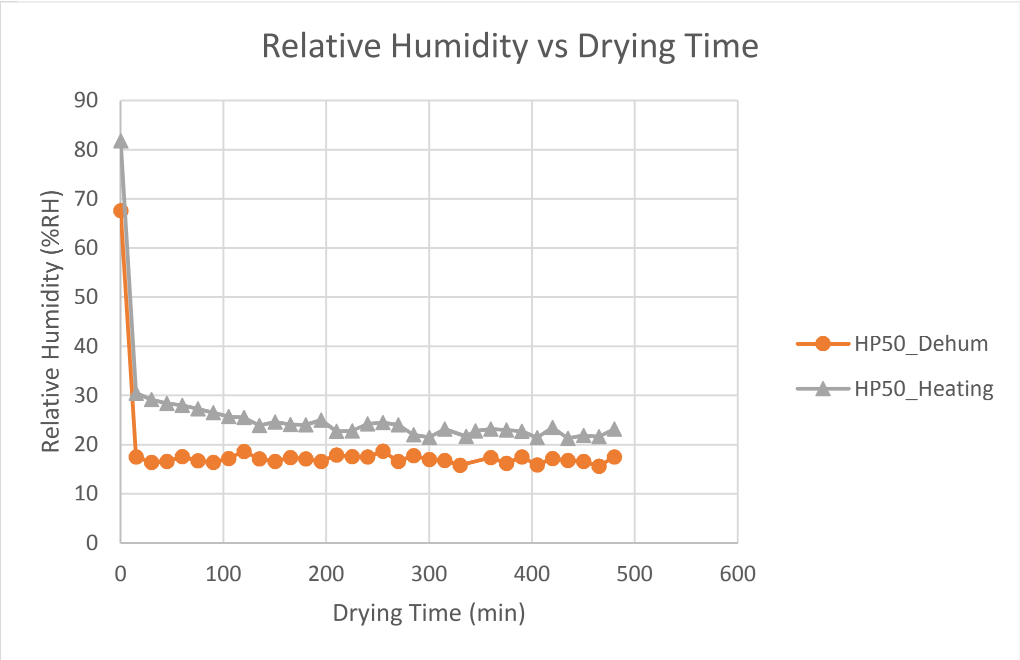

Figure 4-40 Relative humidity of drying air medium during heat pump drying with dehumidifying mode and heating mode

Figure 4-41 and Figure 4-42 show the drying kinetics and energy consumption of heat pump drying 50°C with dehumidifying mode (HP50_Dehum) and heating mode (HP50_Heating), respectively. In agreement with the findings in previous sections, the drying rate and energy consumption in dehumidifying mode (HP50_Dehum) were higher than that in heating mode. It was found that the drying rate of samples under the dehumidifying mode was about 13% higher than that in heating mode. This demonstrates that a low relative humidity in drying air medium plays a crucial role in enhancing the drying kinetics particularly during initial stage of drying. However, drying during the later stage when the moisture content of samples getting low, then the effect of humidity would become insignificant as compared to heating mode (HP50_Heating) (Zeguang Lu et al, 2016). The energy consumptions of both modes were about the same at the beginning of drying but the energy consumption of dehumidifying mode increased significantly after 75 min of drying as compared to heating mode.

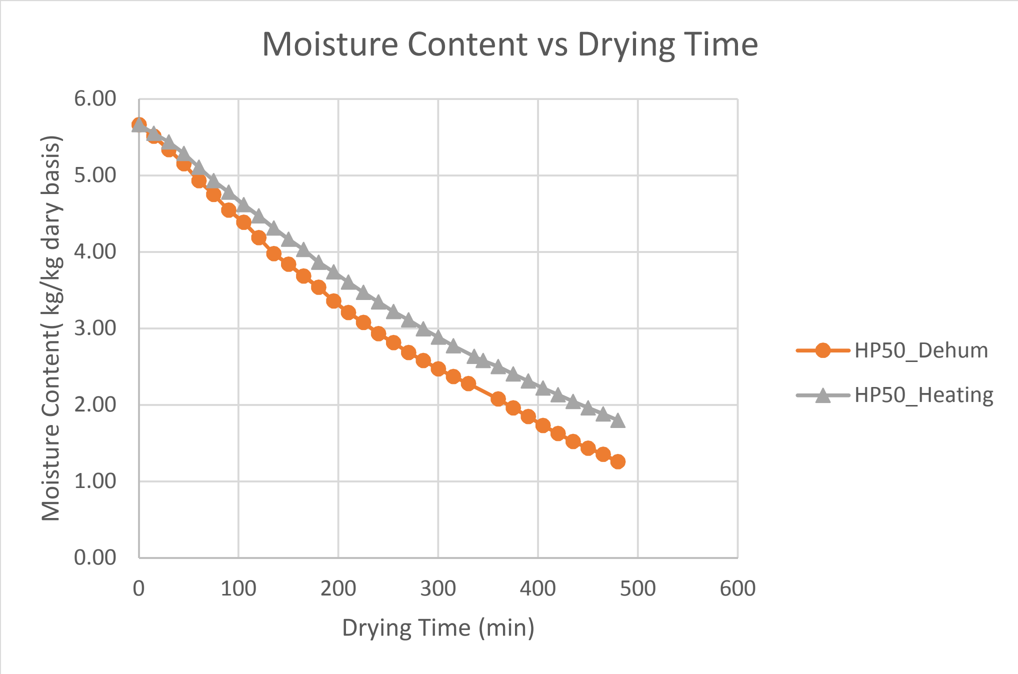

Figure 4-41 Drying kinetics of samples under heat pump drying with dehumidifying mode and heating mode

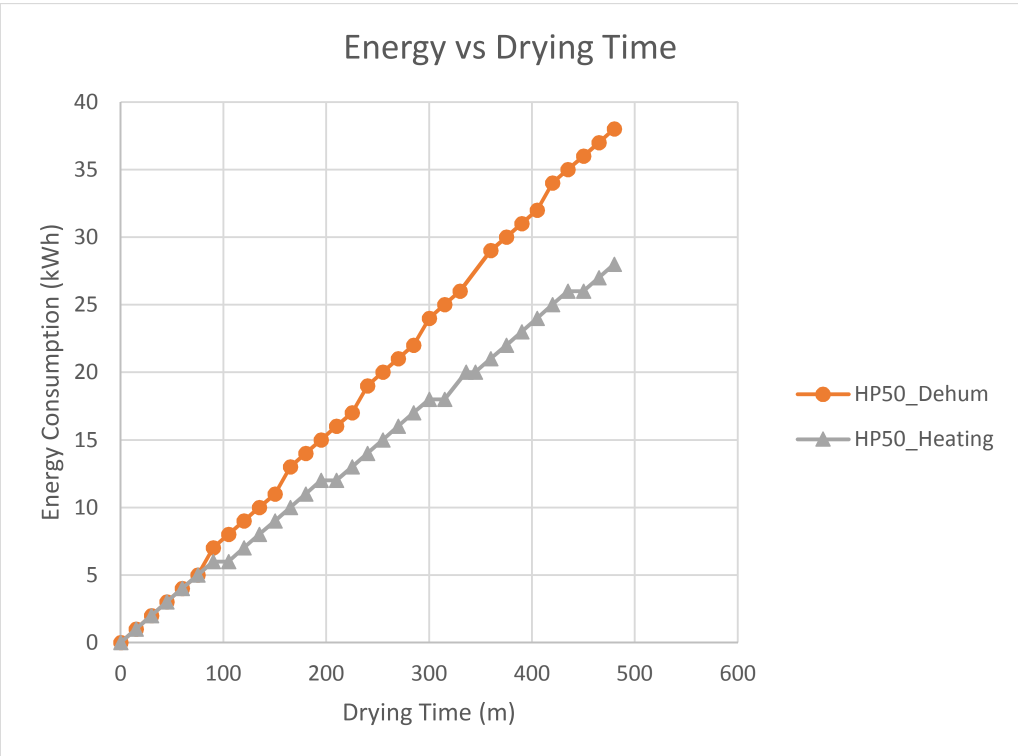

Figure 4-42 Energy consumption of heat pump dryer under dehumidifying mode and heating mode

If drying time is not of concern and only focus on the energy required corresponds to the final moisture content of sample, Figure 4-43 shows the comparison of energy consumption between the dehumidifying mode and heating mode at various moisture contents. It appeared that at the early stage of the drying process, HP50_Dehum mode consumed about the same energy as HP50_Heating mode, but when the moisture content of the sample dropped below 4.00 kg/kg dry basis, HP50_Dehum mode gradually consumed more energy compared to HP50_Heating mode. The total energy used in dehumidifying mode was recorded at 29kWh which was about 38% higher than that in heating mode, where the energy usage was just 21 kWh. This could be due to the continuous operation of the compressor in the HP50_Dehum while periodic operation of compressor in HP50_Heating.

Besides the compressor, the main energy consumption in HP50_Heating was from its auxiliary condenser fan. During the drying process, when the temperature at the heating coil (condenser) was too high, then the extra heat would be ejected to the surrounding through the auxiliary condenser, hence triggered the operation of the auxiliary condenser fan. On the other hand, as for the HP50_Dehum mode, drying air medium that approaching the heating coil was a cold dehumidified air that exhausted from the dehumidifying coil (evaporator) where its temperature was much lower and could absorb more heat that being ejected from the heating coil, hence reduced the operation of the auxiliary condenser. Nonetheless, results showed that the energy consumption of the auxiliary condenser fan was lower as compared to the compressor.

In addition, SMER for both drying modes were calculated and illustrated in Figure 4-43. It was observed that at initial stage, the SMER of dehumidifying mode was much higher than the heating mode. However, after the peak value of 0.275 kg/kWh at the 75^{th} min, the SMER dropped rapidly. Meanwhile in the heating mode, the SMER was low initially, but slowly reached the peak value of 0.265kg/kWh at about the 100^{th} min. Then the SMER slowly dropped to about 0.230 kg/kwh at the end of experiment. This suggested that the drying efficiency could be higher for a heat pump dryer operating in dehumidifying mode in the initial stage when the drying air medium was moisture laden and the dehumidifying coils could perform effectively. Though, when the relative humidity of drying air medium was reduced to a stage where the dehumidifying coil was no longer performing effectively, then the drying efficiency would drop and eventually lower than that could be achieved in heating mode (Minea, 2016). Therefore, it can be proposed that dehumidifying mode should be used in the beginning of the drying operation when the moisture content of sample is high while it must change to heating mode when the moisture content of sample is lower than 4 kg/kg dry basis.

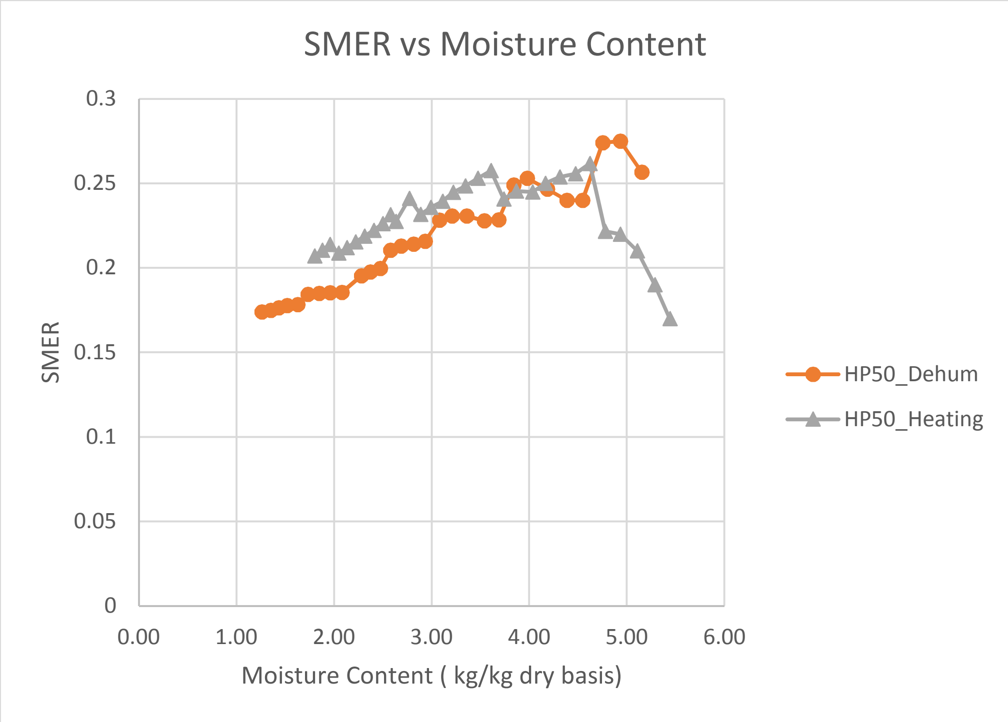

Figure 4-43 SMER of heat pump dryer under dehumidifying mode and heating mode

4.2.8 Effect of heat pump compressor capacity

Drying trials were conducted at 50°C by employing heat pump dryer coupled with compressors of 4.0 HP, 2.0 HP and 0.5 HP. Results from hot air drying 50°C were used as comparison purpose.

Figure 4-44 shows the drying kinetic under hot air drying and heat pump drying with compressors of 4.0 HP, 2.0 HP and 0.5 HP. It was observed that all the drying curves were superimposed to each other. The results showed that the drying kinetics were mainly governed by drying air condition, regardless of drying mode and heat pump size. As long as the drying air temperature, air velocity and relative humidity are the same, then the drying kinetics will be the same.

Figure 4-45 shows the total energy consumption that required to dry the sludge samples to various moisture contents at the temperature of 50°C. In order to dry the sample to a moisture content of 3.00 kg/kg dry basis, HP50_4.0HP records the highest energy consumption at 16 kWh while the lowest energy consumption was achieved by HP50_0.5HP at about 9 kWh. HP50_2.0HP and HA50 were in the between, recorded at 13 kWh and 11 kWh, respectively. According to the results (for 10 kg sludge sample), when the drying air conditions and sample load were the same, then heat pump dryer with a smaller compressor would be more efficient. This had implied that for an energy efficient heat pump drying, the compressor capacity must be sized according to the sample load and desired drying rate. As demonstrated in the previous sections that the most energy consumption part in the heat pump dryer was the compressor. Therefore, oversize of compressor in the heat pump system for sure would result in higher energy consumption rather than enjoying the benefits from it.

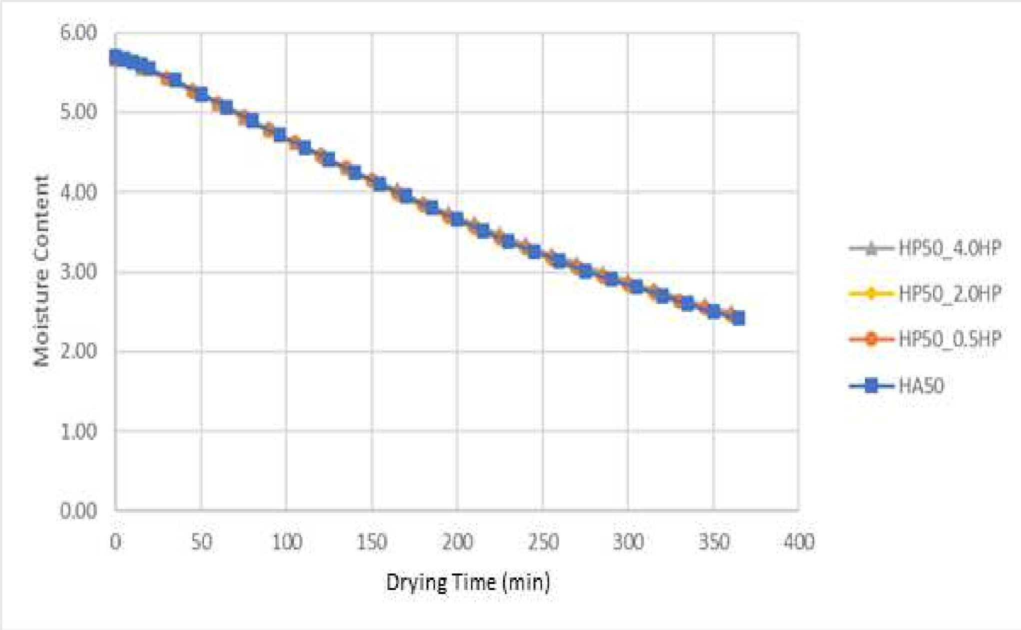

Figure 4-44 Moisture Content of samples under heat pump drying with various compressor sizes

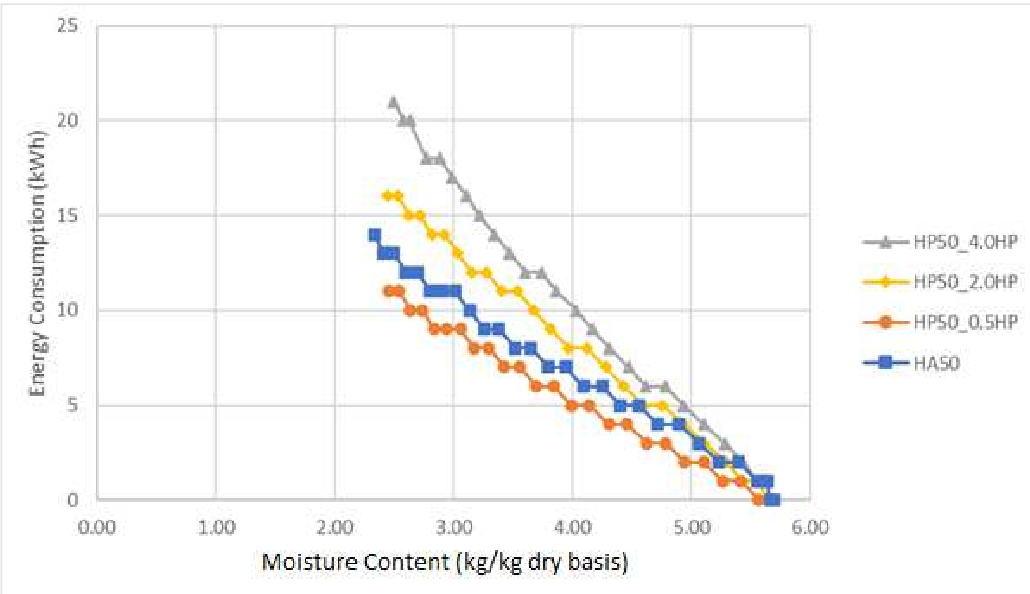

Figure 4-45 Energy consumption under hot air mode and heat pump mode with various compressor sizes

4.3 Quality analysis of dried sludge samples

Figure 4-46 shows the total organic carbon content while Figure 4-47 shows the heavy metal content in raw sample as well as samples under heat pump drying at 50°C (HP50) and hot air drying at 50°C (HA50) and 70°C (HA70). It was observed that the total organic carbon content in samples had increased to 0.16% to 0.21% after drying. The results implied that drying below 70°C would not degrade much the total organic carbon but would concentrate it instead after the removal of moisture content. Nonetheless, the total organic carbon in HA70 was slightly lower in the sludge composition as compared to HP50 and HA50 probably due to some thermal degradation during the drying at slightly high temperature.

On the other hand, it was observed that total amount of most heavy metals was reduced after drying, except platinum (no significant reduction) and zinc (significant increment). Apparently, the composition of the heavy metals had changed after the drying though all the heavy metals were not heat labile materials. Referring to , boiling points of the heavy metals (327.46°C to 1907°C) were far above from the drying temperature (50°C to 70°C). Therefore, the reduction was not caused by thermal degradation or evaporation. Instead, it was postulated that some of the heavy metal particles were flying and then trapping inside the dryer chamber and air flow ducting as some powder precipitations were observed on the wall surfaces. The loss of the heavy metals became more obvious when the final moisture content was low, for instance total amount of heavy metals in HP50 and HA70 was lower as compared to HA50. Physically, sludge samples with lower final moisture content would appear powderier and looser. This made the heavy metals particles easier to fly and carried over by the drying air medium. According to Table 4-7, atomic number and standard atomic weight of zinc and platinum were higher as compared to other heavy metals. Hence, this had made zinc and platinum less tendency to fly and deposit on the wall surface. Consecutively, amount of zinc and platinum was well preserved in the dried samples.

Results revealed that although the drying did not degrade the heavy metals in the sludge samples thermally, safety concerns must be given to the flying particles particularly if the drying air medium would be exhausted during the drying process. Discharge of heavy metal particles in the drying air exhaust would then bring safety and health problems to the users. Furthermore, deposit of the heavy metals could bring other issues like fouling and corrosion as well to the components in the dryer. Therefore, proper attention must be given when designing the drying trays, air pathway, particles filtration and collection in order to reduce the flying powder particles and discharge of harmful substances.

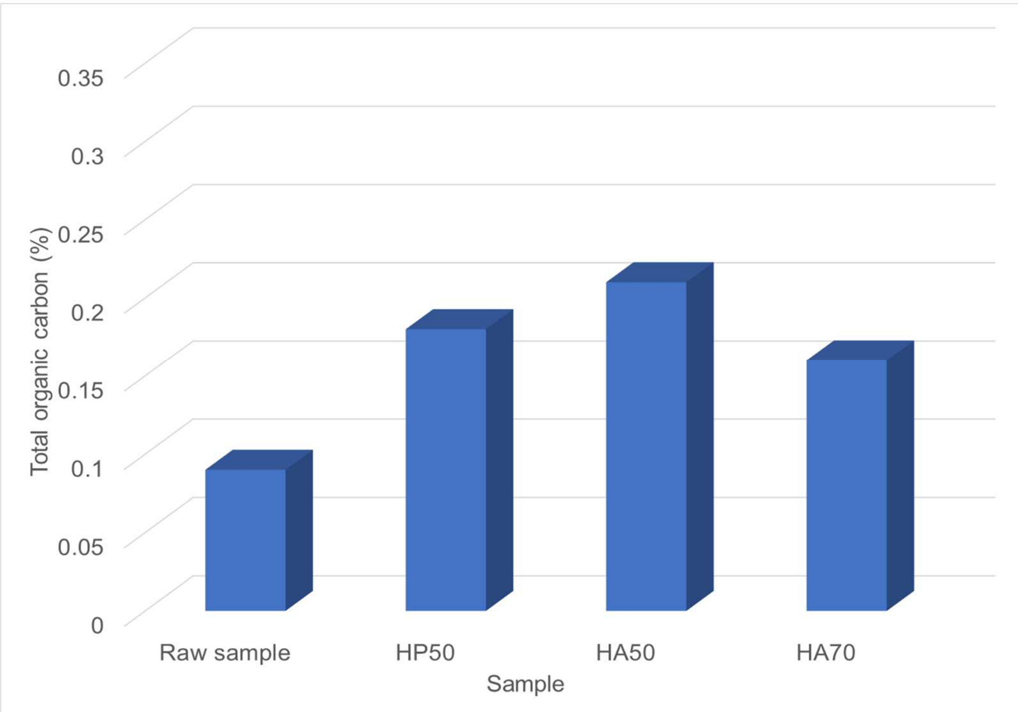

Figure 4-46 Total organic carbon content in samples

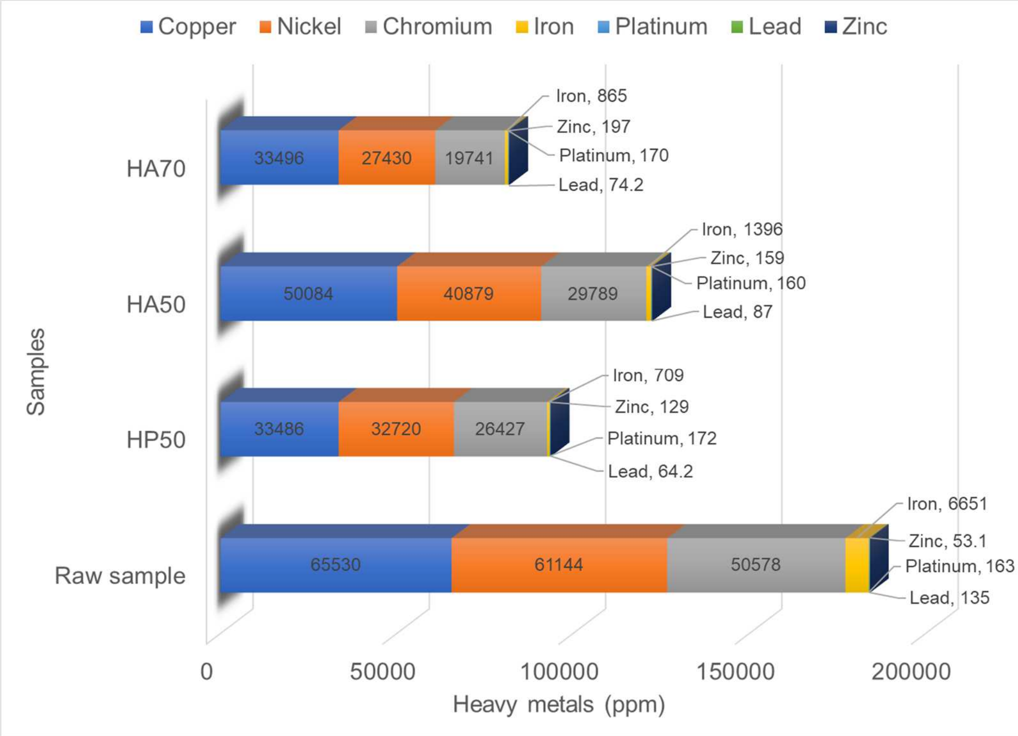

Figure 4-47 Heavy metal content in samples

Table 4-7: Properties of heavy metals

Parameter	Boiling temperature (°C)	Atomic number	Standard atomic weight Ar°(E)
Chromium	1907	24	51.996
Iron	1538	26	55.845
Nickel	1455	28	58.693
Copper	1084.6	29	63.546
Zinc	419.5	30	65.38
Platinum	3827	78	195.08
Lead	327.46	82	207.2

CHAPTER 5

CONCLUSION & FUTURE WORKS

5.1 Conclusion

The present study represents a scarce investigation on drying of industrial electroplating sludge by using a heat pump dryer which rarely being reported in open literatures. Industrial electroplating sludge samples were dried under various conditions using a pilot-scale heat pump dryer. Both drying characteristics of sample and energy efficiency of heat pump dryer were studied. Comparisons were made against conventional hot air drying. In overall, heat pump drying with proper dryer configurations and settings was found to be a good drying method for industrial sludge as it allowed better drying rate and enhanced energy efficiency as compared to other drying methods. Hence, this justified the feasibility of heat pump drying for industrial sludge. Followings are the significant findings from the present study.

i. **Drying kinetics and characteristics of the industrial sludge**

It was found that drying kinetics of all sludge samples conformed to a typical drying curve when undergoing heat pump drying, where they consisted of constant rate period and falling rate period. During constant rate period, the drying rate was proportion to the wet bulb depression of drying air medium when the air flow was remained constant and the heat transfer surface was the same.

Whereby the wet bulb depression could be increased by either increasing the dry bulb temperature or reducing the humidity. Generally, higher drying rate could be obtained with higher drying temperature and lower relative humidity. Similar trend was observed in the effective moisture diffusivity as well (Hosain *et al.*, 2016). Comparing to hot air dryer, heat pump dryer with dehumidification capability could achieve higher drying rate at same drying air temperature. This was because heat pump dryer could generate drying air medium with lower humidity and hence having higher wet bulb depression as compared to a conventional hot air dryer.

ii. **Energy efficiency of a heat pump dryer for sludge drying application**

In overall, heat pump dryer would be more energy efficient than hot air dryer if proper configuration and control strategy were used. Hot air drying trials revealed that drying temperature was the key parameter to obtain high drying rate, where the higher the drying temperature, the higher the drying rate. However, the high drying rate did not imply high energy efficiency. In fact, higher drying temperature would consume more energy to achieve the same moisture content of sludge sample that could be obtained at a lower drying temperature. Hot air drying at 70°C recorded the lowest SMER as compared to 50°C and 35°C. On the other hand, results illustrated that SMER curves were different between heat pump dryer (concave) and hot air dryer (convex). SMER for the hot air dryer tended to increase at the beginning of the drying session while SMER for the heat pump dryer was in reducing trend from the beginning. This was due to the heating mechanism of both dryers when generating the drying air medium.

iii. Impacts of configurations of heat pump components and control strategies

a. Effect of relative humidity control

SMER of heat pump dryer was much lower than hot air dryer when a controller was used to maintain low relative humidity in the drying air medium, where high power consumption was required to run the compressor continuously in order to perform the dehumidification and meet the set point. In addition, due to the limitation on the wet bulb temperature that could be achieved in the heat pump system and also the moisture evaporation rate of sludge sample, the additional energy input to control the relative humidity did not bring much benefit to the drying rate.

b. Effect of condenser type

Drying kinetics were similar regardless of the condenser type as both condensers were able to produce the drying air medium with the similar properties and drying force. Nonetheless, temperature control in water heating mode (WH) was slightly more stable than direct air heating mode (DH) though DH mode possessed much higher SMER in the early stage of drying. Nevertheless, SMER for both condenser types became similar in the end of drying when the WH mode stopped heating and storing thermal in the water tank once it had reached its set limit.

c. Effect of air flow

Simulation of air flow profile and dynamics showed that there was variation of air velocity in the drying chamber where the uneven air distribution could reduce the overall drying efficiency. Therefore, it is essential to review and improve the air flow path to reduce the effect of the uneven air flow and consequently causing the sporadic drying kinetics. Drying trials disclosed that the effect of air velocity was more prominent than relative humidity. In addition, when drying at the same temperature, higher air flow would promote higher effective moisture diffusivity. It was observed that the energy consumption was increasing with fan speed. Heat pump drying with the highest fan speed (HP50_60Hz) had logged the highest electricity consumption but at the same time it recorded the highest SMER among the heat pump drying trials. The result revealed that the electric power input for the fan in heat pump dryer was worthy as the higher air velocity could help to enhance the drying rate. However, when comparing with hot air drying, SMER of hot air drying was higher than heat pump drying. It could be postulated that the fan electricity consumption was relatively small as compared to the heat pump compressor electricity consumption.

d. Effect of bypass air ratio

Results showed that the drying kinetics for partially open mode (50% bypass) and open mode (100% bypass) were almost the same since their air velocities were not far different. Meanwhile, drying kinetic would drop significantly in closed mode (0% bypass) due to the ineffective dehumidification of drying air medium at the evaporator when there was overwhelm of warm and moisture laden drying air medium passing through it. On the other hand, it is observed that drying under open mode consumed the highest energy while drying under the close mode consumed the least energy. It was recommended that the bypass air ratio should be adjusted and controlled based on the surface temperature of the evaporator.

e. Effect of dehumidification

Results showed that the drying kinetics of samples under the dehumidifying mode (HP50_Dehum) was about 13% higher than that in heating mode (HP50_Heating). However, the dehumidifying mode became energy inefficient at the later stage of drying. Therefore, it was proposed that dehumidifying mode should be used in the beginning of the drying operation when the moisture content of sample is high while it must change to heating mode when the moisture content of sample was lower than 4 kg/kg dry basis.

f. Effect of heat pump compressor capacity

Results revealed that drying kinetics were mainly governed by drying air condition, regardless of heat pump compressor size. As long as the drying air temperature, air velocity and relative humidity were the same, then the drying kinetics would be the same. To obtain energy efficient heat pump drying, the compressor capacity must be sized according to the sample load and desired drying rate. Oversize compressor would result in higher energy consumption rather than enjoying the benefits from it. For a 10 kg sludge sample, a 0.5 HP compressor (HP50_0.5HP) was the most energy efficient as compared to other bigger sizes.

iv. **Quality analysis of dried sludge samples**

The total organic carbon did not degrade in the heat pump drying but was concentrated instead. It was found that the heavy metals in the dried samples were not degraded thermally but were carried over to air flow ducting and deposit on the wall surface. Proper design of the drying tray, air filtration and particles collection were needed to ensure the safety of the users.

5.2 Limitations and future works

There are still a lot of improvement work for the present pilot heat pump dryer based on the limitations that we encountered during the fabrication and construction stage of the heat pump dryer. There are a few improvement works are suggested to be considered on the design and construction of the heat pump dryer to increase the drying performance. The limitations and suggestions are listed as follow:

i. The current pilot heat pump dryer can only deliver up to around 50°C drying air temperature. However, since the experiments have concluded that better drying kinetic can be achieved at higher drying temperature, there would be an essential design consideration to develop a heat pump dryer which capable to deliver higher drying air temperature. Compressors operated with low or medium pressure refrigerant such as R134a shall be consider due to the capability to deliver higher drying temperature at lower operating pressure. The maximum drying air temperature that can be achieved by using such compressor shall be determined by carefully study the operating envelop of the compressor.

ii. Currently, the heat pump dryer was fitted with fix speed compressor. Thus, whenever system reaching the desired temperature set point, the compressor will stop operating. Compressor will be turned on again when the drying air temperature is lower than the temperature set point. The Frequent start stop of the compressor will cause the system to operate less efficiently and consume more energy compare to variable speed compressor. Variable speed compressor can regulate its output by varying the rotating speed based on the heating demand of the system. Adjusting the heating capacity according to the heating load would prevent capacity fluctuation that cause by the start stop of the fix speed compressor. Variable speed compressor coupled with electronic expansion valve would achieve 30% and 40% energy saving according to compressor manufacturers (Kuppusamy, Shanmugasundaram and Kumar, 2019).

iii. There are corrosion stains found inside the drying chamber after the drying process had been carried out for few months. It was clearly indicated that the sludge sample has contained corrosive solvent such as sulphuric acid. After drying process, the corrosive particles enter the drying air stream and cause acidic drying air which could corrode the heat pump dryer. To overcome the problem, the drying air path and drying chamber of the heat pump dryer can be considered to be made by corrosion resisting material such stainless steel 316 casing while the condenser and evaporator fin shall be coated with anti-corrosion coating or constructed with corrosion resisting material also. Besides that, the dried sample in powder form shall be trap with filtration system to avoid leaking of heavy metal to outside environment.

iv. The current pilot heat pump dryer is designed for experiment purpose which can only process around 10kg of sludge sample. Total 6 trays with each tray size at 350mm x350mm x25mm, are insufficient to dry big quantity of sludge and thus, bigger volume of drying chamber is required for huge quantity of sludge. The volume of drying chamber should be aligned with heating capacity for better of energy efficiency. The basic commercial size of drying chamber for sludge drying is looking at around 300kg/batch. Therefore, the next design of heat pump dryer shall start with 300kg/batch.

v. The drying experiments had shown that the heat pump dryer is operate efficiently at the constant period, but not as efficient as hot air drying at the falling period. Therefore, continue using heat pump drying during falling period will reduce the overall efficiency of the dryer. Therefore, the next development of heat pump dryer shall incorporate programmable logic controller (PLC) to control the drying stages with different setting of drying air temperature and humidity at individual stage. The drying process can be shifted to subsequent drying stage base on drying period or moisture reduction weight.

vi. The current pilot heat pump dryer with manual damper opening is difficult to control the require airflow pass through the dehumidification evaporator. Too much airflow with high drying air temperature will cause lesser condensation at the evaporator and therefore, higher humidity in the drying air stream. In order to have better control of condensation rate at the evaporator, the bypass damper should be fitted with a motorized actuator with analogue signal control. The bypass opening will be controlled based on evaporator surface temperature. If evaporator temperature is higher than the set point, then bypass opening shall be increased and vice versa.

vii. The air finned heaters shall be installed inside an air flow adapter box to reduce the air bypass ratio. If the air bypass ratio is high, the drying air does not contact the air finned heater effectively and thus reduce the heat exchange efficiency. The research study (Hall, 2018) has shown that the fan energy consumption is relatively small compare to compressor. Therefore, with the installation of the air flow adaptor box, the fan energy consumption will not significantly increase while the effectiveness of heat transfer from heater will increase effectively.

viii. The existing pilot heat pump dryer is assisted by hot air system. However, there are other hybrid heat pump dryers can be considered to achieve further energy saving. Heat pump dryer assisted by microwave or infra-red might have better energy saving compare to hot air heater (Hosain *et al.*, 2016),(Zielińska *et al.*, 2020). Further study shall be carried out on the new combination drying system and therefore, could provide alternative solution to industrial owner for their sludge drying application.

LIST OF REFERENCES

Aja & Joo (2016) *Overview of Hazardous Waste Management Status in Malaysia*. Intech.

Aktaş, M. *et al.* (2015) 'Performance analysis and modeling of a closed-loop heat pump dryer for bay leaves using artificial neural network', *Applied Thermal Engineering*, 87, pp. 714–723. doi: http://dx.doi.org/10.1016/j.applthermaleng.2015.05.049.

Ananthanarayanan, P. N. (2013) *Basic Refrigeration and Air Conditioning*. Tata McGraw-Hill Education, 2013.

Chua, K. J., Chou, S. K. and Yang, W. M. (2010) 'Advances in heat pump systems: A review', *Applied Energy*, 87(12), pp. 3611–3624. doi: http://dx.doi.org/10.1016/j.apenergy.2010.06.014.

Ferrarini, G. *et al.* (2017) 'Thermal diffusivity measurement of ring specimens by infrared thermography', in *Proc.SPIE*, p. 102140Z. doi: 10.1117/12.2262512.

Flaga (2015) 'Sludge Drying', *Institute of Heating Engineering and Air Protection, Cracow University of Technology*, ul Warszaw.

Fudholi, A. *et al.* (2011) *The effects of drying air temperature and humidity on the drying kinetics of seaweed*.

GEANKOPLIS, H. J. (2003) *Transport Processes and Unit Operations*.

Hall, S. M. (2018) 'Chapter 8 - Fans, Blowers, and Compressors', in Hall, S. M. B. T.-R. of T. for C. E. (Sixth E. (ed.). Elsevier, pp. 143–159. doi: https://doi.org/10.1016/B978-0-12-811037-9.00008-4.

Hanif, S. *et al.* (2017) *Effect of drying air parameters on energy consumption in desiccant grain drying*.

Hosain, M. *et al.* (2016) 'Effect of temperature and loading density on drying kinetics of wheat', 4, pp. 210–217. doi: 10.18006/2016.4(2).210.217.

Iain Grace (2002) 'Comparison of Hermatic Scroll and reciprocating compressors operating under varying refrigerant charge and load'.

Indah Water Konsortium Sdn Bhd (2015) 'Effects Of The Reuse of Sludge To Environment Health, 2015', in.

Je Myoung Moon (2003) 'Better Controls To Improve Air-Conditioning System efficiency'.

Ju, H.-Y. *et al.* (2018) 'Energy efficient improvements in hot air drying by controlling relative humidity based on Weibull and Bi-Di models', *Food and Bioproducts Processing*, 111, pp. 20–29. doi: https://doi.org/10.1016/j.fbp.2018.06.002.

Kivevele & Huan (2014) 'A review on opportunities for the development of heat pump drying systems in South Africa'. doi: 10.1590/ sajs.2014/20130236.

Kuppusamy, K., Shanmugasundaram, N. and Kumar, S. P. (2019) 'Variable Speed Compressor based Energy Savings in Air Condition system'.

Lee, K. H., Kim, O. J. and Kim, J. (2010) 'Performance Simulation of a Two-Cycle Heat Pump Dryer for High-Temperature Drying. Dry. Technol. 2010, 28, 683–689. http://dx.doi.org/10.1080/07373931003799210'.

Leniger, H.A., Beverloo, W. A. (2012) *Food Process Engineering*. Springer Science & Business Media, 2012.

Léonard, A. (2010) 'No Title', *SOME PRACTICAL PROBLEMS ENCOUNTEREDWHEN DRYING WASTEWATER SLUDGE*.

Leonard, V. (2004) 'Wastewater sludge convective drying: Influence of sludge origin."'.

Liu, H. *et al.* (2018) *Design and Thermal Analysis of an Air Source Heat Pump Dryer for Food Drying, Sustainability*. doi: 10.3390/su10093216.

Marinos-Kouris, D. and Maroulis, Z. (2006) '4 Transport Properties in the Drying of Solids', *Handbook of Industrial Drying*. doi: 10.1201/9781420017618.ch4.

Minea, V. (2010) 'Improvements of high-temperature drying heat pumps', *International Journal of Refrigeration*, 33(1), pp. 180–195. doi:

http://dx.doi.org/10.1016/j.ijrefrig.2009.09.010.

Misha, S. *et al.* (2015) *Simulation of Air Flow Distribution in a Tray Dryer by CFD*.

Mujumdar, A. S. (2007) *Handbook of Industrial Drying*. third edit. Edited by A. S. Mujumdar. CRC Press.

Patel, H. and Vashi, R. T. (2015) 'Chapter 2 - Characterization of Textile Wastewater', in Patel, H. and Vashi, R. T. B. T.-C. and T. of T. W. (eds). Boston: Elsevier, pp. 21–71. doi: https://doi.org/10.1016/B978-0-12-802326-6.00002-2.

Patel, K. K. and Kar, A. (2012) 'Heat pump assisted drying of agricultural produce—an overview', *Journal of Food Science and Technology*, 49(2), pp. 142–160. doi: 10.1007/s13197-011-0334-z.

Putra, R. N. and Ajiwiguna, T. A. (2017) 'Influence of Air Temperature and Velocity for Drying Process', *Procedia Engineering*, 170, pp. 516–519. doi: https://doi.org/10.1016/j.proeng.2017.03.082.

Rao, B. and Cao, L. (2012) *Technical research on sludge drying by solar energy and heat pump*, *Nongye Gongcheng Xuebao/Transactions of the Chinese Society of Agricultural Engineering*. doi: 10.3969/j.issn.1002-6819.2012.05.031.

S. Parker, D. *et al.* (1997) *Impact of evaporator coil airflow in residential air-conditioning systems*, *ASHRAE Transactions*.

Schnotale, A. F. and J. (2018) 'SEWAGE SLUDGE THERMAL DRYING AND HYGIENIZATION IN A CLOSED LOOP ENERGY RECOVERING SYSTEM'.

Shen, J. *et al.* (2018) 'Design and Experimental Study of an Air Source Heat Pump for Drying with Dual Modes of Single Stage and Cascade Cycle.'

Slim, R., Zoughaib, A. and Clodic, D. (2008) 'Modeling of a solar and heat pump sludge drying system', *International Journal of Refrigeration*, 31(7), pp. 1156–1168. doi: https://doi.org/10.1016/j.ijrefrig.2008.03.003.

Soponronnarit, S., Wetchakama, S. and Kanphukdee, T. (2000) *Seed drying using a heat pump*.

Spinosa, L. (2011) *Wastewater Sludge - A Global Overview of the Current Status and Future Prospects*. 2nd Editio.

WEC, W. E. F. (2017) 'The Global Competitiveness Index 2017–2018', *Geneva, Switzerland*.

Wikipedia (no date) 'Wastewater treatment', *Wikipedia*.

Www.iwapublishing.com (no date) 'Sludge Drying view'.

Yang, Z., Zhu, Z. and Zhao, F. (2016) 'Simultaneous control of drying temperature and superheat for a closed-loop heat pump dryer', *Applied Thermal Engineering*, 93, pp. 571–579. doi: https://doi.org/10.1016/j.applthermaleng.2015.09.117.

Yi H, Guo QW, Li XH, X. Z. (2014) (2014) 'Design characteristics of wastewater treatment and reutilization in a printing and dyeing industrial park in Xintang Town of Guangzhou City. China Water Wastewater 2014;30(2):34–7 [in Chinese]'.

Yu, L. *et al.* (2012) 'Influence of drying medium relation humidity on drying rate of wood base on X-ray scanning method', in *Proceedings of 2012 International Conference on Biobase Material Science and Engineering*, pp. 117–120. doi: 10.1109/BMSE.2012.6466194.

Zhang, J. *et al.* (2016) 'A comprehensive review on advances and applications of industrial heat pumps based on the practices in China', *Applied Energy*, 178, pp. 800–825. doi: 10.1016/j.apenergy.2016.06.049.

Zielińska, M. *et al.* (2020) 'Review of recent applications and research progress in hybrid and combined microwave–assisted drying of food products: Quality properties', *Critical Reviews in Food Science and Nutrition*, 60, pp. 2212–2264. doi: 10.1080/10408398.2019.1632788.

APPENDIX 1

Calculation of Heat Transfer Coefficient

During the constant rate period, assuming all the heat transfer from the air to the sludge has vaporized the water on it, then the heat transfer from the air to the sludge,

$$\dot{m}\lambda_w = hA(T_a - T_w)$$

where $\dot{m}$ is drying rate, T_a is dry bulb temperature of drying air, T_w is the web bulb temperature of drying air and λ_w is the latent heat of vaporization at temperature T_w. We can also express the above equation as,

$$\dot{m}\lambda_w = hA\ x\ wet\ bulb\ depression\ of\ drying\ air$$

Latent heat of vaporization of water at corresponding temperature can be calculated from the equation below,

Latent heat of vaporization (kJ/kg) = 2500.8 – 2.36T + 0.0016T^2 – 0.00006T^3

where T is water temperature in degree Celsius.

Taken the data from Table *4-2*, the heat transfer of sludge drying is calculated and shown in table below,

	T_w (°C)	WB Depression (°C)	Drying Rate (-kg/min)	λ_w (kJ/kg)	$\dot{m}\lambda_w$ (kW)
HA50	32.4±1.5	17.6±1.5	0.0167±0.0005	2424±3.4	0.67±0.002
HP50	25.8±1.5	24.2±1.5	0.0200±0.0005	2440±3.4	0.81±0.002
HA35	26.6±1.5	8.4±1.5	0.0078±0.0005	2438±3.4	0.32±0.002
HP35	20.8±1.5	14.2±1.5	0.0133±0.0005	2452±3.4	0.54±0.002

Plotting heat transfer against wet bulb depression, we get the chart below,

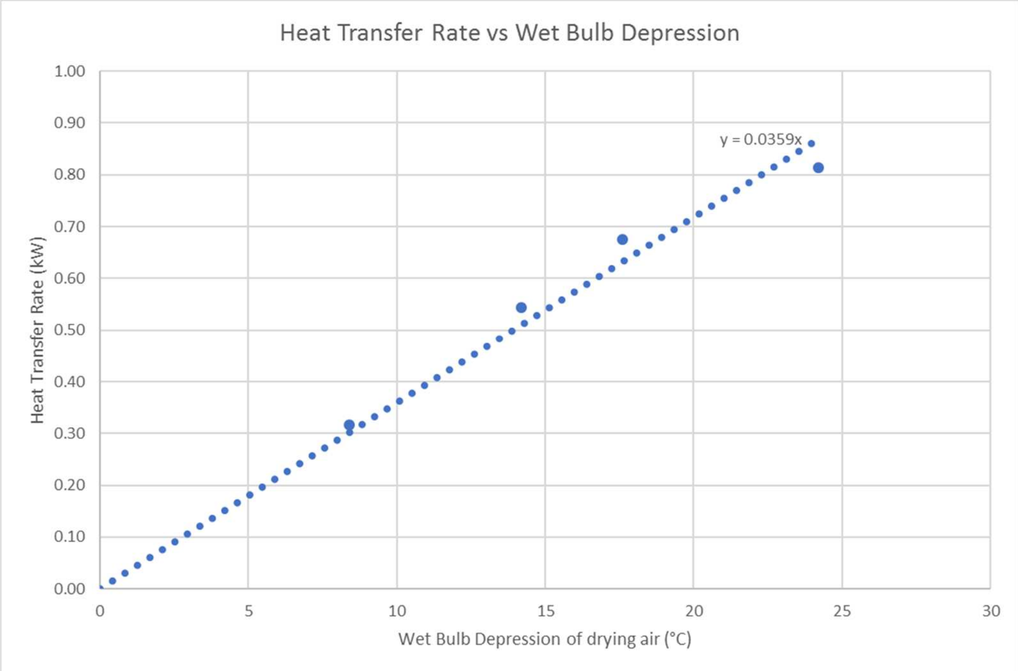

From the chart above, the hA is approximated as 0.0359 kW/°C. Since the heat transfer surface area, A is unknown, then the heat transfer coefficient is calculated based on tray area, h_{tray} hence

$$hA = h_{tray}A_{tray}$$

where total tray area is 6 x 0.315m x 0.365m = 0.690 m^2. Therefore,

$$h_{tray} = 0.0359/0.690 = 0.0520 \text{ kW/m}^2\cdot°\text{C}.$$

Drying trials were conducted with 3 different fan speeds to investigate the effect of air velocity on drying rate. Three frequencies (30Hz, 50Hz and 60Hz) were selected by adjusting the frequency inverter. In the drying chamber, air flow is passing through a stack of trays. The passages between trays are approximated as 365mm x 95mm. There are 6 passages in total and thus the total cross section area of passages is,

$$6 \text{ x } 0.095\text{m x } 0.365\text{m} = 0.208 \text{ m}^2$$

Hence, the air velocity inside the passage, u can be written as

$$u = V/0.208$$

Table below shows the result of measurement and calculated data for different air flow.

Frequency	Fan Speed (rpm)	V (m^3/s)	u (m/s)
30Hz	870	0.33	1.59
50Hz	1450	0.53	2.55
60Hz	1740	0.61	2.93

Reynold's number of the flow is defined as,

$$Re = \frac{\rho u D_h}{\mu}$$

where ρ is air density, D_h is hydraulic diameter and μ is the dynamic viscosity.

For rectangular passage, D_h is defined as,

$$D_h = \frac{4A}{P}$$

where A is surface area and P is wetted perimeter. Therefore, for the passage,

$$D_h = \frac{4(0.365 \times 0095)}{2(0.365 + 0.095)} = 0.151\text{m}$$

Viscosity of air can be calculated using the Sutherland Equation,

$$\mu = \frac{bT^{3/2}}{T + S}$$

where b and S are constants while T is temperature in Kelvin.

For air, b = 1.458 x $10^{-6}\ \frac{\text{kg}}{\text{m·s.K}^{1/2}}$ and S = 109.1 K.

For drying air at 50°C,

$$\mu = \frac{1.4592 \times 10^{-6} \times (50 + 273.15)^{3/2}}{(50 + 273.15) + 109.1} = 1.961 \times 10^{-5}\ \frac{\text{kg}}{\text{m} \cdot \text{s}}$$

Density of the air can be calculated using perfect gas equation,

$$\rho = \frac{P_{atm}}{RT}$$

where P_{atm} is atmospheric pressure, R is gas constant R = 0.287 kJ/kg·K.

At 50°C, the density of air is

$$\rho = \frac{101.325}{0.287 \times (50 + 273.15)} = 1.0925\ \frac{\text{kg}}{\text{m}^3}$$

Substitute the calculated values into Re equation, the Reynold's numbers for 30Hz, 50Hz and 60Hz air flow are as shown in the Table (Page 138). For flow in rectangular passage, the flow is turbulent when Re > 10000 (2009 ASHRAE Handbook – Fundamental (SI), 4.17). Thus, all the air flows in drying trials were turbulent in the drying chamber.

For turbulent flow in rectangular passage, Gnielinski correlation is used to calculate the heat transfer coefficient of the air flow. Gneilinski correlation is written as

$$Nu = \frac{\left(\frac{f}{8}\right)(Re - 1000)Pr}{1 + 12.7\left(\frac{f}{8}\right)^{\frac{1}{2}}\left(Pr^{\frac{2}{3}} - 1\right)} \cdot \left[1 + \left(\frac{D_h}{L}\right)^{2/3}\right]$$

where Nu is Nusselt number, Pr is Prandtl number and f is Darcy friction factor.

Prandtl number is defines as

$$Pr = \frac{\mu C_p}{k}$$

where C_p is specific heat capacity and k is thermal conductivity. The correlation of thermal conductivity and temperature using Sutherland equation is

$$k = \frac{2.334 \times 10^{-6} \times T^{3/2}}{T + 164.54} \frac{\mathrm{kW}}{\mathrm{m} \cdot \mathrm{K}}$$

Thus, for air at 50°C

$$k = \frac{2.334 \times 10^{-6} \times (50 + 273.15)^{3/2}}{50 + 273.15 + 164.54} = 2.78x10^{-5} \frac{\mathrm{kW}}{\mathrm{m} \cdot \mathrm{K}}$$

The specific heat of air can be calculated using the quadratic equation,

$$C_p = 1.0305 - 1.9975x10^{-4}T + 3.9734x10^{-7}T^2$$

Substitute T with 323.15 K,

$$C_p = 1.0074 \frac{\mathrm{kJ}}{\mathrm{kg} \cdot \mathrm{K}}$$

Hence, the Prandtl number for air at 50°C is

$$Pr = \frac{1.961 \times 10^{-6} \times 1.0074}{2.78 \times 10^{-5}} = 0.71$$

With turbulent flow, the Darcy friction factor can be calculated using relationship developed by Churchill (1977) which available in 2013 ASHRAE Hand book – Fundamental 3.7.

$$f = 8\left[\left(\frac{8}{Re}\right)^{12} + \frac{1}{(A+B)^{1.5}}\right]^{1/12}$$

$$A = \left[2.457 \ln\left(\frac{1}{(7/Re)^{0.9} + (0.27\varepsilon/D_h)}\right)\right]^{16}$$

$$B = \left(\frac{37530}{Re}\right)^{16}$$

where ε in this case, is the roughness height of sludge surface. The roughness height is estimated at 8.5mm, then ε/D_h = 0.0085/0.151 = 0.056.

Once Nusselt number is calculated using the above correlation, then heat transfer coefficient can be calculated as

$$h = \frac{Nu.k}{D_h}$$

Table below shows the result of calculation.

Frequency	Fan Speed (rpm)	*Re*	*A*	*B*	*f*	*Nu*	*h* (kW/m^2·K
30Hz	870	13322	1.188E+16	1.573E+07	0.0783	185.62	0.0342
50Hz	1450	21396	1.304E+16	8.028E+03	0.0774	303.08	0.0559
60Hz	1740	24626	1.332E+16	8.467E+02	0.0772	349.99	0.0645

With the heat transfer coefficients known, drying rate can be calculated by using equation,

$$\dot{m}_w = \frac{hA(T_a - T_w)}{\lambda_w}.60$$

where $\dot{m}_w$ is drying rate in kg/min.

Calculated drying rate for respective flow rate are as shown in the Table below.

Frequency	DB Temp	Rel. Hum	WB Temp	DB - WB	h (kW/m^2.K)	λ_w (kJ/kg)	$\dot{m}_w$ (kg/min)
30Hz	50	28.2%	31.7	18.3	0.0342	2426	0.0107
50Hz	50	30.0%	32.4	17.6	0.0559	2424	0.0168
60Hz	50	27.5%	31.4	18.6	0.0645	2426	0.0205

Comparing the calculated data with the measured data (chart below), the deviation is within 5%.

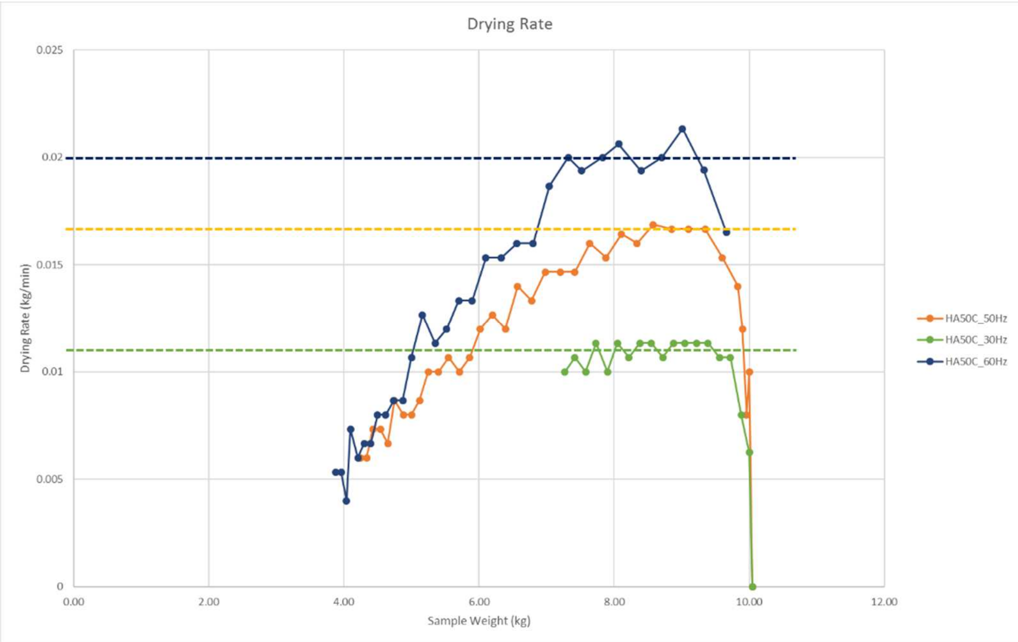

APPENDIX 2

Drying Formula Information

Item	Formula Name/Descriptions	Formula	Explanation of symbols	References
1	Coefficient of Performance (COP)	$$\text{COP} = \frac{\text{Actual Heat Output}}{\text{Power Input}}$$		Handbook of Industrial Drying Arun S. Mujumdar (editor)3rd Edition ;Chapter47.equa 47.1 (Mujumdar, 2007)
2	Heat Pump efficiency by Carnot efficiency	$$COP_{Carnot} = \frac{\dot{T}_{Cond}}{TCondenser - T\ Evaporator}$$		Handbook of Industrial Drying Arun S. Mujumdar (editor)3rd Edition ;Chapter47.equa 47.2 (Mujumdar, 2007)

Item	Formula Name/Descriptions	Formula	Explanation of symbols	References
3	COP of heat pump system	$$COP_{HP} = \frac{\dot{Q}_{Cond}}{\dot{W}_C}$$	$\dot{Q}_{Cond}$ is heating output at the condenser (kW) $\dot{W}_C$ is input power of compressor (kW)	A review on opportunities for the development of heat pump drying systems in South Africa. Thomas Kivevele1 Zhongjie Huan1 Equa 1. (Kivevele & Huan, 2014)
4	COP of heat pump dryer	$$COP_{HPD} = \frac{\dot{Q}_{Cond}}{\dot{W}_C + \dot{W}_F + \dot{W}_P}$$	$\dot{W}_F$ is input power of circulation fan (kW) $\dot{W}_P$ is input power of circulation pump (kW) if liquid is used	A review on opportunities for the development of heat pump drying systems in South Africa. Thomas Kivevele1 Zhongjie Huan1 Equa 3.

Item	Formula Name/Descriptions	Formula	Explanation of symbols	References
5	Specific Moisture Extraction Rate (SMER)	$SMER_{HP} = \frac{\dot{m}_{CW}}{\dot{W}_C}$	$\dot{m}_{CW}$ is rate of moisture condensation at the evaporator (kg/s)	A review on opportunities for the development of heat pump drying systems in South Africa. Thomas Kivevele1 Zhongjie Huan1 Equa 6.
6	Drying efficiency of heat pump dryer	$SMER_{HPD} = \frac{\dot{m}_{CW}}{\dot{W}_C + \dot{W}_F + \dot{W}_P}$		Handbook of Industrial Drying Arun S. Mujumdar (editor)3rd Edition ;Chapter47.equa 47.3
7	Energy relationship between condenser and evaporator	$\dot{Q}_{Cond} = \dot{Q}_{Evap} + \dot{W}_C$		Heat pump assisted drying of agricultural produce—an overview Krishna Kumar Patel & Abhijit Kar ; Equation5 (Patel and Kar, 2012)

Item	Formula Name/Descriptions	Formula	Explanation of symbols	References
8	Wet basis moisture content	$M_w = \frac{m_w}{m_t}$	M_w is defined as the mass of water in the product m_w divided by the total mass of the product m_t,	Handbook of Industrial Drying ArunS.Mujumdar (editor)3rdEdition ;Chapter1.equa 1.50
9	Dry basis moisture content	$M_d = \frac{m_w}{m_d}$	M_d is defined as the mass of water in the product divided by the total mass of the product m_d,	Performance analysis and modeling of a closed-loop heat pump dryer for bay leaves using artificial neural network Mustafa Aktas¸ a, 1, Seyfi S¸ evik b, *, M. Bahadır €Ozdemir a, 2, Emrah G€onen Equa:4 (Aktaş *et al.*, 2015)

Item	Formula Name/Descriptions	Formula	Explanation of symbols	References
10	Water activity	$A_w = \frac{Partial\ vapour\ pressure\ in\ a\ product}{Partial\ vapour\ presure\ of\ pure\ water}$		Methods to Measure Water Activity JOHN TROLLER
11	Fick's second law of diffusion	$\frac{\partial M}{\partial t} = D_{eff}\nabla^2 M$	• M is local moisture content • is the time (h) • D_{eff} is the moisture diffusivity (m^2/h)	Transport Properties in the Drying of Solids Dimitris Marinos-Kouris and Z.B. Maroulis Equation 4.1 (Marinos-Kouris and Maroulis, 2006)
12	Thermal diffusivity	$\alpha = \frac{k}{\rho Cp}$	• k is thermal conductivity (W/(m·K)) • ρ is density (kg/m^3) • Cp is specific heat capacity (J/(kg·K))	Determination of thermal diffusivity of austenitic steel using pulsed infrared thermography (Ferrarini *et al.*, 2017)

Item	Formula Name/Descriptions	Formula	Explanation of symbols	References
				k. kochanowski∗ , w. oliferuk∗ , z. płochocki∗∗, a. adamowicz∗Equa:1
13	Pressure of air is related to the altitude of atmosphere	$P = 101.325 [1 – (2.25569x\ 10^{-5}) Z]^{5.2561}$	*P* is in kPa and *Z* is in meters	From NACA # 1235 (1955)- Pressure of air is related to the altitude of atmosphere
14	Partial water vapour pressure	$p_{ws} = e^{B1}$	$B1 = [(C_8 / T) + C_9 + C_{10}T + C_{11}T^2 + C_{12}T^3 + C_{13}(InT)]$ p_{ws} is in Pa; *T* in K and constants are: $C_8 = -5.8002206 \times 10^3$ $C_9 = +1.3914993$ $C_{10} = -4.8640239 \times 10^{-2}$ $C_{11} = +4.1764768 \times 10^{-5}$ $C_{12} = -1.4452093 \times 10^{-8}$	From ASHRAE Handbook- Fundamentals, chapter 6, 1993, equation 4

Item	Formula Name/Descriptions	Formula	Explanation of symbols	References
			C_{13} = +6.5459673	
15	Dew point temperature (T> 0°C)	$t_d = a + b [\ln(p_w)] + c [\ln(p_w)]^2 + d [\ln(p_w)]^3 + e (p_w)^{0.1984}$	pw is in kPa; t_d is in ^{0}C, and constants are: a = 6.54 b = 14.526 c = 0.7389 d = 0.09486 e = 0.4569	ASHRAE Handbook-Fundamentals, chapter 6, 1993, equation 35
16	Humidity ratio	$W = 0.62198 (p_w) / (p- p_w)$	p and p_w are in kPa ; W is kg moisture / kg dry air ratio.	ASHRAE Handbook-Fundamentals, chapter 6, 1993, equation 20
17	Relative humidity	$\varphi = p_w / p_{ws}$	p_{ws} and p_w are in kPa or consistent units.	ASHRAE Handbook-Fundamentals, chapter 6, 1993, equation 22

Item	Formula Name/Descriptions	Formula	Explanation of symbols	References
18	Specific volume	$v = R_aT /(p – p_w) = 0.287055T /(p – pw)$	V is in m^3/kg, p_w and p are in kPa , T is in K	ASHRAE Handbook-Fundamentals, chapter 6, 1993, equation 25
19	Enthalpy	$h = t + W(2501 + 1.805t)$	h is in kJ/kg, t is in ^{0}C and W is the (kg moisture / kg dry air) ratio.	ASHRAE Handbook-Fundamentals, chapter 6, 1993, equation 30
20	Wet bulb temperature ($T \geq 0^0$C)	$t^* = [2501W_s^* - c_{pa}t – W(2501 +1.805t)]/ (2.381W_s^* - c_{pa} – 4.186W)$	t and t^* is in ^{0}C ; W and W_s^* are the (kg moisture / kg dry air) ratio, and c_{pa} is the specific heat of dry air (kJ/kg.°C).	ASHRAE Handbook-Fundamentals, chapter 6, 1993, equation 33 a
21	*Total Cooling Capacity*	$T_c = \dot{m}\Delta H$ $= \frac{Q}{Spv\ x\ 3600}\ (H_{entering} – H_{Leaving})\ldots kW$	Q = Flowrate of unit (m^3/hr) Spv = Specific volume (m^3/kg) with value of 0.8323 m^3/kg H = Enthalpy (kJ/kg) U = $C_p\Delta T$	2001 *ASHRAE Handbook* Chapter 6 : Equation 42

Item	Formula Name/Descriptions	Formula	Explanation of symbols	References
			$\dot{m}$ = mass flowrate (m^3/hr) C_p = Specific heat for air at 300K with 1.007 kJ/kg.K	
22	Sensible Heat	$qs = Q\rho cp\Delta t = 1200Q\Delta t$	*qs = sensible heat load, W* *Q = air flow rate, m3/s* *ρ = air density, kg/m3 (about 1.2)* *cp = specific heat of air, J/(kg·K) (about 1000)* *Δt = temperature difference between indoors and outdoors, K*	2001 *ASHRAE Handbook* Chapter 26 :26.9 Equation 27

Item	Formula Name/Descriptions	Formula	Explanation of symbols	References
23	Moisture removal rate (kg water / kg dry solid)	$mc = \frac{W1 - Wc}{tc}$	*mc = moisture removal rate (kg water/ kg dry solid)* *W1 = initial moisture content (kg water/kg dry solid)* *Wc = critical moisture content (kg water./ kg dry solid)* *tc = time for constant rate period (s)*	Performance analysis and modeling of a closed-loop heat pump dryer for bay leaves using artificial neural network Mustafa Aktas¸ a, 1, Seyfi S¸ evik b, *, M. Bahadır €Ozdemir a, 2, Emrah G€onen Equa:6
24	*Heat transfer (W)*	$q = h A (Ta – Ts)$	*q = rate of heat transfer (W)* *h = convective heat transfer coefficient* W/m^2C *A = surface area of product* *Ta = heated air temperature* ^0C *Ts = product surface air temperature* *During constant rate of drying, product surface*	Handbook of Industrial Drying ArunS.Mujumdar (editor)3rdEdition ;Chapter4 ; equa 4.5

Item	Formula Name/Descriptions	Formula	Explanation of symbols	References
			temperature equal to wet bulb temperature of air stream	
25	Drying time at constant rate, *tc*	$$t_c = \frac{w_1 - w_c}{R_c A}$$	t_c = *constant rate drying period* initial moisture content w_1 critical moisture content w_c. R_c is the rate of drying A is the area of exposed surface.	Chemical Engineering Chapter 16 ; equation 16.10

Item	Formula Name/Descriptions	Formula	Explanation of symbols	References
26	*Thermal energy transfer*	$q = h A (Ta - Ts)$ $q = mc (HL)$ $mc = \frac{W1 - Wc}{tc} = \frac{hA(Ta - Ts)}{HL}$ $tc = \frac{HL(W1 - Wc)}{hA(Ta - Ts)}$	HL = latent heat of vaporisation at wet bulb temperature (J/kg water)	Transport Processes and Unit Operations Chapter9; equation 9.3.17 (GEANKOPLIS, 2003)

Item	Formula Name/Descriptions	Formula	Explanation of symbols	References
27	Drying time at Falling rate, *tc*	$\frac{w-we}{wc-we} = \frac{8}{\pi^2} e^{\left(-\frac{\pi^2 Dt}{4dc^2}\right)}$ $tf = \frac{4dc^2}{\pi^2 D} \ln[\frac{8}{\pi^2}(\frac{w-we}{wc-we})]$	*dc* = characteristic dimension. Half thickness of the slab (m) *D* = effective mass diffusivity m^2/s *tf* =drying time, (s) *w*= moisture content *we* = equilibrium moisture content *wc* = critical point moisture content between constant and falling period	Transport Processes and Unit Operations Chapter9 ;equation 9.9.6